Appendixes

DARHT EIS

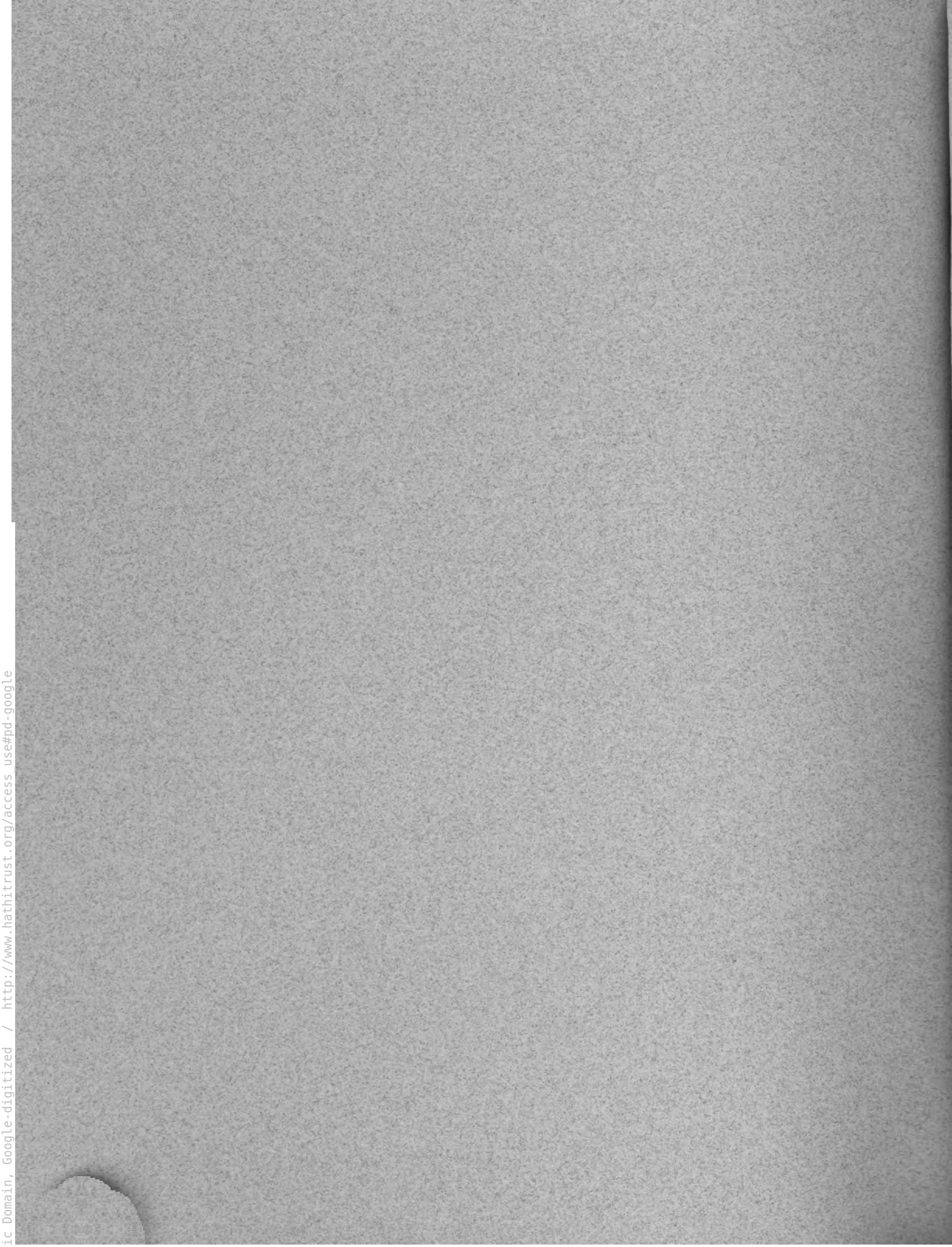

Appendix A
Federal Register Notices

DARHT EIS

APPENDIX A: FEDERAL REGISTER NOTICES

This appendix presents the following U.S. Department of Energy notices published in the *Federal Register*:

- **Notice of Intent** – Environmental Impact Statement; Dual Axis Radiographic Hydrodynamic Test Facility, Los Alamos National Laboratory
- **Notice of Availability** – Availability of the Dual Axis Radiographic Hydrodynamic Test Facility Draft Environmental Impact Statement
- **Notice of Additional Information** – Availability of Information Related to the Dual Axis Radiographic Hydrodynamic Test Facility; Draft Environmental Impact Statement

DEPARTMENT OF ENERGY

Environmental Impact Statement; Dual Axis Radiographic Hydrodynamic Test Facility, Los Alamos National Laboratory

AGENCY: Department of Energy.

ACTION: Notice of intent to prepare an environmental impact statement.

SUMMARY: The United States Department of Energy (DOE) provides notice of its intent to prepare an environmental impact statement (EIS) on the DARHT facility at its Los Alamos National Laboratory (LANL), Los Alamos, New Mexico. The EIS will be prepared pursuant to the National Environmental Policy Act of 1969 (NEPA) (42 U.S.C. 4321 et seq.), the Council on Environmental Quality NEPA Regulations (40 CFR Parts 1500–1508), and the DOE NEPA Regulations (10 CFR Part 1021). The EIS will analyze the impacts of completing construction and operating the DARHT facility at LANL, and reasonable alternatives.

With this Notice, DOE initiates a public comment period to solicit suggestions on the scope of analysis for this EIS. DOE also extends an invitation to attend public scoping meetings in Los Alamos and Santa Fe, New Mexico, and to provide suggestions for public participation opportunities for this NEPA review.

DATES: Written comments on the scope of the EIS are invited from the public. To ensure consideration, comments should be postmarked by Tuesday, January 10, 1995. Comments sent after that date will be considered to the fullest extent practicable. Public scoping meetings will be held as follows:

Wednesday, December 7, 1994, Los Alamos, 1:00 pm–4:30 pm, and 6:30 pm9:00 pm, Hilltop House, 400 Trinity Drive, Los Alamos, New Mexico.

Thursday, December 8, 1994, Santa Fe, 1:00 pm–4:30 pm, and 6:30 pm–9:00 pm, Sweeney Center, 201 West Marcy Street, Santa Fe, New Mexico.

The meetings will use a workshop format to facilitate dialogue among DOE, LANL, and the public and will provide an opportunity for individuals to provide written or oral statements.

ADDRESSES: Written comments on the scope of the DARHT EIS, or other matters regarding this environmental review, should be addressed to: Ms. Diana Webb, NEPA Compliance Officer, Los Alamos Area Office, Department of Energy, 528 35th Street, Los Alamos, NM 87544, Attn: DARHT EIS. Ms. Webb may be contacted by phone at (505) 665–8353, facsimile (505) 665–4872.

FOR FURTHER INFORMATION CONTACT: For general information on the DOE NEPA process, please contact: Carol M. Borgstrom, Director, Office of NEPA Oversight, EH–25, Department of Energy, 1000 Independence Ave., SW, Washington, DC 20585. Ms. Borgstrom may be contacted by leaving a message at (800) 472–2756 or by calling (202) 586–4600.

SUPPLEMENTARY INFORMATION:

Purpose and Need for Action

One of the most urgent and difficult technical tasks facing the DOE is to assess the effects of aging on the weapons that remain in the nation's nuclear stockpile, and to ensure the continuing safety of those weapons. Because the President has decided not to build any new nuclear weapons for the foreseeable future, but instead to continue to rely upon a smaller stockpile of existing but aging weapons as a nuclear deterrent, DOE must ensure that the weapons remaining in the stockpile are safe, secure and reliable. Under the Atomic Energy Act, this mission rests with DOE and essentially requires DOE to certify that the weapons will not accidentally detonate during storage and handling, that the weapons would thwart any attempts for unauthorized use, and that they would function as designed in the event of authorized use.

To fulfill this mission, DOE needs to collect diagnostic information regarding the condition of the weapons which remain in the enduring stockpile. Some of these weapons are approaching the end of their design life, and DOE is not certain how they may be affected by the aging process. One important type of information that is currently lacking concerns the three-dimensional condition of the various internal components of aging weapons. These are often shielded by thick and dense materials. Multiple view hydrodynamic testing (experiments to look at the flow of adjacent materials as they are driven by high explosives) and dynamic testing (experiments to study other effects of high explosives), combined with computer modeling, provide the only means of obtaining this data in the absence of nuclear testing. The President has endorsed hydrodynamic testing as the preferred means of conducting experiments in support of stockpile stewardship and maintenance. Hydrodynamic testing has become more important since the United States moratorium on nuclear testing was extended. A future Comprehensive Test

Ban Treaty, moreover, would foreclose the acquisition of additional performance and safety data through nuclear testing.

Proposed Action

DARHT would be a specialized high energy X-ray machine that would take three-dimensional, sequential and high-resolution X-ray pictures of the dynamic behavior of dense materials that are being shocked and compressed by high explosives. DARHT would be used to evaluate the nonnuclear behavior of nuclear weapons components and would provide the nation with a significantly improved diagnostic capability to evaluate and assess the safety and reliability of the existing nuclear weapons stockpile. DARHT would consist of an existing support lab, a new firing site, and the necessary infrastructure, all located at Technical Area 15 at LANL. DARHT would be used to detonate high explosives, and to use very high-speed, tightly-focused radiographic (X-ray) photography to determine the motions (dynamic experiments) or flow (hydrodynamic tests) of the explosive-driven materials. Two X-ray machines at right angles to each other (dual-axis lines of sight) would be powered by two 16 million electron volt (MeV) electron accelerators, each housed in a building about 225 feet long. By using two machines, DARHT would be able to provide three-dimensional, sequential information on occurrences within millionths of a second during a test. The accelerators' small beam size would allow DARHT to provide a very high-quality resolution of the radiographic image. This resolution is necessary to resolve the fine details of the material flowing in these experiments.

DARHT experiments would variously involve radioactive materials (primarily depleted uranium), beryllium and other hazardous materials, and other metals. Additionally, experiments involving plutonium contained in steel vessels may be conducted. DARHT would not test materials that could result in nuclear yield, or a nuclear detonation. Experiments at DARHT would be expected to result in metal fragments and other airborne debris being deposited up to 750 meters from the open-air explosives testing (standard operating procedures would require the evacuation of this area before any experiments were conducted)

In addition to testing the nonnuclear behavior of nuclear weapons components, DARHT would be used to evaluate conventional weapons systems, explosives-driven materials for non-weapons uses, and high-velocity impact phenomena. The facility would also be used to support non-proliferation and counter-proliferation efforts, such as experiments intended to disable a terrorist-designed or proliferant-designed nuclear weapon. Although DARHT could be used to collect information relevant to the design of new weapons, no new weapons are anticipated to be designed in the foreseeable future.

Design of DARHT began in the early 1980's. Memoranda to File, describing the environmental impacts of constructing and operating DARHT, were completed in 1983 and 1987. DARHT construction began in 1988 with the Radiographic Support Laboratory, which was completed in 1990. The Radiographic Support Laboratory is currently being used to support the development of the accelerator equipment that is planned to be used in DARHT. In May 1994, DOE began construction of the Hydrodynamic Firing Site. Approximately 20 percent of the Hydrodynamic Firing Site construction work (e.g., site preparation, foundation pouring) has been completed. Current schedules call for the Hydrodynamic Firing Site construction to be completed, and the first X-ray machine to be operating, in 1997 at a cost of approximately $86 million, and the second X-ray machine, if approved, would begin operation in 2000. The total estimated project cost of DARHT in its final two-axis configuration is $124 million; to date, approximately $44 million has been spent or obligated on the project.

In response to public concern, the DOE has decided to prepare this EIS at this time to allow for a full dialogue between DOE and the State, tribes, other agencies and the general public regarding the environmental impacts of completing and operating DARHT, and the impacts of other alternatives. The EIS will also assist in ensuring that appropriate mitigation measures are developed if DARHT is completed and put into operation. Construction and related work on the facility will continue during the preparation of the EIS.

Proposed Alternatives

DOE has tentatively identified the following alternatives for analysis in the EIS and seeks public comment on their adequacy, inclusiveness, and reasonableness:

(1) Proposed action

Under this alternative, DOE would complete construction and operate the DARHT facility as currently planned. This alternative would provide a state-of-the-art diagnostic capability for ensuring the safety, security and reliability of the aging nuclear weapons stockpile. If DARHT becomes operational, operation of the Pulsed High Energy Radiation Machine Emitting X-Rays (PHERMEX) facility, an existing facility at LANL also located at Technical Area 15, near the DARHT site, will be phased out.

(2) No Action (status quo) Alternative

Under this alternative, DARHT would not be completed and DOE would continue to operate the Pulsed High Energy Radiation Machine Emitting X-Rays and the Flash X-Ray facility at the Department's Lawrence Livermore National Laboratory Site 300 located near Livermore, California. The Pulsed High Energy Radiation Machine Emitting X-Rays, a single-axis radiographic facility, was built in the mid-1960's and has been used continuously since that time. It uses a pulsed power accelerator to power the X-ray machine, and does not have the small beam size (tight focus) planned for DARHT, thereby precluding the high-resolution images that DARHT would provide. Flash X-Ray, also a single-axis radiographic facility, was built in 1982 and has been used continuously since that time. It uses a linear induction accelerator to power the X-ray machine and also does not have the small beam size planned for DARHT.

(3) Containment Alternative

Under this alternative, DOE would modify the construction and/or operation of DARHT to contain some or all airborne emissions of fragments or other debris. Under one approach, the X-ray pictures would be taken through the walls of a containment vessel. Another approach would be to construct a building to enclose and contain the explosive experiments; X-ray pictures would be taken within the containment building. These two approaches may be considered separately or together, for some tests or for all tests.

(4) Institutional Control Alternative

Under this alternative, DOE would complete and operate DARHT, but would limit use of the facility to exclude any applications involving experiments with plutonium.

(5) Single-Axis Alternative

Under this alternative DOE would complete construction of the Hydrodynamic Firing Site but would operate only a single axis of DARHT with one accelerator. This alternative would provide an improved technical

capability over present accelerators with a single view (i.e., the Pulsed High Energy Radiation Machine Emitting X-Rays and Flash X-Ray).

(6) Upgrade Alternative

Under this alternative DOE would upgrade the present Pulsed High Energy Radiation Machine Emitting X-Rays capability with the new technology developed for DARHT.

DOE does not intend, in this EIS, to analyze alternatives or issues beyond the construction and operation of DARHT that relate to the nation's nuclear weapons policies, the DOE mission of stockpile stewardship and management, the need for hydrodynamic testing or dynamic testing that are part of the stockpile stewardship and management program, the mission of LANL, or continued operation of other facilities at LANL. To the extent that these matters are under the purview of DOE, they will be considered in the Programmatic EIS on Stockpile Stewardship and Management or the LANL Sitewide EIS, as discussed below in the section on related NEPA reviews.

Proposed Issues

The EIS will identify and analyze the direct, indirect and cumulative effects resulting from the completion and operation of DARHT. DOE has tentatively identified the following environmental and socioeconomic issues for consideration in the EIS and seeks public comment on the adequacy and inclusiveness of these issues:

- Natural ecosystems, including air quality, surface and groundwater quality, and plants and animals.
- Cultural resources, including archeological sites, historic resources, other facilities and infrastructure at LANL, and actual and potential uses of the site including Native American cultural, traditional and religious uses; DOE has previously identified Native American archeological sites in the vicinity of DARHT and has conducted mitigating activities.
- Economic impacts, including those from constructing, equipping and operating DARHT.
- Socioeconomic impacts, including any disproportionately high and adverse impacts on minority and low income populations.
- Health and safety impacts to on-site workers, other LANL personnel, local communities and tribes, and the general population of northern New Mexico.
- Other construction and operational impacts, such as transportation of people and materials.
- Waste management considerations, including the eventual decontamination and decommissioning of the facility after the end of its useful life (approximately 30 years).
- Health and safety, environmental, and other impacts related to the transport, storage and use of hazardous and radioactive materials and generation of X-ray radiation.
- Other relevant issues identified by DOE or the State, tribes, other agencies, or the public through this scoping process.

Related NEPA Reviews

The Department is currently preparing to undertake two related NEPA reviews. The planned LANL Sitewide EIS (59 FR 40889, August 10, 1994) will consider the cumulative impacts of operations and planned activities foreseen within the next 5 to 10 years. The planned Stockpile Stewardship and Management Programmatic EIS (59 FR 54175, October 28, 1994) will evaluate activities required to maintain a high level of confidence in the safety, reliability, and performance of nuclear weapons in the absence of nuclear testing, and to be prepared to test weapons if so directed by the President.

Classified Material

The Department will review classified material while preparing this EIS. Within the limits of classification, DOE will provide to the public as much information as possible. If DOE needs to generate classified material to explain the purpose and need, use, materials, or impacts from this project, that material will be segregated into a classified appendix.

Public Involvement Opportunities

DOE will develop a stakeholder involvement plan to guide the public review aspects of this EIS. To assist with developing the stakeholder involvement plan, DOE requests suggestions by the public on how this EIS process should be conducted, including suggestions regarding the type, format and conduct of public involvement opportunities.

Through this Notice, DOE formally invites the State, tribes, other government agencies and the public to comment on the scope of the EIS. DOE will offer informational briefings to tribal governments, local (county and municipal) governments, and the State of New Mexico.

A second formal opportunity for comment will be provided after DOE issues the draft EIS, expected in mid-1995. Public hearings will be held in conjunction with that comment period. DOE will inform the State, tribes, local governments, other agencies and the general public of its final decisions at the time the Record of Decision is issued, expected in October 1995.

In addition to formal opportunities for comment, any person may submit comments at any time during the NEPA review process; however, to ensure that comments are considered at specific points in the NEPA review, and to best assist DOE, the public is encouraged to comment during the formally established comment periods.

Copies of DARHT design and other background documents, written comments, records of public meetings, and other materials related to the development and analyses of the EIS have been and are being placed in the Los Alamos National Laboratory Community Reading Room, 1450 Central Avenue, Suite 101, Los Alamos, New Mexico 87544. For information on the availability of specific documents and hours of operation, please contact the reading room at (505)665–2127 or (800)543–2342.

Signed in Washington, D.C., this 18 day of November 1994, for the United States Department of Energy.

Tara O'Toole,

Assistant Secretary, Environment, Safety and Health.

[FR Doc. 94–28889 Filed 11–18–94; 11:46 am]

BILLING CODE 6450–01–P

Environmental Management Site Specific Advisory Board, Nevada Test Site

AGENCY: Department of Energy.

ACTION: Notice of open meeting.

DEPARTMENT OF ENERGY

Availability of the Dual Axis Radiographic Hydrodynamic Test Facility Draft Environmental Impact Statement

AGENCY: Department of Energy.

ACTION: Notice of availability and public hearings.

SUMMARY: The Department of Energy (DOE) announces the availability of the Dual Axis Radiographic Hydrodynamic Test (DARHT) Facility Draft Environmental Impact Statement (EIS), DOE/EIS–0228D, for public review and comment, and the dates, times and places for public hearings on the Draft EIS. The alternative actions analyzed in the Draft EIS would occur at the DOE's Los Alamos National Laboratory (LANL) in northern New Mexico.

DATES: Written comments on the Draft EIS are invited from the public. Comments must be postmarked by Monday, June 26, 1995, to ensure consideration; late comments will be considered to the extent practicable. The DOE will use the comments received to help prepare the final version of the DARHT EIS. Public hearings on the Draft EIS will be held as follows:

Wednesday, May 31, 1995, Los Alamos, New Mexico, 2:00pm–4:00pm and 6:30pm–9:00pm, Los Alamos Inn, 2201 Trinity Drive, Los Alamos, NM, (505) 662–7211.

Thursday, June 1, 1995, Santa Fe, New Mexico, 2:00pm–4:00pm and 6:30pm–9:00pm, High Mesa Inn, 3347 Cerrillos Road, Santa Fe, NM, (505) 473–2800.

The meetings will use a workshop format to facilitate dialogue among DOE, LANL, and the public and will provide opportunities for information exchange and discussion as well as submitting prepared statements.

ADDRESSES: Requests for copies of the Draft DARHT EIS, written comments on the Draft EIS, or other matters regarding this environmental review should be addressed to: Ms. Diana Webb, DARHT EIS Project Manager, Los Alamos Area Office, Department of Energy, 528 35th Street, Los Alamos, NM 87544. Ms. Webb may be contacted by telephone at (505) 665–6353 or by facsimile at (505) 665–1506.

FOR FURTHER INFORMATION CONTACT: For general information on the DARHT project, interested parties may contact Ms. Webb at the address and phone number above. For general information on the DOE NEPA process, please contact Ms. Carol M. Borgstrom, Director, Office of NEPA Policy and Assistance, EH–42, Department of Energy, 1000 Independence Ave., SW, Washington, DC 20585. Ms. Borgstrom may be contacted by leaving a message at (800) 472–2756 or by calling (202) 586–4600.

SUPPLEMENTARY INFORMATION: The Draft EIS was prepared pursuant to the National Environmental Policy Act of 1969 (NEPA) (42 U.S.C. 4321 *et seq.*, the Council on Environmental Quality NEPA regulations (40 CFR 1500) and the DOE NEPA regulations (10 CFR 1021).

The Department proposes to provide enhanced high-resolution radiography (x-ray) capability for the purpose of performing hydrodynamic tests and dynamic experiments in support of its national defense mission. The enhanced radiography facility would be a key component of the Department's near-term science-based stockpile stewardship and management program. These hydrodynamic tests and dynamic experiments are required to assist DOE in ensuring the continued safety, security, and reliability of existing nuclear weapons as they age.

The Draft DARHT EIS analyzes the environmental consequences of alternative ways to accomplish the proposed action. The DOE's preferred alternative would be to complete and operate the DARHT facility at LANL in northern New Mexico. Radiographic hydrodynamic testing is now conducted in two existing facilities within the DOE complex—a 30-year-old facility at LANL, and a 10-year-old facility at the DOE's Lawrence Livermore National Laboratory in California. The Draft DARHT EIS compares the environmental impacts that would be expected to occur from continuing to operate existing facilities (the No Action Alternative) with the consequences that would be expected to occur if DOE implemented the Preferred Alternative or one of four other operational alternatives. The Draft EIS has a classified supplement that provides additional information and analysis. DOE has distributed copies of the Draft DARHT EIS to appropriate Congressional members and committees, the State of New Mexico, American Indian tribal governments, local county governments, other federal agencies, and other interested parties. DOE expects to complete the Final EIS in August 1995, and reach a Record of Decision in September 1995.

Signed in Washington, D.C., this 17th day of May, 1995, for the United States Department of Energy.

Victor H. Reis,

Assistant Secretary for Defense Programs.

[FR Doc. 95–12628 Filed 5–23–95; 8:45 am]

BILLING CODE 6450–01–P

Availability of Information Related to the Dual Axis Radiographic Hydrodynamic Test Facility; Draft Environmental Impact Statement

AGENCY: Department of Energy.

ACTION: Notice of availability of information.

SUMMARY: On May 12, 1995, the Environmental Protection Agency (EPA) announced the availability of the Department of Energy's (DOE) Dual Axis Radiographic Hydrodynamic Test (DARHT) Facility draft Environmental Impact Statement (EIS), DOE/EIS–0228D, for public review and comment (60 FR 25717). The alternative actions analyzed in the draft EIS would occur principally at the DOE's Los Alamos National Laboratory (LANL) in northern New Mexico. By this notice, DOE is announcing the availability of additional information related to the draft DARHT EIS that has recently been placed in the Los Alamos National Laboratory Community Reading Room for public review.

ADDRESSES: Information discussed in the supplementary information section is available for public review at the Los Alamos National Laboratory Community Reading Room, 1450 Central Ave., Suite 101, Los Alamos, New Mexico 87544. For information on the availability of specific documents, availability of copies of documents and hours of operation, please contact the reading room at (505) 665–2127 or (800) 543–2342.

FOR FURTHER INFORMATION CONTACT: For general information on the DARHT EIS, or for copies of the draft EIS, interested parties may contact Ms. Diana Webb, DARHT EIS Project Manager, Los Alamos Area Office, Department of Energy, 528 35th Street, Los Alamos, NM 87544. Ms. Webb may be contacted by telephone at (505) 665–6353 or by facsimile at (505) 665–1506.

SUPPLEMENTARY INFORMATION: The draft EIS was prepared pursuant to the National Environmental Policy Act of 1969 (NEPA) (42 U.S.C. 4321 et seq.), the Council on Environmental Quality NEPA regulations (40 CFR parts 1500–1508) and the DOE NEPA regulations (10 CFR Part 1021).

The Department proposes to provide enhanced high-resolution radiography (x-ray) capability for the purpose of performing hydrodynamic tests and dynamic experiments in support of its national defense mission. The enhanced radiography facility would be a key component of the Department's near-term science-based stockpile stewardship and management program. These hydrodynamic tests and dynamic experiments are required to assist DOE in ensuring the continued safety, security, and reliability of existing nuclear weapons as they age.

The draft DARHT EIS analyzes the environmental consequences of alternative ways to accomplish the proposed action. The DOE's preferred alternative would be to complete and operate the DARHT facility at LANL in northern New Mexico. Public hearings are scheduled (Los Alamos, May 31, 1995 and Santa Fe, June 1, 1995) as previously announced in DOE's Notice of Availability dated May 24, 1995 (60 FR 27498). The comment period will extend through Monday, June 26, 1995. DOE expects to complete the final EIS in August 1995, and reach a Record of Decision in September 1995.

Following is a list of documents currently available for public review in the Los Alamos National Laboratory Community Reading Room:

1. Nuclear Weapons Stockpile Stewardship: the Role of Livermore and Los Alamos National Laboratories.
2. Congressional Budget Office Papers, The Bomb's Custodians.
3. An Alternative Budget for Lawrence Livermore National Laboratory and How to Get There—Los Alamos Study Group (LASG).
4. The Conversion of LANL to a Peacetime Mission—Concerned Citizens for Nuclear Safety (CCNS).
5. 1979 LANL Environmental Impact Statement.
6. Transcript from the September 14 SWEIS Public Meeting at the Los Alamos Civic Auditorium.
7. Environmental Impact Statement for Transuranium Solid Waste Development Facility, LASL, 4/73.
8. Implementation Plan Nuclear Weapons Complex Reconfiguration Programmatic Environmental Impact Statement.
9. Pantex Site-Wide EIS Scoping Plan.
10. Scoping Comments/Documents for the Nuclear Weapons Disposition PEIS, Oak Ridge Institute for Science & Education.
11. Fueling A Competitive Economy: US DOE Strategic Plan.
12. National Security Strategic Plan, Working Paper.
13. DOE Albuquerque Operations Office Strategic Plan.
14. September 13, 21, 22, 28, 29, SWEIS Public Meeting Transcripts.
15. Stormwater Pollution Prevention Plan for DARHT 10/25/94.
16. DARHT Hydrotest Project Cultural Resource Survey Report 10/25/94.
17. Hydrotest Firing Site Drawing List 10/25/94.
18. NESHAPS for DARHT Construction Project 10/25/94.
19. DARHT Amendment of Solicitation 10/25/94.
20. DARHT Construction Documents Vol 1–3, 10/25/94.
21. Action Description Memorandum DARHT Facility, TA–15.
22. Results of the Soil Sampling Survey Conducted Over Active RCRA Firing Site TA–15–184 (PHERMEX) 10/28/94.
23. Baseline Soil Uranium and Beryllium Concentrations Around The Proposed DARHT Facility at TA–15 10/28/94.
24. Construction Contract for DARHT.
25. Programmatic Cost Impact Due to Project Delay for EA 11/8/94.
26. Programmatic Cost Impact Due to Project Delay for EIS DARHT 11/8/94.
27. Total Regional Economic Impact Resulting from DARHT Cancellation 11/8/94.

28. DARHT Archaeological Site Protection 11/8/94.
29. Welcome to DARHT Day 11/28/94.
30. NEPA and Related Environmental Documentation History for DARHT.
31. 1979 Site-Wide EIS at LANL. Portions Addressing Dynamic Testing 1/5/94.
32. Soil/Sediment Studies Conducted at the DARHT and PHERMEX Firing Sites 1/5/95.
33. Implementation Plan for the Continued Operation of the Pantex Plant and Associated Storage of Nuclear Weapons Components EIS 1/12/95.
34. Initial Data Request for DARHT EIS 1/17/95.
35. DARHT Public Scoping Meeting Roundtable Discussion and Comments 12/7/95.
36. DARHT Scoping Comment Reference Documents 1/17/95.
37. Background Information on the Nuclear Weapons Stockpile Memorandum 1/31/95.
38. DARHT EIS Implementation Plan 2/14/95.
39. DARHT Feasibility Assessment Independent Consultants (DFAIC) Panel Final Report 9/9/2.
40. Hydrotest Program Assessment 10/92.
41. Report of Independent Consultants Reviewing Integrated Test Stands Performance and Readiness of DARHT Construction Start 8/93.
42. Letter to Jennifer Fowler-Propst—U.S. Fish and Wildlife Service—Att. Biological and Floodplain/Wetland Assessment for DARHT.
43. DOE NEWS—Draft Environmental Impact Statement Available for DARHT Facility at LANL 5/10/95.
44. DOE—Notice of Pre-Scoping Workshop for the Stockpile Stewardship and Management Programmatic Environmental Impact Statement 5/2/95.
45. The Stockpile Stewardship and Management Program—Maintaining Confidence in the Safety and Reliability of the Enduring U.S. Nuclear Weapon Stockpile.
46. Notice of Intent to Prepare a Site-Wide Environmental Impact Statement for the Los Alamos National Laboratory.
47. Statement of Hazel O'Leary, Secretary of Energy, Before the Committee on Armed Services, United States Senate April 4, 1995.
48. Federal Register Notices for the LANL DARHT and SWEIS 5/12/95.
49. Newspaper clippings.
50. Aerosolized U and Be from LASL Dynamic Experiments (1977).
51. DARHT Environmental Monitoring 1/30/95.
52. Stockpile Stewardship and Management Programmatic Environmental Impact Statement—Pre-Scoping Workshop (Viewgraphs) 5/19/95.
53. U.S. Department of Energy Environmental Justice Strategy Executive Order 12898—4/95.
54. DOE—Notice of Availability and Public Hearings.
55. Summary of Environmental Impacts from Classified Supplement, DARHT EIS—5/95.
56. DOD Nuclear Posture Review.
57. Letter exchange with LASG—4/95.
58. Letter from LASG—11/94.
59. Letter from LASG—12/94.
60. Letter to President Clinton from J. Stroud (LASG)—2/28/95.
61. Letter responding to J. Stroud (LASG) from V. Reis, Department of Energy—4/19/95.
62. Letter responding to Kathleen Sabo (LASG) from James Dorskind, White House—4/17/95.
63. Letter responding to Greg Mello (LASG) from D. Webb—3/20/95.
64. Letter responding to Greg Mello (LASG) from D. Webb with LLNL attachment—4/17/95.

Signed in Washington, DC, this 26th day of May, 1995, for the United States Department of Energy.

Everet H. Beckner,

Principal Deputy Assistant Secretary for Defense Programs.

[FR Doc. 95-13435 Filed 5-31-95; 8:45 am]

BILLING CODE 6450-01-P

Appendix B
PHERMEX Baseline

DARHT EIS

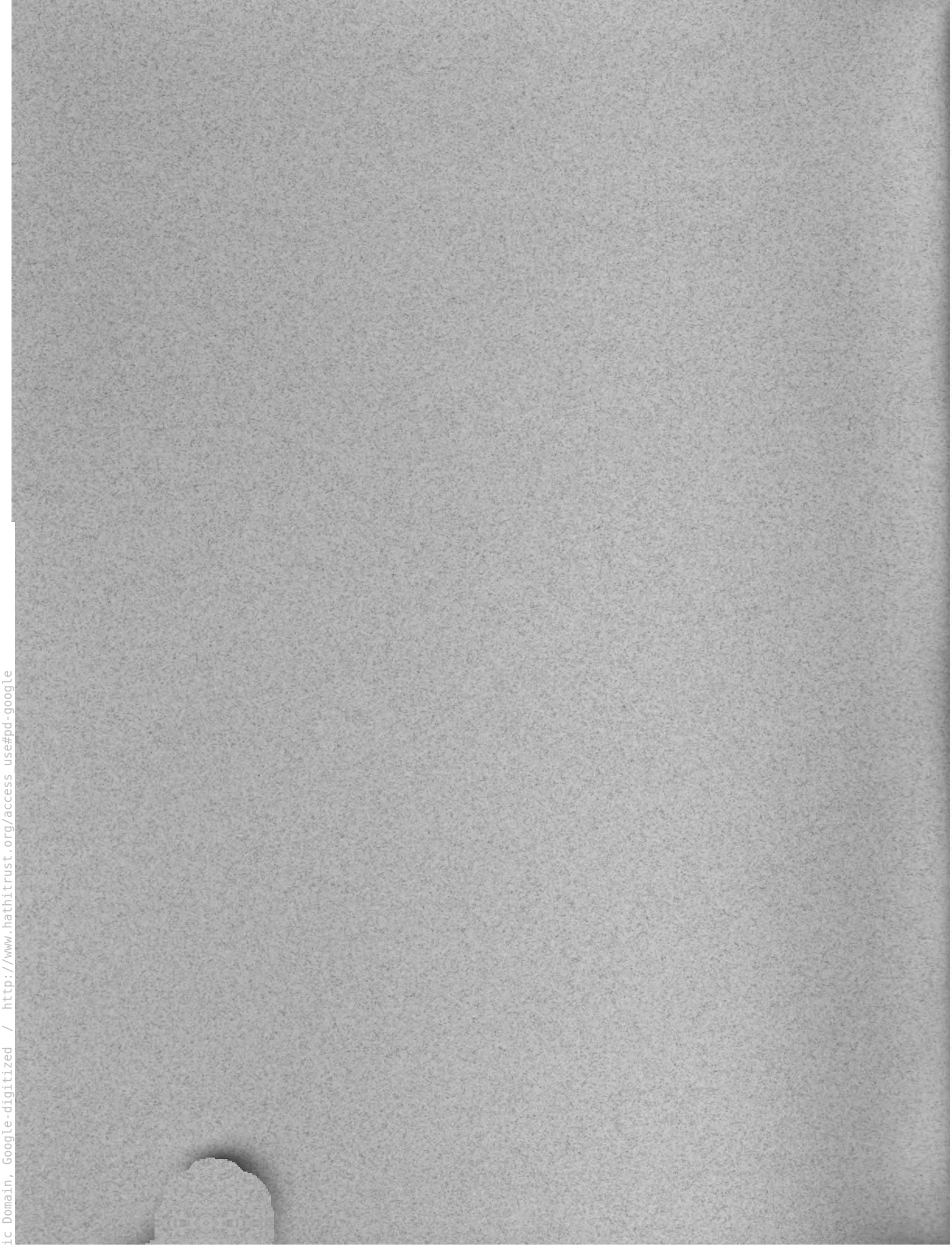

APPENDIX B
PHERMEX BASELINE

This section describes the current condition of the PHERMEX firing site and summarizes the materials used to conduct current operations and the materials that have been released to the immediate environment of the firing point. This baseline represents PHERMEX conditions before any decision is made on the hydrodynamic testing alternatives. This baseline information was compiled to develop reasonable testing activities which are analyzed under each alternative in this EIS in order to determine valid impacts and to establish a comparative analysis of alternatives with respect to current conditions. Historically, numbers of tests and quantities of various materials have varied by year, in accordance with program needs. Material usage over the past five years has been used in this EIS to establish the baseline for material usage. This baseline does not reflect projected future changes in the activities at PHERMEX under various alternatives. The current levels of migration of materials by air and water pathways are discussed, as well as the disposition of materials removed from the site during periodic cleanup activities. Waste streams resulting from the current operation are also discussed.

B.1 AIR QUALITY AND NOISE

This section describes the nonradioactive ambient air criteria pollutants emitted from PHERMEX operations as well as the noise impacts from PHERMEX experiments.

B.1.1 Air Quality

The ambient air criteria pollutants potentially released due to PHERMEX operations include nitrogen dioxide, PM_{10} (aerosolized material assumed to be respirable), beryllium, heavy metals (depleted uranium and lead), and lead (the concentration of pollutants is similar to those presented in section 5.1.2; see related discussion in section 4.2.4). Cleaning chemicals are not used on a scale large enough to produce measurable releases. Materials used are rags dampened with acetone, chlorinated hydrocarbons, toluene, xylene, or 1,1,1-trichloroethane.

Since the PHERMEX operations are classified as intermittent fugitive emission sources, no stations are established to directly monitor potential emissions from PHERMEX (see related discussion in section 4.2.5 and figure 4-6). A sitewide sampling network is available at LANL to provide air monitoring data for the site. The radiological dose from TA-15 operations has been estimated at 1 percent or less of the total LANL dose to the public.

Waste wood from the platforms used to support the experiments is taken to TA-36 for disposal in an open burn. An existing open burn permit from the NMED indicates approximately four to five burns per year are required to reduce the fire and safety hazards due to the accumulation of wood. Some of the wood waste may be contaminated with small quantities of high explosives and/or depleted uranium.

In support of the open burn permit application, the DOE Los Alamos Area Office submitted dose dispersion estimates. The nearest residential community, White Rock 1.8 mi (3 km) from the burn site,

was estimated to receive 1.1 x 10^{-8} rem using the HOTSPOT 6.5 modeling program and 2.9 x 10^{-8} rem using the DISPERSION modeling program (DOE 1993). The NMED Air Quality Bureau reviewed the dose estimates and concluded that the results indicate reasonable assurance of no health effects in White Rock from this source (NMED 1993).

B.1.2 Noise

Noise from a 150-lb (70-kg) test explosion, the largest in normal operation at PHERMEX, was measured March 11, 1995, at several locations in and around LANL (Burns 1995; Vigil 1995; Vibronics 1995). Peak overpressure in the air, reported in dB, is the important measurement for assessing the potential effects of an air wave but is not the same as a dBA noise measurement (see section 4.2.6). These peak overpressure measurements showed 138 dB at a distance of 2,150 ft (655 m) from the 150-lb (70-kg) shot, and 137 dB at the Nake'muu ruin site, a distance of 3,880 ft (1,180 m). If the largest explosive charge for PHERMEX, 1,000 lb (450 kg), were fired, the expected pulse would be about 6 dB higher than for the 150-lb (70-kg) explosion.

Two types of instrumentation were used for the noise measurements recorded during the tests conducted at PHERMEX on March 11, 1995. A sound level meter set up for a broad frequency range (about 20 to 12,000 Hz), slow time response, and frequency sensitivity corresponding to human hearing (A scale, ANSI-S1.4-1971) was used. The results are reported in decibels weighted for hearing response, dBA. The peak overpressure was measured in the air with a microphone sensitive to low frequencies (2 to 200 Hz) and having fast time response. These results are reported in decibels (dB) and are important for assessing potential effects of an air wave but are not the same as "noise" measurements.

Both types of instruments were used at only one location, on State Highway 4, which is the closest possible public approach to the firing point [1.3 mi (2 km) to the south]. The slow time response and frequency sensitivity corresponding to human hearing measured 71 dBA while the fast time response instrument measured 120 dB; the peak pulse energy was at about 20 Hz. These two values are comparable because the A-scale weighing at 20 Hz is about -50 dB (ANSI-S1.4-1971). Using the sound level meter, 60 dBA was measured near the entrance to Bandelier National Monument [closest permanent residences, 2.6 mi (4.3 km)], and about 70 dBA in White Rock [a nearby residential community, 4 mi (6.4 km)]. At these levels and distances, variations in local atmospheric conditions may account for the louder noise at the more distant site, but measurements under a range of known atmospheric conditions have not been made. These measured levels can be used to estimate a sound level of 61 to 68 dBA in southern Los Alamos, the closest residential area to PHERMEX at a distance of 3 mi (5 km).

B.2 SOILS

In 1993, LANL collected and analyzed over 20 surface soil samples and 2 sediment samples at the PHERMEX firing site (Fresquez 1994). These soil sampling surveys indicated that no lead, beryllium, or mercury were observed beyond 200 ft (60 m) of the firing point. The samples were analyzed for RCRA-regulated metals (silver, arsenic, barium, cadmium, chromium, lead, mercury, beryllium, selenium) using the Toxicity Characteristics Leaching Procedure (TCLP); total beryllium, gallium, lead, thorium, and uranium; semivolatile organic compounds (SVOCs); and high explosive residues. The sampling plan and the results for uranium, beryllium, and lead are described in appendix D. Most TCLP metals in surface

soil samples were detected below proposed U.S. Environmental Protection Agency (EPA) action levels; however, two soil samples contained lead above the EPA action level of 5 ppm. Among the other metals analyzed, most beryllium values were above the EPA action level (see appendix D). No sediment samples from drainage channels leading away from the PHERMEX site contained TCLP metals above EPA action levels or other metals above their background level. The PHERMEX area soils contained traces of 21 SVOCs, but no detectable high explosive residues.

B.3 HUMAN HEALTH

The average dose received for 92 workers who were assigned dosimetry badges in 1993 and who worked regularly or occasionally at PHERMEX was 0.003 rem/person. LANL has established an administrative dose limit of 2 rem/year, which is below the DOE limit of 5 rem/year.

The PHERMEX facility operated an internal dosimetry program for three years beginning in 1992. No dose equivalent greater than 0.003 rem was detected, and over 50 percent of the participants registered doses at or below natural background levels. It was concluded that no radiological hazard exists for PHERMEX and the program was discontinued except for suspected exposures. Chemical toxicity has also been evaluated, and calculated fractions of nephrotoxic limits have not approached any levels of concern (Kottmann 1994).

B.4 ACCIDENTS

Operations at PHERMEX pose accident hazards expected at industrial sites. In addition, there are unique hazards associated with high explosives, high voltages, high densities for energy stored in capacitor banks, intense x-rays, and test materials. Hazards that have the potential to lead to accidents at a hydrodynamic test facility are summarized in table B-1.

The accident hazards in table B-1 are addressed by physical barriers, interlock systems, and administrative controls. The accidents with the most serious potential consequences (i.e., radiation exposure, high explosive detonation, and electrical discharges) were analyzed for likelihood of occurrence. An annual probability of less than 10^{-4} was estimated for each of these accidents, with no likely common-mode accidents identified. Probabilities for the other hypothetical accidents are based on commercial industry experience. All these accident probabilities are shown in table B-2.

During the most recent 10-year period (1985 to 1994), the accident statistics for PHERMEX indicate that there were a total of 19 lost-work days due to injury. None of these injuries were considered serious; they consisted of a contusion, a concussion, and numerous back strains. The most recent incident that resulted in lost time occurred in 1991 when an employee who suffered a strain injury as a result of a lifting activity lost three workdays. There have been no reported accidents that were initiated by the detonation of explosives.

TABLE B-1.—*Hazards at Hydrodynamic Test Facilities*

Hazard	Location	Comments
Ionizing Radiation Exposure		
Personnel inside exclusion areas during beam pulsing	Accelerator bay, optical room, and firing pad	Beam pulse with up to 2,000 rad x-rays at one meter on axis
Nonionizing Radiation		
Operating personnel intersect laser beam	Laser room	
Electrical		
Personnel in contact with the power supplies or capacitor banks	Accelerator room and power supply rooms	Power supplies with voltages up to 4MV, high energy-densities in capacitor banks
Personnel in contact with laser power supplies	Accelerator bay and laser rooms	Power supplies with voltages up to 35 kV
High Explosives Blast		
Personnel in the hazard radius exclusion area during testing	Firing site exclusion area	Area radius is 2,500 ft (750 m), personnel OK in R-184 and R-310
Accidental detonation of explosive	Firing pad	
Mechanical		
Crane maintenance and operation	Accelerator bay, power supply rooms, equipment and assembly rooms	Potential for misuse
Occupational		
Slippery surfaces due to fluids	Accelerator bay, power supply rooms, equipment room	Leaks or spills from tanks, valves, or connections
Gases		
Helium	Firing pad, diagnostics area	Used to drive high-speed cameras
Sulfur hexafluoride	Accelerator hall, power supply room	Leaks from spark gaps
Chemicals/Solvents		
Acetone, ethanol	Accelerator bay and assembly room	Inhalation hazards
Fire		
Insulating oil	Accelerator bay and power supply rooms	EXXON 1830 type insulating oil has a flash point above 149°C (330°F)
Wicking of insulating oil	Power supply rooms	Oil-soaked rags
Acetone, ethanol	Accelerator bay and assembly room	Volatile cleaning solvents
Electrical control cables, high-voltage cables, and components	Accelerator bay, power supply rooms, equipment room	Faulty items may cause sparks to ignite oil, etc.
Fire from parked vehicles	Parking and delivery area	Gasoline in fuel tanks
Natural gas	Equipment room	Hot water boiler
Trash and rag accumulation	Accelerator bay, power supply rooms, equipment room	Ignition source for oil
Forest or brush fire	External to building	May arise from explosives or natural causes
Natural Phenomena		
High winds	TA-15	Damage to utilities
Lightning	TA-15	Damage to utilities
Earthquake	TA-15	Damage to any of LANL infrastructure, design level is 0.22 G for DARHT, current expectation is 0.5 to 0.6 G for maximum earthquake.

TABLE B-2.—*Hypothetical Accidents and Probabilities*

Accident	Levels[a]	Probability
Unplanned exposure to radiation	III–IV	$< 10^{-4}$
Laser hazards	III	$< 10^{-4}$
Electrical energy hazards	III–IV	$< 10^{-4}$
Blast hazards	II	$< 10^{-4}$
Accidental detonation	II	$< 10^{-4}$
Mechanical hazards	IV	$< 10^{-2}$
Occupational hazards	IV	$< 10^{-2}$
Confined space	IV	$< 10^{-4}$
Pressurized containers and distribution systems	IV	$< 10^{-4}$
Toxic gases and vapors	IV	$< 10^{-4}$
Chemicals/solvents	IV	$< 10^{-2}$
Fire hazards	IV	$< 10^{-4}$
Natural phenomena	IV	$< 10^{-4}$

[a] System failure level categories are as follows:

II – Critical: May cause severe injury, severe occupational illness, major damage to a facility operation, or major environmental damage.
III – Marginal: May cause minor injury, minor occupational illness, or minor environmental damages.
IV – Negligible: Will not result in a significant injury or occupational illness, or have a significant environmental effect.

B.4.1 Radiation Exposure

The safety system associated with radiation protection provides controls and barriers to prevent radiation exposure. This system consists of positive interlocks, alarms, warning lights, television monitors, and personnel accountability sweeps of the area prior to testing. These functions can be monitored from the control room. Extensive operator training, personnel radiation dosimetry, and use of thermoluminescent dosimeter (TLD) surveys for facility radiation monitoring are integral parts of facility operations to monitor exposures and prevent accidental overexposure. The following two accident scenarios have been analyzed to provide the unplanned exposure to radiation probability in table B-2:

- The walk-through clearance plan fails to detect personnel in the exclusion areas
- The interlock safety system fails, and the accelerator is pulsed while personnel are in the accelerator hall

B.4.2 Electrical Discharge

Controls and barriers associated with electrical energy hazards are designed into the PHERMEX facility. Physical barriers, such as cabinets around power supplies and capacitor banks and the injector power supplies, along with an interlocked high-voltage safety system, prevent entry during pulsing or

hydrodynamic testing. Only experienced, trained personnel are allowed to perform the operations at the firing point. Potential accident scenarios include personnel contact with power supplies, charged capacitor banks, or laser power supplies.

B.4.3 Explosives

The most serious hazard to operation personnel is from firing high explosives during a hydrodynamic test. The buildings and structures at the firing site are designed to withstand repetitive explosions, but only R-184 and R-310 may be occupied during a test. Safety interlocks prevent firing the high explosives if personnel exit these buildings during the firing sequence. Hazards involved with handling explosives are well recognized and are based on long experience. The hazard radius around the firing site varies from test to test depending on the size of the shot. Two main accident scenarios have been analyzed to provide the blast hazards and accidental detonation probabilities in table B-2.

- By error, some personnel are within the hazard radius during a test.
- Predetonation of the explosives occurs during test setup.

Occupational injuries at PHERMEX have primarily dealt with injuries such as strains, lacerations, and contusions that have resulted from the movement of equipment and materials associated with the experiments.

B.5 MITIGATION AND MONITORING

B.5.1 Mitigation

The PHERMEX facility employs mitigation systems and administrative controls in a defense-in-depth approach to facility safety. Physical barriers consisting of passive shielding for radiation control and blast protection form the first level of barrier to prevent injury to personnel. Active barriers are in place, consisting of locked and interlocked gates and roadblocks or passageway closures to prevent entry to radiation areas or explosives areas. Audible and visual warning systems are in place which are activated whenever the imminent exposure to radiation or explosive blast is possible. Red stop or scram buttons are placed near visual alarms to allow any personnel inadvertently left in the area to abort the test or hazardous condition. In-place administrative procedures control the transportation and movement of explosives and hazardous materials and limit the number of personnel who might be exposed to a given hazard. Trucks and cranes may be operated only by personnel who are trained and experienced in the operation being conducted.

Access is controlled to ensure that no personnel are within the hazard area for each shot. Clearance personnel maintain radio contact with each other, and the access control office visually checks the hazard area from the firing point to the clearance radius before each test and then establishes road blocks to prevent inadvertent entry to the area until the test has completed. Small fires after a test are not unusual, and the fire suppression personnel are available at the boundary to the hazard area for each explosive shot. Fire suppression personnel, trained for the hazards to be expected when fighting fires immediately following explosives tests, are allowed access to the firing point immediately after the all-clear is sounded to extinguish any resulting fires.

B.5.2 Monitoring

Monitoring consists of radiological area monitors and visual television monitoring of critical areas. The accelerator hall and firing point are monitored annually for radioactivity. TLDs are placed at potential exposure areas in and around the facility and are read annually to monitor cumulative doses. Except for the expected high dose observed at the firing point and on the axis of the PHERMEX beam, all recorded doses are in the mrem/year range.

Environmental Surveillance at Los Alamos during 1992 describes LANL's surveillance and monitoring program (LANL 1994). LANL routinely monitors radioactive and nonradioactive pollutants in environmental media (air, water, soil) on the LANL site and in the surrounding region.

Three air-monitoring networks are operated or accessed by LANL. Nonradiological ambient air monitors are used to measure criteria pollutants, beryllium, acid precipitation, and visibility. A network of continuously operating sampling stations measures ambient airborne radioactivity. Thermoluminescent dosimeters are used to monitor doses of external penetrating radiation. LANL's air-monitoring program is discussed in detail in section 4.2.5.

Surface waters and ground water are monitored to detect any contaminants from LANL operations. Water monitoring is discussed in detail in section 4.4.3.

B.6 MATERIALS USED

The materials used at the PHERMEX site include water, industrial chemicals, and materials comprising the test assemblies. Water at the PHERMEX site is not separately metered, but is supplied through an 8-in (20-cm) line from a 250,000-gal (946,000-L) tank located near TA-15. Water is used in a cooling tower, and deionized water is used in a closed cycle for magnet cooling. Sulfur hexafluoride is used as an insulating material. The major uses of industrial chemicals on an annual basis for the No Action Alternative are:

- Helium – 6,000 ft^3 (170 m^3)
- Sulfur hexafluoride – 3,100 ft^3 (90 m^3)
- Acetone – 3 gal (11 L)
- Ethanol – 6 gal (23 L)

The tests themselves contain materials that are released to the environment during uncontained tests. Table B-3 shows the number of separate tests conducted at both PHERMEX and FXR during CY 1990 to 1994. The tables include all tests at the facility, not only those using the accelerator radiographic diagnostics. A large range of complexity exists among high-explosives tests, and simply counting the number of tests serves only as a broad summary of the testing efforts at each facility. Table B-4 shows the corresponding materials released as a result of these tests, prior to regular firing-point cleanups.

For this EIS, DOE averaged the amount of material used at PHERMEX over the past five years to estimate the expected amounts of material that will be used in the future. However, operations at PHERMEX during the last five years underrepresent the facility's use of depleted uranium. For this

TABLE B-3.—*Number and Type of Tests at PHERMEX (P) and FXR (F) for CY 1990 to CY 1994*

Area of Research	CY90		CY91		CY92		CY93		CY94	
	P	F	P	F	P	F	P	F	P	F
Weapon Development	2	3	2	13	6	5	0	0	0	0
Stockpile Support	9	12	8	48	5	23	6	14	4	8
Predictive Capability	10	—[a]	12	—[a]	8	—[a]	26	—[a]	11	—[a]
Proliferation Assessment and Disablement	0	4	0	4	1	3	1	1	5	11
Conventional Munitions	70	5	0	22	0	22	7	18	3	3
Measurement Technique Development	0	0	0	0	10	0	5	0	15	0
Other Applications	6	5	3	10	1	20	0	0	0	0
TOTALS	97	30	25	97	31	73	45	33	38	22

[a] Due to record-keeping differences, the FXR totals under Stockpile Support include both Stockpile Support and Predictive Capability.

Definition of research areas:

1. **Weapon Development** – This type of testing supported engineering development of new weapon systems.
2. **Stockpile Support** – This type of testing was directed to stockpile surveillance, benchmarking against the underground nuclear test database, stockpile life extension, and nuclear safety. Experiments included large, full-scale mock-ups of weapons systems to observe integrated operation and smaller-scale mock-ups of weapons systems to observe integrated operation and smaller-scale experiments dedicated to observing selected phenomena isolated as much as possible from other effects. Each large-scale test was accompanied by a smaller test used to calibrate experimental timing and recording instruments and this smaller test is also counted in this category.
3. **Predictive Capability** – This type of testing included smaller-scale experiments to validate or develop parts of computer simulations and to gather data for computer models of equations-of-state, turbulence, high-explosive detonation, etc. This type of testing was also meant to explore new or poorly understood phenomena. Large tests were done of weapons geometries to benchmark three-dimensional or other advanced computer simulation tools that integrated several complex models.
4. **Proliferation Assessment and Disablement** – Tests done to evaluate actual or potential foreign, proliferant, or terrorist nuclear devices. This included tests to develop and evaluate disablement technologies.
5. **Conventional Munitions** – Tests done to develop and evaluate non-nuclear, conventional munitions, usually for the Department of Defense.
6. **Measurement Technique Development** – Tests done to develop and evaluate new diagnostics and techniques for radiographic hydrodynamics and other high-explosives experiments.
7. **Other Applications** – Experiments not covered by the other categories.

estimate, DOE looked at use over the past 30 years. For example, the average annual release of depleted uranium during the mid-1980s was approximately 450 lb (200 kg) per year. Earlier use expended even greater amounts of material. Based on the known use of depleted uranium during the period from 1963 until 1994, DOE estimates that the expected use of depleted uranium would be higher than the average of the past five years, as shown in table B-4.

For this EIS, DOE estimates that the average annual releases over the past 32 years to the environment as a result of high-explosives testing, prior to regular firing-point cleanups, were:

- Depleted uranium – 1,100 lb (500 kg)
- Beryllium – 15 lb (7 kg)
- Lead – 22 lb (10 kg)

TABLE B-4.—*Materials Released to the Environment Before Regular Firing-site Cleanup at PHERMEX and FXR for CY 1990 to CY 1994*

Year	DU (kg)	Be (kg)	Pb (kg)	Cu (kg)	Other Metals	HE (kg)	Tritium (Ci)	LiH (kg)	Fluoride Salts (kg)
PHERMEX									
CY94	66	4	12	7	77	148	0[b]	9	—[a]
CY93	251	4	20	75	91	269	0[b]	12	—[a]
CY92	244	2	48	0[b]	29	146	0.8	17	—[a]
CY91	245	2	0[b]	0[b]	156	340	0[b]	21	—[a]
CY90	71	—[a]	0[b]	11	75	301	0[b]	—[a]	—[a]
FXR									
CY94	204	4	0	14	4	371	0	5	0
CY93	186	2	0	20	3	413	0	9	0
CY92	154	10	10	22	19	1,744	0	13	0
CY91	214	6	0	41	14	1,466	0	14	0
CY90	315	16	0	19	15	411	0	15	9

[a] None reported.
[b] The material was reported as 0.

Notes: "DU," short for depleted uranium, refers to uranium in which the isotope uranium-235 has been depleted below the content of 0.7 percent found in naturally occurring uranium. The majority isotope in the material is uranium-238.

When referring to PHERMEX, "other metals" means the sum of all aluminum, boron, brass, iron, inconel, niobium, nickel, silver, tin, tantalum, titanium, tungsten, and vanadium used during each year. For FXR, "other metals" includes those metals listed above, plus barium, chromium, cobalt, and molybdenum.

Standardized symbols are used for the following materials: beryllium (Be), lead (Pb), copper (Cu), high explosives (HE), and lithium hydride (LiH).

- Copper – 155 lb (70 kg)
- Other metals – 310 lb (140 kg): consists of 50 percent aluminum, 35 percent stainless steel, and 15 percent other metals and alloys, including tantalum, brass, nickel, silver, tin, and very small quantities of others.
- Tritium – 2 Ci
- Lithium hydride – 155 lb (70 kg)
- High explosives – 2,400 lb (1,100 kg)

The alternatives analyzed in this EIS predict an increase in hydrodynamic testing and dynamic experiments. This predicted increase incorporates conservative estimates for the purpose of analyzing impacts in this EIS. It reflects the increased use of radiographic hydrodynamic testing and dynamic experiments over the next few years for reasons such as: the cessation of underground nuclear testing and the pursuit of a Comprehensive Test Ban treaty, the need for stewardship of the nuclear weapons stockpile, benchmarking computer simulations of the stockpile that will be compared to the past data obtained from underground nuclear tests, increases in proliferation assessment and disablement, and the need for tests to improve nuclear weapons safety, security, and reliability.

B.7 WASTE MANAGEMENT

During more than 30 years of PHERMEX operations, a total of about 35,000 lb (16,000 kg) of depleted uranium has been used. This amount of depleted uranium represents a total volume of about 35 ft^3 (1 m^3). LANL has estimated that at least 70 percent of the depleted uranium remained on or near the firing point after test assembly detonations and has been removed during routine operational cleanup of the firing site. The depleted uranium and other firing-site debris are handled as low-level radioactive waste. Approximately 10 to 12 truck loads, each having an average weight of 7 tons (6,400 kg) are sent to TA-54 Area G for disposal each year, totaling about 160,000 lb (70,000 kg). This material consists mainly of firing-site soil, wood, metal, glass, plastic, rubber, and cabling used to set up a test assembly detonation. The average quantity of depleted uranium in this waste would be about 770 lb (350 kg), less than 1 percent of the total waste mass.

Lead has been a constituent of a small number of test assemblies fired at the site; however, when lead is present in a test assembly, the site is cleaned both before and after the test so that the site is cleared of lead before the next test. The firing-site debris (including soil on and around the firing site) is characterized periodically for the presence of RCRA-controlled metals. The negative findings of these characterizations have always resulted in the firing-site debris being classified as low-level radioactive waste (not mixed waste). Other lead is used for shielding (rather than as part of a test assembly) which may become contaminated with radioactive material and is kept onsite for reuse. Approximately 10 percent, less than one 55-gal drum or 220 lb (100 kg) per year, of the lead shielding that is potentially radioactively contaminated is considered unusable, becomes waste, and is transferred to the established LANL mixed-waste program.

As shown in table 3-1, plastics, glues, foams, binders, and other organic materials are used in constructing test assemblies. However, only small quantities, less than a few pounds total for each assembly, are used, and these are mostly destroyed when the assembly is detonated. What little remains would be part of the shot-point debris described above.

A small amount of industrial chemicals and solvents are routinely used to support normal operations at PHERMEX. The major industrial chemicals used on an annual basis are solvents: 3 gal (11 L) of acetone and 6 gal (23 L) of ethanol. Other solvents, which are used on rags for cleaning and are used in very small quantities, are chlorinated fluorocarbons, toluene, 1,1,1-trichloroethane, and xylene. The cleaning rags are collected and disposed as solid potentially hazardous waste following laboratory guidelines. Historically, no more than 220 lb (100 kg) of solid hazardous waste and 1,800 lb (800 kg) of liquid hazardous waste have been disposed for every 1,000 lb (450 kg) of depleted uranium used at PHERMEX firing site.

Nonhazardous solid waste from the building is sent to the county landfill. Approximately one dumpster of nonhazardous solid waste is generated per week.

Wastes generated under current operations and under the proposed alternatives would be subject to treatment, storage, and disposal in other LANL Technical Areas. Transportation of these wastes is conducted using DOE- or DOT-approved containers carried on government vehicles using public roads between LANL facilities, as needed.

The PHERMEX facility has sanitary and storm water management systems. The sanitary system employs a septic tank and leach field. The storm system directs rainwater away from buildings. The sanitary system is registered with Los Alamos County and the storm system has an EPA authorization to discharge. Cooling tower blowdown consisting of a few gallons per year is discharged into the sanitary system.

When containment was used for a test shot, the containment vessel was taken to another LANL facility for cleaning and refurbishing. The blast debris removed was taken to appropriate LANL facilities for processing and disposition.

B.8 DISTRIBUTION OF MATERIAL RELEASED TO THE ENVIRONMENT

For the purposes of this EIS, DOE has estimated the distribution of test assembly material released to the environment to support evaluation of potential impacts for the proposed alternatives. Approximately 50 percent of the depleted uranium in test assemblies at the PHERMEX site is contained in simulated secondaries and blast pipes of pin experiments. During detonation this fraction of the depleted uranium is ejected as relatively large fragments (see figure B-1) that remain in the immediate vicinity of the firing point and are collected during routine cleanup operations. Another approximately 40 percent of the total depleted uranium may be dispersed as relatively small, platelet-shaped fragments having surface areas ranging from 0.08 to 1.1 in^2 (0.5 to 7 cm^2). About half of this material remains in the immediate vicinity of the firing point and is also collected during routine cleanup. Therefore, about 70 percent of the total depleted uranium used on the firing site is collected during cleanup operations. The remaining depleted uranium (about 10 percent of the total) may be released as an aerosol, all of which was considered respirable for the EIS analyses. Respirable particles are those with an activity median aerodynamic diameter (AMAD) of 3.94×10^{-4} inches (10 μ) or less.
The other half of the small depleted uranium fragments (20 percent of the total depleted uranium) dispersed as a result of detonation typically falls within a 4,100-ft (1,250-m) circle. Larger particles of the aerosolized fraction may also fall out from the plume of released material and be deposited near the firing point. These two fractions constitute the majority of depleted uranium contamination that has been detected in the soil (McClure 1995).

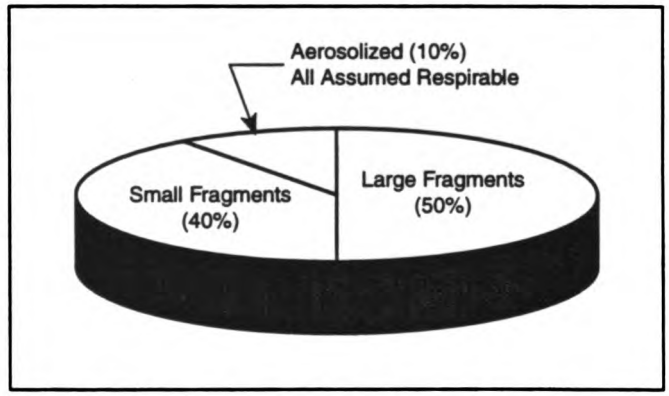

FIGURE B-1.—*Depleted Uranium Debris from a Typical Test.*

The release and aerosolization fractions described above are also used to estimate the dispersion of other constituents in test assemblies detonated on the PHERMEX firing site. Thus, the other metals (beryllium, lead, copper, and "other metals" in table B-4) are presumed to distribute in ways similar to depleted uranium. Lithium hydride converts to the hydroxide and is not an environmental problem. The high explosives convert to water, NO_2, and CO_2; any residues are extremely minor.

B.9 TRANSPORTATION

Test assemblies that include high explosives are shipped using DOE and LANL trucks, containers, and tie-down techniques from the assembly area at TA-16 to the PHERMEX site. This is a total distance of about 3.5 miles under a speed limit of 35 miles per hour. This shipment is conducted on LANL secure roads and is not conducted on public roads. Transportation requirements consist of one trip for each assembly and up to three trips for shipment of support materials. Support shipments might include high explosives or surrogate materials, but not both simultaneously. Shipments of radioactive surrogate materials exhibit no external radiation exposure characteristics either because of the nature or the characterization of the shipping container.

B.10 REFERENCES CITED IN APPENDIX B

Burns, M.J., 1995, *White Rock Noise Measurements During PHERMEX Tests*, 11 March 1995, LANL Memorandum No. DC-DO: DARHT-95-31, March 13, Los Alamos National Laboratory, Los Alamos, New Mexico.

DOE (U.S. Department of Energy), 1993, *1992 LANL Dose* [Annual Air Emissions Report for the calendar year 1992], June, Los Alamos, New Mexico.

Fresquez, P., 1994, *Results of the Soil Sampling Survey Conducted Over Active RCRA Firing Site TA-15-184 (PHERMEX)*, LANL Memorandum No. ESH-8/EFM-94-111, May 26, Los Alamos National Laboratory, Los Alamos, New Mexico.

Kottman, J.H., 1994, *Discontinuance of Uranium Bioassay Program*, LANL Memorandum No. DX-11:94-287, June 22, Los Alamos National Laboratory, Los Alamos, New Mexico.

LANL (Los Alamos National Laboratory), 1994, *Environmental Surveillance at Los Alamos During 1992*, LA-12764-ENV, UC-902, July, Los Alamos, New Mexico.

McClure, D.A., 1995, *DARHT EIS Section 3.1.3.2 Effluents (Mass Balance)*, Internal memorandum to S.T. Alexander March 21, Los Alamos National Laboratory, Los Alamos, New Mexico.

NMED (New Mexico Environment Department), 1993, Letter from L. Gay (NMED) to S. Fong (Department of Energy, Los Alamos Area Office), May 27, New Mexico Environment Department, Santa Fe, New Mexico.

Vibronics, Inc., 1995, *Acoustic and Seismic Testing at the PHERMEX Facility, Conducted for : Environmental Impact Statement for DARHT Facility, Los Alamos National Laboratory, March 10, 1995 - March 11, 1995*, Vibronics, Inc., Evansville, Indiana.

Vigil, E.A., 1995, *Noise Measurement at State Road 4 and Bandelier Turn Off at State Road 4 During PHERMEX Test on March 11, 1995*, LANL Memorandum No. ESH-5:95-11825, March 17, Los Alamos National Laboratory, Los Alamos, New Mexico.

Appendix C
Air Quality and Noise

DARHT EIS

APPENDIX C
AIR QUALITY AND NOISE

This appendix presents the methods used for analyzing potential impacts to air quality and potential noise impacts. Appendix C1, Air Quality, addresses routine emission of nonradiological air pollutants from the DARHT and PHERMEX sites from construction activities and normal operations. Pollutants addressed in this appendix include nitrogen dioxide (NO_2), sulfur dioxide (SO_2), respirable particulate matter (PM_{10}), heavy metals, beryllium, and lead. Appendix C2, Noise, provides methods and information on potential noise impacts from explosive detonation activities, construction, and traffic that would be associated with the DARHT or PHERMEX facilities.

APPENDIX C1: AIR QUALITY

Emission of nonradiological air pollutants into the atmosphere is regulated by Federal and State ambient air quality standards. Nonradioactive air pollutants at LANL are summarized in chapter 4. Estimates of the air quality impacts that would result from the emission of nitrogen dioxide (NO_2), sulfur dioxide (SO_2), and particulate matter with a 10-μ or less aerodynamic diameter (PM_{10}) were presented in chapter 5. Other criteria pollutants are carbon monoxide (CO) and ozone (O_3), but these pollutants are not emitted in any significant quantities by the operation of the facilities. Modeling tools and assumptions used to estimate impacts on air quality are presented in this appendix. In formulating inputs for air quality modeling, a series of conservative assumptions was made (i.e., assumptions which tended to maximize air quality impacts).

C1.1 MODELS

The Industrial Source Complex (ISC2) computer code was used to estimate the annual air quality impacts, as well as some of the short-term air quality impacts of criteria pollutants. The ISC2 model consists of the ISC2 short-term model (ISCST2) and the ISC2 long-term model (ISCLT2). The two models use steady-state Gaussian plume algorithms to estimate pollutant concentrations from a wide variety of sources associated with industrial complexes (EPA 1992a). The models are appropriate for flat or rolling terrain, modeling domains with a radius of less than 31 mi (50 km), and urban or rural environments. The ISC2 models are approved by the EPA for specific regulatory applications and designed for use on personal computers. Input requirements for the ISC2 model include a variety of information that defines the source configuration and pollutant emission parameters. The user may define point, line, area, or volume sources. The ISCST2 model uses hourly meteorological data to compute straight-line plume transport and diffusion, while the ISCLT2 model uses a joint frequency distribution of wind direction, wind speed, and atmospheric stability data to compute the transport and diffusion. Plume rise, stack tip downwash, and building wake can be computed and deposition taken into account. The ISC2 models compute a variety of short- and long-term averaged products (concentrations and depositions) at user-specified receptor locations. Tables C1-1 and C1-2 present input parameters for the short-term and long-term models, respectively.

TABLE C1-1.—*Input Parameters for Modeling Short-term Releases of NO_2 Emissions from Natural Gas Boiler, ISCST2 Model*

Parameter	Value
Pollutant Type	NO_2
Averaging Time	24 h
X-coordinate of Source on Grid	0.0
Y-coordinate of Source on Grid	0.0
Release Height of Source	0.0 m
Emission Rate of Source	4.53×10^{-3} g/s
Exit Temperature of Source	373 K
Exit Velocity of Source	0.0 m/s
Exit Diameter of Source	0.0 m
Origin of Receptor Rings: x-coordinate y-coordinate	 0.0 0.0
Radii of Polar Rings (m)	100. 200. 400. 800. 1000. 1200. 1500. 1800. 2000. 2500. 2700. 3000. 4000. 4400. 5000. 5500. 6000. 7000.
Number of Receptors per Ring	16
Height of Receptors	0.0 m
Starting Angle at each Ring	0.0 deg
Angle between Receptors on Ring	22.5 deg
Meteorological Input File	TA61994.MET
Anemometer Height	10 m

To calculate some of the short-term (24-h or less) criteria pollutant impacts, the SCREEN2 model was used. SCREEN2 is a screening model used to estimate short-term air pollutant concentrations, including estimates of maximum ground-level concentrations from a single source (EPA 1992b). The model uses a steady-state Gaussian plume algorithm to calculate the concentration from a single point, area, or simple volume source. The model can be applied to both simple and complex terrain for modeling domains out to 62 mi (100 km). Input requirements for SCREEN2 include information about the source configuration and pollutant emission parameters. Plume rise, building wake downwash, fumigation, and plume impaction on complex terrain can be computed. While specific meteorological values of wind speed and stability can be input to calculate pollutant transport and diffusion, the model can also calculate a worst-case maximum concentration, in which the model examines a range of stability classes and wind speeds to identify the "worst-case" meteorological conditions. Output of the SCREEN2 model is 1-h maximum concentration at specified distances. Adjustment factors can be applied to estimate concentrations for longer averaging periods (i.e., up to 24 h). The SCREEN2 model is approved by the EPA for specific screening procedures and is designed to run on personal computers.

TABLE C1-2.—*Input Parameters for Modeling Long-term NO_2 Emissions from Natural Gas Boiler, ISCLT2 Model*

Parameter	Value
Pollutant Type	NO_2
Averaging Time	24 h
X-coordinate of Source on Grid	0.0
Y-coordinate of Source on Grid	0.0
Release Height of Source	0.0 m
Emission Rate of Source	4.53×10^{-3} g/s
Exit Temperature of Source	373 K
Exit Velocity of Source	0.0 m/s
Exit Diameter of Source	0.0 m
Origin of Receptor Rings:	
x-coordinate	0.0
y-coordinate	0.0
Radii of Polar Rings (m)	100. 200. 400. 800. 1000. 1200. 1500. 1800. 2000. 2500. 2700. 3000. 4000. 4400. 5000. 5500. 6000. 7000.
Number of Receptors per Ring	16
Height of Receptors	0.0 m
Starting Angle at each Ring	0.0 deg
Angle between Receptors on Ring	22.5 deg
Meteorological Input File	LANLTA6.JFD
Anemometer Height	10 m
Average Wind Speed for Six Wind Speed Categories (m/s)	1.23 2.40 4.08 6.46 9.30 13.28
Average Temperature for Six Stability Classes	282 K
Averaging Mixing Height for:	
Stability A	2600.0 m
Stability B	2170.0 m
Stability C	1740.0 m
Stability D	1310.0 m
Stability E	880.0 m
Stability F	450.0 m

C1.2 RECEPTORS

Maximum ground-level pollutant concentrations for regulatory-significant time periods are reported at the maximally impacted receptor location. To capture this impact, ISC2 model runs have at least one receptor

location in each of the 16 transport directions (north, north-northeast, etc.) used by the model. Receptors are positioned at points of public access along publicly accessible roads within the boundaries of LANL, along the LANL fenceline, and in existing residential areas (figure C1-1).

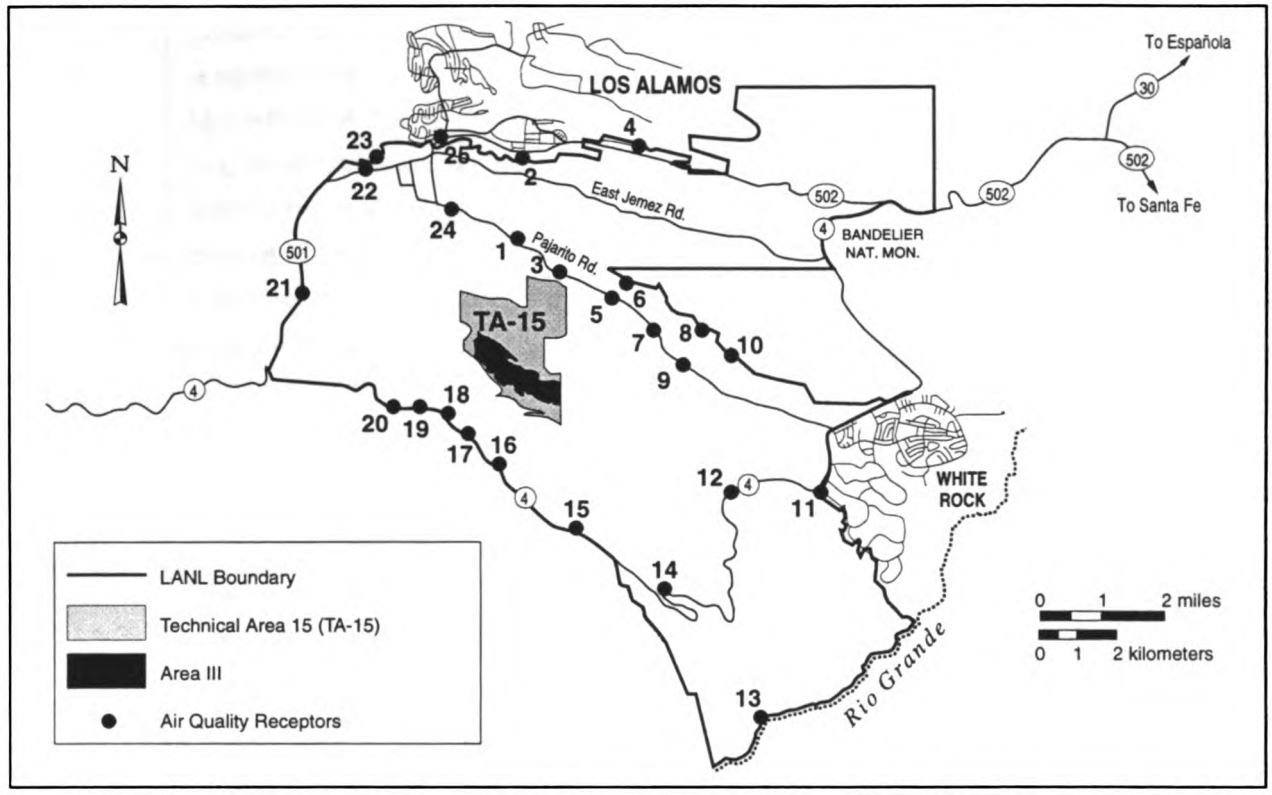

FIGURE C1-1.—*Location of Receptors used in Air Quality Modeling.*

To determine maximum short-term (i.e., exposure periods from 1 to 24 h) impacts, pollutant concentrations are reported for the maximally impacted point of public access. This involves assessing impacts at receptors located within, along, and outside of the LANL fenceline. For long-term impacts (i.e., annual exposures), pollutant concentrations are reported for the maximally impacted point of unrestricted public access. This involves the assessment of impacts at receptor locations along and outside of the LANL fenceline. Onsite points of public access are not considered because of the limited time any member of the public would spend at an onsite location over the course of an entire year; however, receptor locations along large segments of the LANL fenceline are considered even though current land-use restrictions do not allow permanent residents in these areas.

ISC2 model runs indicate that the maximum short-term (i.e., 1, 3, 8, and 24 h) pollutant concentrations would occur along the LANL fenceline at a point 1.0 mi (1.5 km) southwest of the proposed DARHT Facility (receptor 18 on figure C1-1). Maximum long-term (annual) pollutant concentrations would occur along the LANL fenceline at a point 1.1 mi (1.8 km) south of the DARHT Facility (receptor 16 on figure C1-1). Because of the close proximity of the DARHT and PHERMEX sites, emissions from both facilities are conservatively assumed to occur at the DARHT Facility.

C1.3 SOURCE TERM AND IMPACTS

The increases in the airborne concentration of criteria pollutants, as described for each alternative in chapter 5, is assumed to result from construction activities and routine operation of the DARHT or PHERMEX facilities. Construction activities release NO_2, SO_2, and PM_{10} as a result of the operation of diesel- and gasoline-powered construction equipment. PM_{10} emissions also occur, in the form of fugitive dusts, as a result of the movement of construction equipment over the disturbed ground. Operations activities release NO_2 and PM_{10} as a result of emissions during hydrodynamic testing and NO_2, SO_2, and PM_{10} as a result of the operation of the natural gas boiler used in heating the DARHT Facility.

In all but one case, pollutants were assumed to be released from a ground-level point source located on flat terrain; the only exception to this is that fugitive dust emissions during construction are assumed to come from an area source. The use of more realistic pollutant release heights, accounting for buoyant and mechanical plume rise, and the consideration of initial plume spreading (e.g., as would result from hydrodynamic testing) are factors that would tend to reduce maximized ground-level impacts, but were not included in this analysis.

To calculate annual pollutant concentrations using the ISCLT2 model, a joint frequency distribution of wind speed, wind direction, and atmospheric stability data from tower TA-6 was used (exhibit C1-1). The TA-15 area, where the proposed DARHT and PHERMEX facilities are located, does not have routine meteorological monitoring. As described in appendix H, meteorological data from TA-6 were also used to compute human health impacts from the airborne transport of pollutants.

The ISCLT2 model also required estimations of average mixing layer depth for the six stability classes (A-F). Because no mixing height data is available from Los Alamos, the annual morning mixing height of Albuquerque, 1,500 ft (450 m), is assumed to be the average mixing layer depth for stability class F (very stable), and the annual afternoon mixing height of Albuquerque, 8,500 ft (2,600 m), is assumed to be the average mixing layer depth for stability class A (very unstable) (Holzworth 1972). The mixing layer depths at stability classes between A and F are estimated by linear interpolating between the mixing heights at stability class A and F.

To calculate the short-term averaged concentration using the ISCST2 model requires hourly meteorological data of wind speed, wind direction, atmospheric stability, air temperature, and mixing heights. The hourly meteorological data for 1994 at tower TA-6 were used as meteorological input in the ISCST2 model. Because mixing layer depth is not measured at Los Alamos, a conservative estimate of the morning mixing height for Albuquerque for all stability classes was used (Holzworth 1972). The morning mixing height varied by season.

For estimating the short-term averaged concentration using the SCREEN2 model, no meteorological input is required. The worst-case maximum concentration option is used in which the SCREEN2 model estimates the maximum concentration by examining a range of wind speed and stability classes to find the worst-case meteorological conditions. For a ground-level release, the worst-case meteorological variables are a 2 mi/h (3.6 km/h or 1 m/s) wind speed and a stability class of F (very stable).

C1.3.1 Fugitive Dust

Because it is nearly impossible to accurately predict the amount of dust emitted during construction, a default value of 1.2 ton/ac/mo of total suspended particulates is assumed (EPA 1993). This value was based on EPA measurements of suspended particulates (with aerodynamic diameters ≤ 30 μ) made during the construction of apartments and shopping centers. It takes into account emissions during land clearing, blasting, ground excavation, cut and fill operations, and facility construction (EPA 1993).

The amount of PM_{10} emitted from the construction at the DARHT site should be less than 1.2 ton/ac/mo because many of the particulates suspended during construction are at the larger end of the 30-μ size range and will tend to rapidly settle out of the atmosphere at locations very close to the source (Seinfeld 1986). Experiments on dust suspension due to construction found that at 160 ft (50 m), a maximum of 30 percent of the remaining suspended particulates in the atmosphere were in the PM_{10} size range (EPA 1988). Thus, only 30 percent of 1.2 ton/ac/mo of total suspendable particulates or 0.4 ton/ac/mo are assumed to be emitted as PM_{10} from the construction site. Any active dust suppression activities at the DARHT construction site would further reduce PM_{10} emissions; however, no dust suppression activities are assumed in our analysis.

To estimate the annual and 24-h average PM_{10} concentration requires both the size of the area disturbed and the unit-area emission rate (0.4 ton/ac/mo). For all alternatives except the No Action, a square-shaped area of 8 ac (3 ha) is assumed to be disturbed. For the No Action Alternative, the construction impacts are assumed to be no more than one-half of those from the other alternatives, as some construction occurs on the existing DARHT structure to ready it for other uses. Table C1-3 presents the source term used to calculate the air quality impacts from fugitive dust emissions. Both the annual and 24-h maximum average concentrations are calculated using the ISC2 models. Estimated impacts on air quality from fugitive dust emissions are shown in table C1-4. These impacts apply to all alternatives except the No Action Alternative.

C1.3.2 Construction Equipment

The other major source of criteria pollutant emissions from construction is the operation of diesel- and gasoline-powered construction equipment. To obtain the emission rate for each pollutant from the construction equipment, it is assumed that all the diesel and gasoline are consumed by the heavy-duty construction equipment that emits the maximum amount of each pollutant for the given equipment type. The pollutant emission rate for heavy-duty construction equipment is found in EPA's AP-42 tables 2-7.1 and 2-7.2 (EPA 1991). Table C1-5 presents the estimated average monthly and the peak daily consumption of diesel and gasoline for construction of DARHT. Table C1-6 presents the kilograms of pollutant emitted per cubic meter (m^3) of fuel consumed by the construction equipment. For all pollutants but SO_2, the largest emitter is a wheeled tractor; the motor grader and the wheeled dozer are the largest emitters of SO_2 for diesel- and gasoline-powered equipment, respectively.

The emission rate for the annual concentration is calculated from the average monthly emissions, assuming that the construction is year round. Annual concentrations are calculated using the ISCLT2 model.

TABLE C1-3.—*Source Term for Calculating Fugitive Dust Impacts for All Alternatives Except the No Action Alternative*

Pollutant	Averaging Time	Mass of Pollutant per Time Period per Area	Area of Source (ac)	Maximum Emission Rate ($g/(m^2\text{-}s)$)
PM_{10}	Annual 24-h	4.4×10^3 kg/(yr-ac) 12 kg/(24-h-ac)	8 8	3.4×10^{-5} 3.4×10^{-5}

TABLE C1-4.—*Impacts on Air Quality from Fugitive Dust from Completing Construction for the DARHT Facility*

Pollutant	Averaging Time	Maximally Impacted Point of Unrestricted Public Access ($\mu g/m^3$)	Percent of Regulatory Limit[a]
PM_{10}	Annual 24-h	0.8 17	1.6% 11%

[a] Uses the applicable regulatory limit from table 4-3.

Note: No Action Alternative construction impacts were estimated to be no more than one-half those of other alternatives.

TABLE C1-5.—*Estimated Average Monthly and Peak Daily Consumption of Diesel and Gasoline for Construction of the DARHT Facility*

Fuel	Average Monthly Consumption (gal/mo)	Daily Peak Consumption (gal/day)
Diesel	500	135
Gasoline	500	17

TABLE C1-6.—*Amount of Pollutant Released per m^3 of Fuel Consumed by Construction Equipment with Highest Emissions*

Pollutant	Diesel (kg of pollutant/m^3)	Gasoline (kg of pollutant/m^3)
NO_2	52.4	17.5
SO_2	3.7	0.6
PM_{10}	5.6	1.0

The 3-h average emission rate assumes that all of the full workday ration of fuel is consumed in a 3-h period [i.e., 135 gal (0.5 m^3) of diesel fuel per 3 h]. The 24-h average emission rate assumes that the same workday ration of fuel is consumed over a 24-h period. The short-term average concentrations are calculated using the SCREEN2 model. Because there is no specific information on different fuel consumption rates for the various alternatives, the same annual, 24-h, and 3-h consumption rates are used for all the alternatives except the No Action Alternative.

Table C1-7 presents the source term for the construction equipment emissions used for all alternatives except the No Action Alternative.

Estimated impacts on air quality from construction equipment emissions are shown in table C1-8. These impacts apply to all alternatives except the No Action Alternative, which is estimated to have air quality impacts no more than one-half of the other alternatives for construction-related activities.

TABLE C1-7.—*Source Term for Construction Equipment Emissions for All Alternatives Except the No Action Alternative*

Pollutant and Averaging Time	Averaging Time	Mass of Pollutant per Time Period	Maximum Emission Rate (g/s)
PM_{10}	Annual	150 kg/yr	4.7×10^{-3}
	24-h	2.9 kg/24 h	3.4×10^{-2}
NO_2	Annual	1,600 kg/yr	5.0×10^{-2}
	24-h	28 kg/24 h	3.2×10^{-1}
SO_2	Annual	99 kg/yr	3.2×10^{-3}
	24-h	1.9 kg/24 h	2.3×10^{-2}
	3-h	1.9 kg/3 h	1.8×10^{-1}

TABLE C1-8.—*Impacts on Air Quality from Construction Equipment Emission for All Alternatives Except the No Action Alternative*

Pollutant	Averaging Time	Maximally Impacted Point of Unrestricted Public Access ($\mu g/m^3$)	Percent of Regulatory Limit[a]
NO_2	Annual	0.04	0.06%
	24-h	4.8	3.3%
PM_{10}	Annual	0.004	0.008%
	24-h	0.06	0.04%
SO_2	Annual	0.003	0.007%
	24-h	0.3	0.2%
	3-h	22	2.2%

[a] Uses the applicable regulatory limit from table 4-3.

Note: No Action Alternative construction-related impacts assumed to be no more than one-half those of other alternatives.

C1.3.3. Hydrodynamic Testing

Five ambient air pollutants – NO_2, PM_{10}, beryllium, heavy metals (uranium and lead), and lead – are assumed to be emitted during hydrodynamic testing. These are products of detonation of high explosives and the resultant aerosolization of metals. It is assumed that the high explosives do not contain any significant amounts of sulfur; thus, they are not a source of sulfur dioxide.

For purposes of this analysis, it was assumed that 10 percent of the metals in a device become respirable (PM_{10}) following a test. The remaining materials, detectable above background levels, stay within 460 ft (140 m) of the firing point (see appendix B). Table C1-9 gives the estimated maximum amount of material used each year in the No Action and the Enhanced Containment alternatives. With the exception of the Enhanced Containment Alternative, all the alternatives involve the same amount of material. Under the Enhanced Containment Alternative, the containment building or vessel limits the release of gases, fine particles, and fragments to 6 percent of the values estimated for the other alternatives. The 6 percent release factor is a highly conservative assumption that accounts for potential leakage of the containment structure and vessel/building failure. Annual concentrations are calculated using the ISCLT2 model.

TABLE C1-9.—*Estimated Material Released to the Environment During a Year of Testing for the No Action and Enhanced Containment Alternatives*

Alternative	DU (kg)	Be (kg)	Pb (kg)	Cu (kg)	Other Metal (kg)	HE (kg)	LiH (kg)	Total (kg)
No Action[a]	700	10	15	100	200	1,500	100	~2,600
Enhanced Containment								
Vessel	210	3	4	30	60	1,500	30	~1,800
Building	42	1	1	6	12	1,400	6	~1,500
Phased	330[b]	5[b]	7[b]	50[b]	90[b]	1,500[b]	50[b]	~2,000[b]

DU = Depleted uranium
Be = Beryllium
Pb = Lead
Cu = Copper
HE = High explosives
LiH = Lithium hydride

[a] Other alternatives are the same as the No Action Alternative.
[b] Annual average over 30-year operating life.

For the 24-h concentration of PM_{10}, an estimate of the largest amount of material to be expended in a 24-h period is needed. To provide a rough estimate of the maximum amount of material that could be detonated in a 24-h period, the largest test device detonation was used for all alternatives, assuming detonation of 500 lb (230 kg) of material in a 24-h period. The same emission rate was used for all alternatives except the Enhanced Containment Alternative, for which the emission rate is assumed to be 6 percent of the No Action Alternative. The 24-h PM_{10} concentrations are calculated using the SCREEN2 model.

Nitrogen dioxide can be produced from the detonation of high explosives. Because the type of high explosives to be used during testing is variable, a bounding case is used. The high explosive used in this

assessment was nitroglycerine (even though this specific explosive would not be used in hydrodynamic testing) because it has the highest emission rate of nitrogen dioxide, 53 lb/ton (26 kg/MT), of any of the explosives listed by the U.S. Environmental Protection Agency for stationary point and area sources (EPA 1993). Table C1-9 shows the yearly amount of high explosives to be used for the No Action and Enhanced Containment alternatives. All alternatives except the Enhancement Containment Alternative use the same amount of explosives as the No Action Alternative.

The annual emission rate for nitrogen dioxide from hydrodynamic testing is the product of the number of tons of high explosive used per year and the amount of nitrogen dioxide released per ton of explosive. The emission rate for nitrogen dioxide is the same for all alternatives except the Enhanced Containment Alternative, which uses a smaller quantity of high explosives. The annual concentrations are calculated using the ISCLT2 model.

For the 24-h emission rate of nitrogen dioxide from hydrodynamic testing, the largest amount of high explosive expended in a 24-h period is needed. This quantity is not known. It is assumed that 500 lb (230 kg) of high explosive (nitroglycerine for purposes of nitrogen dioxide emission) will be the maximum amount detonated in a 24-h period. The same emission rate is used for all alternatives. (In the Enhanced Containment Alternative, nitrogen dioxide emissions might initially be contained, but they are soon vented from the building or vessel.) The 24-h concentrations are calculated using the SCREEN2 model.

Table C1-10 gives the source term used to estimate the air quality impacts from PM_{10} and NO_2 due to hydrodynamic testing for the No Action and Enhanced Containment alternatives. As stated before, all alternatives except the Enhanced Containment Alternative are assumed to be the same as the No Action Alternative.

Ambient air concentrations for beryllium, heavy metals (uranium and lead), and lead were estimated using information presented in table C1-11. Twenty-five percent of the annual usage of metals was assumed to be released during the 30-day averaging time for beryllium and heavy metals, and 50 percent was assumed released during the calendar quarter averaging time for lead. Estimated impacts on air quality from releases of metals during hydrodynamic testing are shown in table C1-12. Air quality impacts from uncontained detonations are lower than those from containment releases. There are three major reasons for this.

- Atmospheric Dispersion: There is more atmospheric dispersion from uncontained detonations than from containment releases. Greater dispersion results in lower contaminant concentrations in air. Dispersion of ground-level releases is considerably less than for elevated releases, particularly for nearby locations. In general, ground-level releases impact closer individuals much more than elevated releases, which have greater impact on distant individuals and populations because of the greater dispersion. Thus, even though less material is released via the enhanced containment alternative, the potential for exposure is greater because of the decreased dispersion of ground-level releases.
- Source Term: It is conservatively assumed that 6 percent of the material used inside containment would be released. These releases from containment would be ground-level [< 30 ft (< 10-m high)] releases occurring as part of normal operations (1 percent) or small failures (5 percent) of the containment structure (building or vessel), rather than elevated releases as for uncontained detonations.

TABLE C1-10.—*Source Term for Hydrodynamic Testing for the No Action and Enhanced Containment Alternatives*

Alternative	Pollutant	Averaging Time	Mass of Pollutant per Time Period	Maximum Emission Rate (g/s)
No Action[a]	PM_{10}	Annual	260 kg/yr	8.3×10^{-3}
		24-h	23 kg/24-h	2.6×10^{-1}
	NO_2	Annual	39 kg/yr	1.2×10^{-3}
		24-h	5.9 kg/24-h	6.8×10^{-2}
Enhanced Containment	PM_{10}[b]	Annual	8.8 kg/yr	2.8×10^{-4}
		24-h	1.4 kg/24-h	1.6×10^{-2}
	NO_2	Annual	36 kg/yr	1.1×10^{-1}
		24-h	5.9 kg/24-h	6.8×10^{-2}

[a] Other alternatives are the same as the No Action Alternative.
[b] Values shown are for the Building Containment Option. Values for the Vessel Containment Option and Phased Containment Option would be between the No Action Alternative and Building Containment Option values.

TABLE C1-11.—*Data Used to Estimate Ambient Air Concentrations of Metals from Hydrodynamic Testing*

Parameter	Uncontained Detonation	Containment Release
Release height	elevated (99 m)	ground level (<10 m)
χ/Q'	6.8×10^{-6} s/m^3	5.3×10^{-7} s/m^3
Release fraction	1.0	0.06
Respirable fraction	0.1	1.0

- Comparison point was at State Road 4, approximately 0.9 mi (1.5 km) southwest of the DARHT site.
- Comparisons to 30-day air quality standards for heavy metals and beryllium assumed 25 percent of the annual usage of materials; assumed quantities used were 175 kg uranium, 2.5 kg beryllium, and 3.75 kg lead.
- Comparison to the calendar quarter air quality standard for lead assumed 50 percent of the annual usage of material; assumed quantity used was 7.5 kg lead.
- Uncontained detonation characterized the No Action, DARHT Baseline, Upgrade PHERMEX, Plutonium Exclusion, and Single Axis alternatives.
- The Building Containment Option of the Enhanced Containment Alternative was characterized as 100 percent containment use.
- The Vessel Containment Option of the Enhanced Containment Alternative was characterized as 25 percent uncontained detonation, 75 percent containment use.
- The Phased Containment Option (preferred alternative) of the Enhanced Containment Alternative was evaluated as 1) 5 percent containment release and 95 percent uncontained detonation; 2) 40 percent containment release and 60 percent uncontained detonation; and 3) same as the Vessel Containment Option of the Enhanced Containment Alternative.

TABLE C1-12.—*Impacts on Air Quality from Hydrodynamic Testing for the Enhanced Containment Alternative*

Pollutant	Averaging Time	Maximally Impacted Point of Unrestricted Public Access ($\mu g/m^3$)	Percent of Regulatory Limit[a]
NO_2	Annual	8×10^{-4}	0.001%
	24-h	0.9	0.6%
PM_{10}	Annual	0.003	0.006%
	24-h	0.2[c]	0.1%[c]
		3.2[d]	2.1%[d]
Beryllium	30 days	2×10^{-5}	0.0002%
Heavy Metals[b]	30 days	0.002	0.02%
Lead	Calendar Quarter	1×10^{-4}	0.007%

[a] Uses the applicable regulatory limit from table 4-3.
[b] Sum of the air concentration of uranium and lead.
[c] Building Containment Option.
[d] Vessel Containment and Phased Containment options.

- Receptor Location: The point where a member of the public could receive the maximum offsite exposure is only 0.9 mi (1.5 km) from the firing point, southwest to State Road 4. This relatively short distance to the receptor and point of air quality determination tends to maximize the issues raised in items 1 and 2 above.

Item 1 above relatively decreases the impact of uncontained detonations, item 2 relatively decreases the impact of contained releases, and item 3 relatively increases the impact of contained releases. Taking all these issues into consideration, 100 percent containment releases have an air quality impact about five times those of 100-percent uncontained detonation releases.

Estimated impacts on air quality from uncontained detonations during hydrodynamic testing are shown in table C1-13. These impacts apply to all alternatives except the Enhanced Containment Alternative. Impacts from the Enhanced Containment Alternative are shown in table C1-12.

C1.3.4. Boiler Emissions

The only other primary pollutant source from operation of the facility is emissions from the natural gas boiler used for heating. The natural gas boiler is assumed to be a commercial boiler (80 hp) with an hourly gas input rate of 3,348,000 Btu/hr. The emission rate of each pollutant can be calculated from the emission factors for commercial natural gas boilers given in EPA's AP-42 document (EPA 1993). Table C1-14 gives these emission rates in units of kilograms of primary pollutant (nitrogen dioxide, sulfur dioxide, and PM_{10}) per million m^3 of natural gas. The rates are computed assuming a heating rate of 8,270 kcal/m^3 of natural gas (EPA 1993). To be conservative, the boiler is assumed to run continuously

TABLE C1-13.—*Impacts on Air Quality from Hydrodynamic Testing for All Uncontained Alternatives*

Pollutant	Averaging Time	Maximally Impacted Point of Unrestricted Public Access ($\mu g/m^3$)	Percent of Regulatory Limit[a]
NO_2	Annual 24-h	0.001 0.9	0.001% 0.6%
PM_{10}	Annual 24-h	0.007 3.2	0.01% 2.1%
Beryllium	30 days	5×10^{-6}	0.00005%
Heavy Metals[b]	30 days	5×10^{-4}	0.005%
Lead	Calendar Quarter	2×10^{-5}	0.001%

[a] Uses the applicable regulatory limit shown in table 4-3.
[b] Sum of the air concentration of uranium and lead.

TABLE C1-14.—*Emission of Primary Pollutants from Natural Gas Combustion, Heating Value, and Hourly Gas Input for an 80-hp Commercial Boiler for All Alternatives*

Pollutant	Pollutant Emitted (kg of pollutant per 10^6 m^3 of fuel)	Heating Value ($kcal/m^3$)	Hourly Gas Input (10^3 Btu/hr)
NO_2	1,600	8,270	3,348
SO_2	9.6	8,270	3,348
PM_{10}	192	8,270	3,348

throughout the year. It is also assumed that the boiler has no emissions controls for nitrogen dioxide. Since the hourly gas input rate is known, there is no special requirement for finding the short-term emission rates compared to annual emission rates. The emission rate is the same for all alternatives. Table C1-15 presents the source term used to estimate the air quality impacts due to emissions from the natural gas boiler. All the concentrations are calculated using the ISC2 models.

Estimated impacts on air quality from boiler emissions are shown in table C1-16. These impacts apply to all alternatives.

TABLE C1-15.—*Source Term for Emissions from the Natural Gas Boiler Used in Heating the Facilities for All Alternatives*

Pollutant	Averaging Time	Mass of Pollutant per Time Period	Maximum Emission Rate (g/s)
PM_{10}	Annual	170 kg/yr	5.4×10^{-3}
	24-hr	4.7×10^{-1} kg/24-h	5.4×10^{-3}
NO_2	Annual	1,400 kg/yr	4.5×10^{-2}
	24-hr	3.8 kg/24-h	4.5×10^{-2}
SO_2	Annual	8.6 kg/yr	2.7×10^{-4}
	24-hr	2.4×10^{-2} kg/24-h	2.7×10^{-4}
	3-hr	2.9×10^{-3} kg/3-h	2.7×10^{-4}

TABLE C1-16.—*Impacts on Air Quality from Emissions from the Natural Gas Boiler for All Alternatives*

Pollutant	Averaging Time	Maximally Impacted Point of Unrestricted Public Access ($\mu g/m^3$)	Percent of Regulatory Limit[a]
NO_2	Annual	0.04	0.06%
	24-h	1	0.7%
PM_{10}	Annual	0.004	0.008%
	24-h	0.1	0.07%
SO_2	Annual	0.0002	0.0005%
	24-h	0.006	0.003%
	3-h	0.03	0.003%

[a] Uses the applicable regulatory limit from table 4-3.

Note: Air quality impacts are identical for all alternatives.

APPENDIX C2: NOISE

This evaluation of noise impacts focuses on three sources of noise: construction noise associated with each alternative, increases or decreases in traffic and resulting noise propagation in adjacent communities based on facility construction and operation, and effects of noise from the firing of test shots at the facilities. In support of the evaluation, this appendix reviews how meteorological conditions and terrain influence sound travel, summarizes noise measurements made at a series of testing firings at PHERMEX on March 11, 1995, and documents the tests or methods employed in the noise analysis.

C2.1 GENERAL INFORMATION

Noise is defined as sound that is loud, harsh, or confusing to humans. The standard unit of sound pressure level is the decibel (dB). The decibel (dB) is an expression of sound pressure level that is referenced to a pressure of 20 micropascals expressed on a logarithmic scale,

$$1 \text{ dB} = 20 \log_{10} (p/20)$$

where p is the sound pressure in micropascals. Twenty micropascals approximates the minimum audible sound pressure level in humans and is routinely used for noise levels. The dB(A) is an expression of adjusted pressure levels by frequency that accounts for human perception of loudness; consequently, dB(A) is most often used when evaluating human noise disturbance. For example, at a frequency of 500 Hz, 60 dB are reduced by 3.2 dB to give an a-weighted pressure level of 56.8 dB(A). Frequencies lower than 500 Hz sustain a larger adjustment (from -8.6 to -26.2 dB compared to frequencies greater than 500 Hz (-1.1 to 1.2).

For this assessment, noise is expressed in two forms. A-weighted sound pressure levels (dBA) are adjusted values that are most indicative of adverse community responses to noise. Firing noise levels are reported as peak dBA levels. Noise derived from traffic estimates are reported as 1-h equivalent sound levels (L_{eq}). The L_{eq} (in dBA) is the equivalent steady-state sound level that, if continuous during a specified time period, would contain the same energy as the actual time-varying sound over the monitored or modeled time period (in this case, 1 h). Except for vehicles exceeding 10,000 lb (4,540 kg) Gross Vehicle Weight (GVW), vehicle noise on public thoroughfares is exempted from residential noise standards.

C2.2 NOISE ANALYSIS MARCH 1995 TEST SHOTS

On March 11, 1995, at the PHERMEX pad, a series of test shots was fired to obtain seismic and acoustic measurements at selected locations. The coordinates at the PHERMEX firing point were North 35°49.957′ and West 106°17.739′. Acoustic (sound pressure) readings were taken by instruments fitted with wind screens at three locations: Technical Area 49 (TA-49), Bandelier National Monument entrance, and the community of White Rock.

C2.2.1 TA-49

The sampling location was located approximately 3/4 mi (1 km) east of the TA-49 Gate along State Route 4 (coordinates for this site were North 35°49.133′ and West 106°18.518′). A multi-spectral IVIE sound-level meter (IVIE #677) was used to record maximum sound pressure levels at nine standard frequencies. This location was the shortest distance between the firing site and the site boundary.

C2.2.2 Bandelier National Monument Entrance

This sampling location was located just off State Route 4 in a turn-off on the east side of the highway about 100 yards west of the entrance to Bandelier National Monument. The coordinates were North 35°47.797′ and West 106°16.545′. A multi-spectral IVIE sound-level meter (IVIE #436) was used to record maximum sound pressure levels at nine standard frequencies. This location represents the closest residence to the PHERMEX firing site.

C2.2.3 White Rock Community

This station was located about 100 to 150 ft (30 to 45 m) east of the intersection of State Route 4 and Karen Circle Road on LANL property just off State Route 4. The mean coordinates of two readings were North 35°82.026′ and West 106°22.182′. A-weighted sound levels were measured with a GenRad Precision Sound Level Meter at 250 Hz. On March 11, 1995, White Rock, which is generally ENE of PHERMEX, was not directly downwind of PHERMEX. Because of terrain and anticipated wind patterns, this location represents the community that is most likely to have the greatest noise levels resulting from blasts.

Acoustic measurements collected on March 11, 1995, measured air over pressure signals (frequencies from 2 to 200 Hz) with a microphone equipped with a wind screen. Measurements were collected at the TA-49 location from two duplicate sensors (Station B1 and Station B2), as shown in table C2-1. Air blast measurements were measured at frequencies (5 to 15 Hz) which do not contribute to the A-weighted measurements for evaluation of human noise impacts. Consequently, air blast measurements are not addressed further.

Meteorological and environmental factors significantly affected the March 11, 1995, noise measurements. Terrain and wind are discussed below.

C2.2.4 Terrain

LANL is situated on the Pajarito Plateau and supports a mixture of conifers, trees, and shrubs. This ground cover will attenuate sound as it travels over land. Generally, the higher frequency sound is more effectively attenuated than lower frequencies. The rate of attenuation through medium-dense woods at 250 Hz is 0.06 dB/m (EEI 1978); hence, attenuation in low-frequency bands that characterize blast noise is significant. The mesas, which run in an east-southeasterly direction, are separated by valleys that may also channel and influence offsite noise measurements.

Portions of the community of Los Alamos are closer to PHERMEX than White Rock (table C2-2), but they are located uphill over heavily forested terrain and beyond a hill. These factors would tend to significantly reduce noise levels at locations north and northwest of PHERMEX. Communities located to the east of LANL are lower in elevation and may have noise channeled into the community down through the valleys.

TABLE C2-1.—*Acoustic (Airblast) Measurement at TA-49 Seismic and Acoustic Monitoring Stations, March 11, 1995*

Shot #	Load[a]	Time	Station B1			Station B2		
			AOP[b]	dB	Hz	AOP[b]	dB	Hz
0942	10	12:15	<0.04	NS	NS	<0.04	NS	NS
0943	25	12:38	<0.04	NS	NS	<0.04	NS	NS
0944	50	13:01	0.17	119	6.6	0.14	117	6.9
0945	50	13:33	<0.04	NS	NS	<0.04	NS	NS
0946	100	13:54	0.11	116	6.0	0.12	116	6.2
0958	150	14:16	0.21	121	7.1	0.20	120	5.0

[a] lb TNT used
[b] Air overpressure in millibars

dB = decibel
Hz = frequency, in Hertz
NS = not sampled

TABLE C2-2.—*Estimated Distances Between PHERMEX Firing Site and Sound Measurement Locations*

Location	Distance
TA-49 (off Route 4)	1.3 mi (2 km)
Bandelier National Monument Entrance	2.6 mi (4 km)
White Rock	4.0 mi (6 km)
Los Alamos	3.0 mi (5 km)

C2.2.5 Wind

Wind measurements are summarized from data collected at the TA-49 weather station (table C2-3). As the firings progressed, wind velocity steadily increased; however, the winds varied and were gusty. The wind measurements do not indicate gusts of possible greater speed that may have occurred at the time of firing. Sound moving into the wind is bent upwards, producing a shadow zone and generally reducing sound levels measured at ground level in an upwind location (EEI 1978). The Bandelier location is located to the south of the firing site and the TA-49 location is located to the SW. The prevailing winds would, therefore, reduce the measurements recorded at these two upwind locations. Sound traveling with the wind is forced downward, which effectively negates any ground-level attenuation that may result from trees, shrubs, terrain, or other sound-attenuating obstructions. This situation is further exacerbated by the

TABLE C2-3.—*Summary of Meteorological Data Collected at TA-49 Weather Station March 11, 1995*

Shot #	Approximate Time	Time	Wind Speed (mi/h)	Wind Direction (Degrees N=0)	Temperature (°F)	Relative Humidity (percent)
		12:00	9.7	183	54.1	37
942	12:16	12:15	12.1	182	57.0	33
		12:30	13.0	182	57.7	31
943	12:39	12:45	15.4	187	56.8	31
944	13:02	13:00	13.9	177	58.6	31
		13:15	16.1	180	59.0	30
945	13:33	13:30	17.4	190	58.1	30
		13:45	13.9	194	57.4	30
946	13:55	14:00	15.4	187	7.0	31
958	14:17	14:15	14.5	189	57.0	31
		14:30	11.0	183	56.5	32

general decrease in slope from the PHERMEX firing site to the White Rock location. Because White Rock is located generally east of PHERMEX, the prevailing wind conditions would tend to increase noise levels there. Daytime winds are generally westerly during the months of March, April, and May (Bowen 1990), hence the selection of the White Rock location. However, during the March 11, 1995, testing, the winds came from the south.

Temperatures and relative humidity varied little over the duration of the firings (table C2-3). The differential effects on noise travel would not significantly affect measured noise levels during the March 11, 1995, tests.

C2.2.6 Measured Sound Levels at White Rock, Bandelier Entrance, and TA-49

During the testing, sound pressure recording generally increased with blast intensity (table C2-4). The noise variation observed by frequency and intensity is caused by the fluctuating wind that changed, not only in direction, but in speed. Under ideal conditions of calm and optimum temperature and humidity, it is possible for sound pressure levels at the TA-49 Site boundary location to exceed 70 dBA with the larger blasts. The lower power firings will have a lower probability of exceeding the 75-dBA Los Alamos County daytime guideline. The nighttime standard imposed from 9:00 p.m. to 7:00 a.m. of 53 dBA can be exceeded at the closest site boundary locations. The diverse terrain and the frequency and directional variability of winds complicate routine noise estimation procedures and introduce a high level of uncertainty.

TABLE C2-4.—*Noise Measurements Conducted at LANL on March 11, 1995*

		Frequency, in Hertz									
Firing No.	**Load (lb TNT)**	**31.5**	**63**	**125**	**250**	**500**	**1,000**	**2,000**	**4,000**	**8,000**	**dBA**
TA-49 (I)											
942	10	32	42	54	52	50	46	42	44	48	NR
943	20	<46	52	58	58	46	52	46	NR	NR	66
944	50	48	52	62	62	60	58	48	NR	NR	68
945	50	NR	54	56	54	54	50	48	NR	NR	64
946	100	48	50	60	64	62	60	50	50	NR	70
958	150	NR	62	68	64	64	58	54	48	NR	71
Bandelier (II)											
943	20	NR	NR	NR	NR	NR	NR	NR	NR	NR	NR
944	50	38	52	56	54	52	48	42	40	36	NR
945	50	36	42	50	50	54	56	48	40	42	62
946	100	40	46	54	52	48	42	38	36	40	61
958	150	40	48	54	56	52	54	52	36	<36	60
White Rock											
942	10	NR	NR	NR	60.9	NR	NR	NR	NR	NR	NR
943	20	NR	NR	NR	65.3	NR	NR	NR	NR	NR	NR
944	50	NR	NR	NR	69.1	NR	NR	NR	NR	NR	NR
945	50	NR	NR	NR	63.1	NR	NR	NR	NR	NR	NR
946	100	NR	NR	NR	71.6	NR	NR	NR	NR	NR	NR
958	150	NR	NR	NR	68.6	NR	NR	NR	NR	NR	NR
Background Measurements		31.5	63	125	250	500	1,000	2,000	4,000	8,000	dBA
BKG1-67749		49	41	34	30	31	25	25	NR	NR	31
BKGII-436		42	40	38	34	32	30	28	30	28	35
White Rock		NR	NR	NR	38	NR	NR	NR	NR	NR	NR
White Rock (car noise)		NR	NR	NR	51	NR	NR	NR	NR	NR	NR

NR = data not recorded or lost
BKG1-67749 taken at TA-49
BKGII-436 taken at Bandelier entrance

With a base schedule of 20 shots per year, blast noise impacts are considered equivalent for all alternatives except the Enhanced Containment Alternative. In this option, containment may reduce blast noise by as much as 80 percent; however, uncertainties in the choice of a vessel or a building and the design of containment prevent a more specific evaluation of blast noise impacts. The county noise regulations restrict maximum noise levels to 75 dBA for a period of not more than 10 minutes in a single hour during daylight hours (7:00 a.m. to 9:00 p.m.). Monitoring results indicate that it would be extremely unlikely for this guideline to be exceeded as an instantaneous measurement of more than 75 dBA or for 10 min of blast-associated noise to exceed 65 dBA in a given hour. (Under test shot operating procedures, it is not possible for more than three shots to be fired in one hour.) However, the likelihood of exceeding the 53-dBA county limit for nighttime noise imposed from 9:00 p.m. to 7:00 a.m. is high.

C2.3 WORKER PROTECTION

Construction workers are protected by administrative procedures and protective devices (such as ear plugs or muffs). Threshold limit values (ACGIH 1993) for impulse noise are 100 impulses per day at 140 dB. The maximum number of firings in an 8-h period, assuming 20 minutes between shots, is 25, well below the limit. Safety procedures implemented during firing create an exclusion zone that would protect staff from excessive impulse noise due to intensity and frequency.

C2.4 WILDLIFE

Firing noise may potentially impact sensitive wildlife, such as nesting birds. A group of deer observed during the first test shot on March 11, 1995, had an unhabituated startle response to the first firing. This observation suggests that local wildlife have not habituated to routine firings. However, the general health and well-being of deer and elk herds in the area suggest that testing programs involving firings have not had an adverse effect on ungulate populations at LANL or Bandelier National Monument.

C2.5 ESTIMATION OF TRAFFIC NOISE

Traffic noise is exempted under Los Alamos County noise regulations; however, increases in traffic can result in complaints about associated noise or congestion. A regression equation was developed from modeled data of traffic volume (vehicles/h) and estimated noise levels (1-h L_{eq} in dBA). The modeled data was developed to assess traffic noise associated with the New Production Reactor Environmental Impact Statement (DOE 1991). The regression equation was:

$$Y = 48.35549 + 7.25929X$$

where Y is the predicted noise level in 1 h L_{eq} (dBA) and X is the log of the hourly traffic volume.

For the analysis, three baseline levels of traffic volume were used: 10, 100, and 1,000 vehicles/h. The 10-vehicle/h limit might approximate early morning traffic. The 1,000-vehicle/h value is a conservative estimate of rush hour traffic volume. The larger the baseline traffic volume, the less significant the potential impact on overall traffic noise in the community. Incremental increases of traffic for each of these standard traffic volumes were raised by the full-time equivalents (FTEs) associated with each alternative. The impact was then related to the base flow to define the range of impact [the change (Δ) in table C2-5]. The same approach was used to estimate increases in traffic due to construction. Mean and maximum construction forces of 50 and 75 staff, respectively, were used in the assessment and the differences between alternatives resulting from the length of the construction phase.

The increases in traffic noise associated with all alternatives, compared to the No Action Alternative, are inconsequential because, in the modeled assumptions, the expected increases in traffic noise would not increase residential noise levels above 5 dBA. Within Los Alamos County noise standards, operation of motor vehicles on public thoroughfares is exempted from the county noise code.

TABLE C2-5.—*Estimated Traffic Noise Increases by Alternative for Operation and Construction*

Volume (Vehicles/hr)	Log Volume	Estimated L_{eq}	Baseline L_{eq}	Change in L_{eq} (ΔL_{eq})
OPERATIONS				
Analysis Baseline Traffic Flow				
10	1	56	NA	NA
100	2	63	NA	NA
1000	3	70	NA	NA
No Action Alternative (based on 13.4 FTEs)				
23	1.4	58	56	2.7
113	2.1	63	63	0.4
1013	3.0	71	70	0.04
DARHT Baseline Alternative (based on 19.9 FTEs)				
30	1.5	59	56	3.5
120	2.1	63	63	0.6
1020	3.0	70	70	0.06
Enhanced Containment Alternative (based on 28.5 FTEs)				
39	1.6	60	56	4.3
129	2.1	64	63	0.8
1029	3.0	70	70	0.09
Plutonium Exclusion Alternative (based on 19.9 FTEs)				
30	1.5	59	56	3.4
120	2.1	63	63	0.6
1020	3.0	70	70	0.06
Single-Axis Alternative (based on 17.34 FTEs)				
27	1.4	59	56	3.2
117	2.1	63	63	0.5
1017	3.0	70	70	0.05
PHERMEX Upgrade Alternative (based on 19.9 FTEs)				
30	1.5	60	56	3.4
120	2.1	63	63	0.6
1020	3.0	70	70	0.06
CONSTRUCTION				
Maximum				
85	1.9	62	56	6.8
175	2.2	65	63	1.8
1075	3.0	70	70	0.2
Mean				
60	1.8	61	56	5.7
150	2.2	64	63	1.3
1050	3.0	70	70	0.2

L_{eq} is the one-hour equivalent sound level.

C.3 REFERENCES CITED IN APPENDIX C

ACGIH (American Conference of Government and Industrial Hygienists), 1993, *1992-1993 Threshold Limit Values for Chemical Substances and Physical Agents and Biological Exposure Indices*, Cincinnati, Ohio.

Bowen, B.M., 1990, *Los Alamos Climatology*, LA-11735-MS, Los Alamos National Laboratory, Los Alamos, New Mexico.

DOE (Department of Energy), 1991, *Draft Environmental Impact Statement for the Siting, Construction, and Operation of New Production Reactor Capacity*, Vol. 4: Appendices D-R, April, Washington, D.C.

EEI (Edision Electric Institute), 1978, *Electric Power Plant Environmental Noise Guide*, Vol. 1 and 2, New York, New York.

EPA (U.S. Environmental Protection Agency), 1988, *PM_{10} Emission Factors for Selected Open Area Dust Sources*, EPA-450/4-88-003, Office of Planning and Standards, Research Triangle Park, North Carolina.

EPA (U.S. Environmental Protection Agency), 1991, *Supplement A to Compilation of Air Pollution Emission Factors, Volume 2: Mobile Sources*, AP-42, Vol. 2 Suppl. A, Office of Air and Radiation, Office of Mobile Sources, Test and Evaluation Branch, Ann Arbor, Michigan.

EPA (U.S. Environmental Protection Agency), 1992a, *User's Guide for Industrial Source Complex (ISC2) Dispersion Models Volume I - User Instructions*, EPA-450/4-92-008a, Office of Air Quality Planning and Standards, Technical Support Division, Research Triangle Park, North Carolina.

EPA (U.S. Environmental Protection Agency), 1992b, *SCREEN2 Model User's Guide*, EPA-450/4-92-006, Office of Air Quality Planning and Standards, Technical Support Division, Research Triangle Park, North Carolina.

EPA (U.S. Environmental Protection Agency), 1993, *Supplement F to Compilation of Air Pollution Emission Factors, Volume 1: Stationary Point and Area Sources*, AP-42, Vol.1 Suppl. F. Office of Planning and Standards, Office of Air and Radiation, Research Triangle Park, North Carolina.

Holzworth, G.C., 1972, *Mixing Heights, Wind Speeds, and Potential for Urban Air Pollution Throughout the Contiguous United States*, PB-207-102, Office of Air Programs, Research Triangle Park, North Carolina.

Seinfeld, J.H., 1986, *Atmospheric Chemistry and Physics of Air Pollution*, John Wiley and Sons, Inc., New York.

EXHIBIT C1-1.—*Joint Frequency Distribution of Atmospheric Stability, Wind Direction, and Wind Speed for Los Alamos National Laboratory at Tower TA-6*

Wind measurements were made on-site at 32 ft (10 m) above ground level. Data are based on measurements made from 1990 through 1993.

STAB CLASS	WIND DIRECTION FROM WHICH THE WIND IS BLOWING	WIND SPEED CLASS (m/s) 0 - 1.8	1.8 - 3.3	3.3 - 5.5	5.5 - 8.5	8.5 - 11.5	> 11.5
A	NORTH	0.0014	0.0005	0.0000	0.0000	0.0000	0.0000
A	NORTH-NORTHEAST	0.0022	0.0006	0.0000	0.0000	0.0000	0.0000
A	NORTHEAST	0.0048	0.0019	0.0000	0.0000	0.0000	0.0000
A	EAST-NORTHEAST	0.0086	0.0023	0.0000	0.0000	0.0000	0.0000
A	EAST	0.0096	0.0031	0.0000	0.0000	0.0000	0.0000
A	EAST-SOUTHEAST	0.0081	0.0044	0.0000	0.0000	0.0000	0.0000
A	SOUTHEAST	0.0086	0.0076	0.0001	0.0000	0.0000	0.0000
A	SOUTH-SOUTHEAST	0.0066	0.0074	0.0002	0.0000	0.0000	0.0000
A	SOUTH	0.0038	0.0039	0.0003	0.0000	0.0000	0.0000
A	SOUTH-SOUTHWEST	0.0017	0.0013	0.0001	0.0000	0.0000	0.0000
A	SOUTHWEST	0.0010	0.0007	0.0001	0.0000	0.0000	0.0000
A	WEST-SOUTHWEST	0.0007	0.0005	0.0000	0.0000	0.0000	0.0000
A	WEST	0.0007	0.0004	0.0001	0.0000	0.0000	0.0000
A	WEST-NORTHWEST	0.0007	0.0003	0.0001	0.0000	0.0000	0.0000
A	NORTHWEST	0.0009	0.0006	0.0001	0.0000	0.0000	0.0000
A	NORTH-NORTHWEST	0.0007	0.0006	0.0001	0.0000	0.0000	0.0000
B	NORTH	0.0005	0.0004	0.0001	0.0000	0.0000	0.0000
B	NORTH-NORTHEAST	0.0008	0.0012	0.0002	0.0000	0.0000	0.0000
B	NORTHEAST	0.0019	0.0031	0.0004	0.0000	0.0000	0.0000
B	EAST-NORTHEAST	0.0029	0.0032	0.0001	0.0000	0.0000	0.0000
B	EAST	0.0029	0.0032	0.0000	0.0000	0.0000	0.0000
B	EAST-SOUTHEAST	0.0020	0.0041	0.0001	0.0000	0.0000	0.0000
B	SOUTHEAST	0.0019	0.0055	0.0005	0.0000	0.0000	0.0000
B	SOUTH-SOUTHEAST	0.0021	0.0085	0.0022	0.0000	0.0000	0.0000
B	SOUTH	0.0016	0.0066	0.0035	0.0000	0.0000	0.0000
B	SOUTH-SOUTHWEST	0.0008	0.0026	0.0019	0.0000	0.0000	0.0000
B	SOUTHWEST	0.0005	0.0011	0.0010	0.0000	0.0000	0.0000
B	WEST-SOUTHWEST	0.0002	0.0008	0.0004	0.0000	0.0000	0.0000
B	WEST	0.0002	0.0007	0.0002	0.0000	0.0000	0.0000
B	WEST-NORTHWEST	0.0002	0.0007	0.0002	0.0000	0.0000	0.0000
B	NORTHWEST	0.0002	0.0008	0.0004	0.0000	0.0000	0.0000
B	NORTH-NORTHWEST	0.0002	0.0005	0.0003	0.0000	0.0000	0.0000
C	NORTH	0.0008	0.0013	0.0005	0.0000	0.0000	0.0000
C	NORTH-NORTHEAST	0.0016	0.0037	0.0019	0.0000	0.0000	0.0000
C	NORTHEAST	0.0026	0.0058	0.0021	0.0000	0.0000	0.0000
C	EAST-NORTHEAST	0.0035	0.0031	0.0002	0.0000	0.0000	0.0000
C	EAST	0.0040	0.0041	0.0001	0.0000	0.0000	0.0000
C	EAST-SOUTHEAST	0.0021	0.0046	0.0004	0.0000	0.0000	0.0000
C	SOUTHEAST	0.0018	0.0030	0.0007	0.0000	0.0000	0.0000
C	SOUTH-SOUTHEAST	0.0022	0.0087	0.0076	0.0000	0.0000	0.0000
C	SOUTH	0.0026	0.0141	0.0160	0.0000	0.0000	0.0000
C	SOUTH-SOUTHWEST	0.0014	0.0073	0.0090	0.0000	0.0000	0.0000
C	SOUTHWEST	0.0009	0.0039	0.0053	0.0000	0.0000	0.0000
C	WEST-SOUTHWEST	0.0004	0.0021	0.0046	0.0000	0.0000	0.0000
C	WEST	0.0004	0.0014	0.0026	0.0000	0.0000	0.0000
C	WEST-NORTHWEST	0.0003	0.0013	0.0019	0.0000	0.0000	0.0000
C	NORTHWEST	0.0004	0.0016	0.0026	0.0000	0.0000	0.0000

EXHIBIT C1-1.—*Joint Frequency Distribution of Atmospheric Stability, Wind Direction, and Wind Speed for Los Alamos National Laboratory at Tower TA-6 – Continued*

STAB CLASS	WIND DIRECTION FROM WHICH THE WIND IS BLOWING	WIND SPEED CLASS (m/s) 0 - 1.8	1.8 - 3.3	3.3 - 5.5	5.5 - 8.5	8.5 - 11.5	> 11.5
C	NORTH-NORTHWEST	0.0004	0.0009	0.0007	0.0000	0.0000	0.0000
D	NORTH	0.0098	0.0083	0.0011	0.0003	0.0000	0.0000
D	NORTH-NORTHEAST	0.0079	0.0081	0.0031	0.0010	0.0000	0.0000
D	NORTHEAST	0.0067	0.0041	0.0007	0.0001	0.0000	0.0000
D	EAST-NORTHEAST	0.0046	0.0010	0.0001	0.0000	0.0000	0.0000
D	EAST	0.0055	0.0020	0.0001	0.0000	0.0000	0.0000
D	EAST-SOUTHEAST	0.0046	0.0024	0.0003	0.0000	0.0000	0.0000
D	SOUTHEAST	0.0040	0.0012	0.0000	0.0000	0.0000	0.0000
D	SOUTH-SOUTHEAST	0.0060	0.0044	0.0022	0.0002	0.0000	0.0000
D	SOUTH	0.0098	0.0131	0.0041	0.0013	0.0000	0.0000
D	SOUTH-SOUTHWEST	0.0099	0.0221	0.0101	0.0027	0.0000	0.0000
D	SOUTHWEST	0.0085	0.0204	0.0084	0.0019	0.0002	0.0000
D	WEST-SOUTHWEST	0.0065	0.0120	0.0089	0.0038	0.0001	0.0000
D	WEST	0.0062	0.0095	0.0145	0.0090	0.0012	0.0001
D	WEST-NORTHWEST	0.0058	0.0092	0.0147	0.0101	0.0020	0.0012
D	NORTHWEST	0.0080	0.0130	0.0095	0.0030	0.0002	0.0000
D	NORTH-NORTHWEST	0.0079	0.0071	0.0011	0.0002	0.0000	0.0000
E	NORTH	0.0056	0.0027	0.0000	0.0000	0.0000	0.0000
E	NORTH-NORTHEAST	0.0028	0.0011	0.0000	0.0000	0.0000	0.0000
E	NORTHEAST	0.0016	0.0003	0.0000	0.0000	0.0000	0.0000
E	EAST-NORTHEAST	0.0008	0.0000	0.0000	0.0000	0.0000	0.0000
E	EAST	0.0008	0.0001	0.0000	0.0000	0.0000	0.0000
E	EAST-SOUTHEAST	0.0008	0.0001	0.0000	0.0000	0.0000	0.0000
E	SOUTHEAST	0.0009	0.0001	0.0000	0.0000	0.0000	0.0000
E	SOUTH-SOUTHEAST	0.0015	0.0004	0.0000	0.0000	0.0000	0.0000
E	SOUTH	0.0026	0.0013	0.0000	0.0000	0.0000	0.0000
E	SOUTH-SOUTHWEST	0.0047	0.0036	0.0001	0.0000	0.0000	0.0000
E	SOUTHWEST	0.0063	0.0076	0.0001	0.0000	0.0000	0.0000
E	WEST-SOUTHWEST	0.0047	0.0151	0.0007	0.0000	0.0000	0.0000
E	WEST	0.0039	0.0093	0.0029	0.0001	0.0000	0.0000
E	WEST-NORTHWEST	0.0038	0.0096	0.0050	0.0005	0.0000	0.0000
E	NORTHWEST	0.0062	0.0231	0.0010	0.0000	0.0000	0.0000
E	NORTH-NORTHWEST	0.0063	0.0070	0.0000	0.0000	0.0000	0.0000
F	NORTH	0.0058	0.0011	0.0000	0.0000	0.0000	0.0000
F	NORTH-NORTHEAST	0.0031	0.0005	0.0000	0.0000	0.0000	0.0000
F	NORTHEAST	0.0019	0.0001	0.0000	0.0000	0.0000	0.0000
F	EAST-NORTHEAST	0.0005	0.0000	0.0000	0.0000	0.0000	0.0000
F	EAST	0.0008	0.0000	0.0000	0.0000	0.0000	0.0000
F	EAST-SOUTHEAST	0.0009	0.0001	0.0000	0.0000	0.0000	0.0000
F	SOUTHEAST	0.0009	0.0001	0.0000	0.0000	0.0000	0.0000
F	SOUTH-SOUTHEAST	0.0011	0.0001	0.0000	0.0000	0.0000	0.0000
F	SOUTH	0.0020	0.0002	0.0000	0.0000	0.0000	0.0000
F	SOUTH-SOUTHWEST	0.0032	0.0003	0.0000	0.0000	0.0000	0.0000
F	SOUTHWEST	0.0058	0.0013	0.0000	0.0000	0.0000	0.0000
F	WEST-SOUTHWEST	0.0078	0.0068	0.0000	0.0000	0.0000	0.0000
F	WEST	0.0101	0.0307	0.0028	0.0000	0.0000	0.0000
F	WEST-NORTHWEST	0.0100	0.0308	0.0035	0.0000	0.0000	0.0000
F	NORTHWEST	0.0111	0.0149	0.0000	0.0000	0.0000	0.0000
F	NORTH-NORTHWEST	0.0078	0.0030	0.0000	0.0000	0.0000	0.0000

Appendix D

Geology and Soils (Soils Contamination)

DARHT EIS

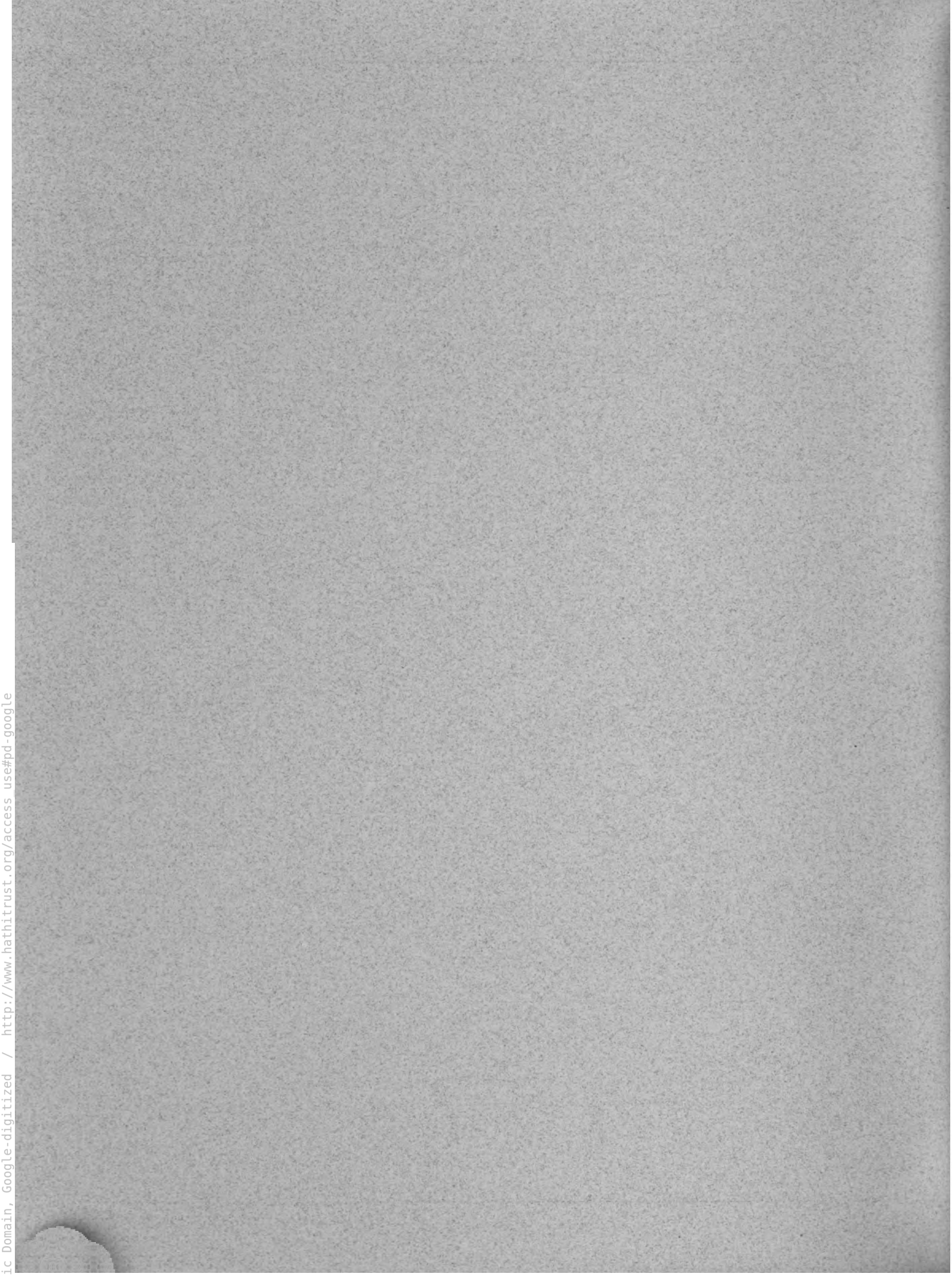

APPENDIX D
GEOLOGY AND SOILS (SOILS CONTAMINATION)

This appendix describes the soils contamination resulting from firing-site activities. The description is presented both in terms of the level of soils contamination evident at firing sites, and in terms of the distance from the firing point (i.e., the soil contamination circle radius) at which levels of contamination cannot be distinguished from known background concentrations of metals.

Observed contamination of the soils surrounding the PHERMEX firing point provides the basis for a reasonable estimate of future soil contamination levels at the PHERMEX or DARHT sites and the soil contamination circle radius applicable to either site. Data from the E-F firing sites, located on the watershed for Potrillo Canyon and also within TA-15, provide additional insight into the maximum soil contamination levels and the levels of contamination as a function of soil depth. Results from an aerial radiological survey provide an integrated assessment of surface soil contamination levels and show that the land area surrounding the PHERMEX firing point exhibits uranium-238 contamination above background levels. Finally, operational aspects of the cleanup of depleted uranium are summarized.

D.1 ABSTRACT

With respect to the soils environment, the existing PHERMEX firing site is an appropriate analogue for future contamination of firing sites located at either the PHERMEX or DARHT sites. PHERMEX is located approximately 2,000 ft (610 m) southeast of DARHT in TA-15 on Threemile Mesa. Soils, precipitation, and vegetation of the two sites are similar. A similar inventory of depleted uranium, i.e., 35,000 lb (~16,000 kg) depleted uranium (Anderson 1995), has been used at PHERMEX, as is planned for the No Action or DARHT Baseline alternatives, i.e., 46,000 lb (~21,000 kg) depleted uranium. Lesser amounts of beryllium and lead are forecast to be used in future tests than have been used in the past 32 years of testing at the PHERMEX firing site (Anderson 1995). Soils contamination observed at the E-F firing sites provides an upper bound to what might be expected under either the No Action Alternative (implying continued use of the PHERMEX site) or DARHT Baseline Alternative (implying use of the DARHT site) because of the higher inventory used at the E-F firing sites between 1943 and 1973. Based on soils contamination data from PHERMEX and E-F firing sites and the ratio of inventory planned for use versus that used at PHERMEX, the maximum average soil contamination level for depleted uranium at the firing point of the DARHT site is not anticipated to be greater than 5,300 ppm. Similarly, the maximum average soil contamination level observed at PHERMEX in the vicinity of the firing point under either the No Action or Upgrade alternatives would be approximately double that observed currently at PHERMEX or 9,300 ppm.

The amount of explosive used in individual tests would be no greater than that used at PHERMEX in the past 32 years. The general pattern and number of tests (i.e., large and small explosives amounts) would be virtually the same over the next 30 years (under any of the proposed alternatives) as that used during the past 32 years. Thus, the radius of a circle defining the area with soils contamination above background (soils contamination circle) at PHERMEX should be virtually the same for either continued operation at PHERMEX or operation of DARHT. That soil contamination circle radius at the PHERMEX site is approximately 460 ft (140 m).

Approximately 70 percent of the depleted uranium used at PHERMEX in open-air experiments is removed from the firing point and disposed during periodic cleanup operations. However, all beryllium, lead, copper, and aluminum used at the firing point in each alternative is assumed to be released to and remain in the environment within the soil contamination circle. Cleanup of these materials has not been documented. Surface soil concentrations of beryllium and lead indicate they drop to background levels within 200 ft (61 m) of the firing point, well within the soil contamination circle radius of 460 ft (140 m). No information was found on the distribution of copper and aluminum in firing site soils; however, it is assumed that they, like the other metals, remain initially within the soil contamination circle.

D.2 PHERMEX FIRING SITE SOIL CONTAMINATION

Results of a soil sampling survey conducted at the PHERMEX firing site have been reported (Fresquez 1994). Over 20 soil surface samples were collected from the 0- to 3-in (0- to 7.6-cm) depth at six distances along the length of four transects radiating outward from the center of the detonation area towards the NE, E, SE, and SSE. Two sediment samples were also collected: one located in a drainage channel about 240 ft (73 m) northeast of the detonation pad and the other located approximately 200 ft (61 m) south of the pad. Results of this sampling effort are summarized in table D-1, showing mean values at various distances from the firing point. Note, the data contained in table D-1 include background and, therefore, are not net values. Note also that the maximum average values, referred to later as the maximum average, does not occur at the same distance from the firing point for the different metals.

TABLE D-1.—*Average Uranium, Beryllium, and Lead Concentrations in Surface Soils at PHERMEX*

Sample Locations or Description – Distance ft (m)	Mean Concentrations (ppm)		
	Total Uranium	Beryllium	Lead
0	161.5	0.6	230.0
20 (6.1)	1746.9	18.5	93.9
40 (12.2)	3789.8	1.6	68.4
80 (24.4)	315.4	3.0	24.5
160 (48.8)	165.7	73.3	39.0
200 (61)	26.8	1.0	13.7
Simple Average	1210	18	52
NE Drainage Channel	105	3.1	16
S Drainage Channel	11.5	1.2	9.5
Background (mean + 2 std dev)	3.4	2.88	54

Source: Fresquez 1994

Total uranium (i.e., the sum of all uranium mass regardless of the isotope mix) in individual soil samples ranged in concentration from 0.8 to 13,398 ppm. The highest concentration, 13,398 ppm, is well above the other observations and resulted from a soil sample taken at the base of a building wall very near the firing point. The wall was exposed to fragments and aerosolized fractions during shots and apparently acts to concentrate depleted uranium in the soils immediately beneath the wall. Most samples were above the upper limit background (mean + 2 standard deviation) uranium concentration of 3.4 ppm for the firing site. Total beryllium (i.e., the sum of all beryllium mass regardless of the isotope mix) in individual surface soil samples ranged from 0.2 to 218 ppm, and total lead (i.e., the sum of all lead mass regardless of the isotope mix) concentrations ranged from 2.9 to 230 ppm. Most beryllium and lead data were also above the upper limit background concentrations of 2.88 and 54 ppm, respectively. However, soil concentrations of both beryllium and lead dropped to background levels at the maximum sampling radius of ~200 ft (~61 m). Simple averages of uranium, beryllium, and lead samples were 1,210, 18, and 52 ppm.

Using the radial measurement point as the center of an annulus having constant contaminant concentration, an area-weighted integration of total uranium concentration was performed. The integration considered only the upper 3 in (7.6 cm) of soil and assumed a dry bulk soil density of 1.4 g/cm^3. If measured surface soil depleted uranium contamination levels were applied to a full circle of radius 200 ft (61 m), the total uranium inventory in the soil would be 1,300 lb (568 kg) uranium. The area-weighted average total-uranium concentration, which takes into account the radial pattern of material deposition, was 456 ppm.

While measured values of beryllium and lead fell to background levels within the ~200 ft (~61 m) radial distance sampled, the total uranium levels did not. A regression analysis on the full (natural log-transformed) total uranium data set (Fresquez and Mullen 1995) showed the distance from the detonation pad to a point where total uranium concentrations would drop to upper limit background levels (i.e., 3.4 ppm) was 279 ± 83 ft (85 ± 25.3 m). The 95 percent upper confidence level of this one-sided estimate was 422 ft (128.6 m). This is an estimate of the soil contamination circle radius enclosing total uranium soil concentrations above background levels.

The drainage channel located northeast of the detonation pad yielded sediments containing 105 ppm total uranium. The channel to the south of the firing pad yielded sediments with only 11.5 ppm total uranium. No TCLP or total heavy metals were detected above EPA or background concentrations in any of the drainage channels. No traces of high explosive materials were detected in any of the soil or sediment samples.

A previous sampling study conducted at the PHERMEX site in 1987 (Fresquez 1995) showed levels of total uranium up to 3,593 ppm and of beryllium up to 470 ppm. A simple average concentration of surface soil samples yielded average uranium and beryllium concentrations for the site of 432 (± 647) ppm and 31.7 (± 83) ppm. Note, these are simple averages of all data and are not area-weighted mean values that would take into account the radial pattern of contaminant distribution.

D.3 E-F FIRING SITES SOIL CONTAMINATION

The E-F firing sites are located within TA-15, in the watershed for Potrillo Canyon. It has been estimated that between 1943 and 1973 up to 150,000 lb (66,500 kg) of uranium (a combination of natural and depleted uranium) were used in tests at the E-F firing sites (Hanson and Miera 1977). This is nearly four

times the inventory used at PHERMEX. The amount of explosive charge in individual tests at the E-F firing sites exceeds that proposed under the DARHT EIS. This implies that both the level of soil contamination and the spatial spread of debris at the E-F firing sites would be greater than has occurred at PHERMEX and is expected to occur under the alternatives examined in this EIS.

In 1976 a polar coordinate sampling pattern was used to collect soil samples at the E-F site for total uranium analysis (Hanson and Miera 1976; Hanson and Miera 1977; Hanson and Miera 1978). Samples were taken at nine distances from 33 to 660 ft (10 to 200 m) on transects that extended outward from the detonation pad every 45 degrees. Total uranium concentrations were determined for six depth increments ranging from 0 to 1 in to 0.66 to 1 ft (0 to 2.5 cm to 20 to 30 cm) depths. The variation in total uranium concentration with horizontal distance from the firing point for the surface soils [0 to 1 in (0 to 2.5 cm)] is presented in table D-2. The area-weighted mean uranium concentration for surface soils in the sampling area was 542 ppm.

Data on the vertical distribution of uranium in site soils were presented in Hanson and Miera (1977). Data collected at the E-F firing sites indicated that uranium had migrated into the soil to the maximum sampling depth; however, sample analyses were incomplete when Hanson and Miera published their work in 1977 and samples from 0.66 to 1 ft (20 to 30 cm) were not reported for all sample distances. Available results are presented in table D-3. The anomaly observed in the 33-ft (10-m) sample from 0.6 to 1 ft (20 to 30 cm) was attributed to a single observation of 22,000 ppm. Deletion of this datum from the mean value calculation resulted in a decreasing uranium concentration with increasing depth for all profiles. Extending the slope of the 33-ft (10-m) sample line in figure 5 Hanson and Miera (1977) results in an approximate value of 1,000 ppm total uranium in the 0.66- to 1-ft (20- to 30-cm) depth interval 33 ft (10 m) from the firing point.

The uranium in the top 2 in (5 cm) ranges between 86 and 43 percent of the total uranium at a sample point, with a regular decrease beyond 66 ft (20 m). Total uranium concentrations presented by Hanson and Miera (1977) show a general decrease with increasing depth. However, even at the maximum sample depths reported, total uranium concentrations were above background.

The E-F firing sites operated over a 30-year period and used on the order of 150,000 lb (66,500 kg) of uranium. The estimate of depleted uranium used at PHERMEX during the past 32 years is 35,000 lb (16,000 kg). The forecasted depleted uranium usage over the next 30 years is 46,000 lb (21,000 kg). Thus, if the No Action Alternative is implemented, the quantity of depleted uranium used at PHERMEX would increment from 35,000 lb (16,000 kg) to 82,000 lb (37,000 kg) depleted uranium over a 30-year period. This represents slightly more than half (57 percent) of the inventory used at E-F during its 30-year operation. Thus, future soil-contamination levels at PHERMEX firing site should not exceed and would likely be less than those observed at the E-F firing sites. If deposition is a linear function of inventory, soil contamination at PHERMEX would be approximately double the levels currently observed at the PHERMEX firing point, [e.g., 9,300 ppm = 4,000 ppm x 82,000 lb (37,000 kg)/35,000 lb (16,000 kg)].

The maximum explosive charge used in tests at the E-F firing sites exceeds that forecast for testing under any DARHT EIS alternative. As a result of tests involving larger explosive charges, uranium contamination in soils is spread over a larger area at the E-F firing sites than is observed at PHERMEX. The amount of explosive used in individual tests under any DARHT EIS alternative would be no greater than that used at PHERMEX in the past 32 years. Additionally, the general pattern and number of tests

TABLE D-2.—*Uranium Distribution in E-F Firing Site Surface Soils [0 to 1 in (0 to 2.5 cm)]*

Distance ft (m)	Mean Concentration (ppm)
0	4,650
33 (10)	4,520
66 (20)	1,000
98 (30)	1,800
130 (40)	745
160 (50)	395
250 (75)	350
330 (100)	520
490 (150)	725
660 (200)	165

Source: Hanson and Miera 1977

TABLE D-3.—*Distribution of Total Uranium with Depth in Surface Soils at the E-F Firing Site*

Distance ft (m)	Percent of total uranium in top 2 in (5 cm) of the column	Lowest Reported Depth [ft (cm)][a]	Concentration[b] (ppm)
0	86	0.33-0.5 (10-15)	650
33 (10)	48	0.66-1 (20-30)	~5000[c]
66 (20)	86	0.33-0.5 (10-15)	80
98 (30)	71	0.33-0.5 (10-15)	250
130 (40)	62	0.33-0.5 (10-15)	450
160 (50)	43	0.66-1 (20-30)	100

[a] Lowest depth presented in figure 5 of the Hanson and Miera report.
[b] Estimate from figure 5 of the Hanson and Miera report.
[c] Includes a value of 22,000 ppm.

Source: Hanson and Miera 1977

(i.e., large and small explosives amounts) would be virtually the same over the next 30 years (under any of the proposed alternatives) as that used during the past 32 years at PHERMEX. Based on the size of explosive forecast for use in the DARHT EIS alternatives, the current areal extent of contamination at

PHERMEX is a better analogue than the E-F firing sites for estimating the areal extent of future soils contamination at either PHERMEX or DARHT.

The E-F firing sites data does reveal that surface soil contamination levels at the PHERMEX firing point can be expected to increase for alternatives that involve continued use of the PHERMEX firing site. Still, average surface-soil total-uranium concentrations local to the firing point do not exceed 5,000 ppm at the E-F firing sites. The depth profile data suggest that uranium concentrations in soil ~1 ft (30 cm) or more below the surface can be expected to exceed background levels within 160 ft (50 m) of the firing point. However, contaminant concentrations at depth were measured to be a factor of 2 to 10 below surface soil contamination levels. Thus, with regard to soils contamination levels, average surface-soil total-uranium concentration levels at the E-F firing sites represent maximums.

D.4 AERIAL RADIOLOGICAL SURVEY

An aerial radiological survey of TA-15 was conducted in 1982 to estimate the extent of uranium (uranium-238) contamination in the vicinity of firing sites (Fritzsche 1989). The survey monitored levels of protactinium (protactinium-234m), a radioactive daughter of uranium-238. Surface contamination was seen to decrease radially as the distance from the test-firing area increased. A surface area of 630,000 ft^2 (58,600 m^2) around PHERMEX was estimated to be contaminated above background. The contaminated area can be represented by a circular area with radius of 450 ft (137 m) centered at the PHERMEX firing point (LATA 1992). The 450-ft (137-m) radius circle is rounded to 460 ft (140 m) for convenience.

D.5 MATERIAL RELEASES AND SITE CLEANUP DURING OPERATIONS

During the 32 years of PHERMEX operations, a total of about 35,000 lb (16,000 kg) of depleted uranium has been used. This amount of depleted uranium represents a volume of about 35 ft^3 (1 m^3). Most of the depleted uranium was used in the form of experimental assemblies of simulated nuclear weapons. Approximately 50 percent of the depleted uranium was contained in simulated secondaries and blast pipes of pin experiments. This depleted uranium is ejected as relatively large fragments. These large fragments remain in the immediate vicinity of the firing point. An estimated 40 percent of the total was dispersed as relatively small, platelet-shaped fragments having surface areas ranging from 0.08 to 1.1 in^2 (0.5 to 7 cm^2). An estimated 10 percent of the depleted uranium was released as an aerosol (McClure 1995).

LANL has estimated that at least 70 percent of the depleted uranium remains on or near the firing point and is removed and disposed of (see Waste Management in appendix B) during routine housekeeping. This 70 percent consists of all of the large fragments, half of the small fragments (i.e., those ejected downward), and some portion of the aerosol. Most of the other half of the small fragments would fall within a 4,100-ft (1,250-m) circle (McClure 1995).

In addition to depleted uranium, the only other materials of regulatory concern for the firing area are beryllium and lead. Materials released during open-air tests at the PHERMEX facility have resulted in observable quantities of beryllium and lead on or near the firing site. The soil sampling mentioned above indicates that no beryllium or lead are observed at levels above background beyond 200 ft (60 m) from the firing point.

Under the Enhanced Containment Alternative, three options are explored: the Vessel Containment Option, the Building Containment Option, and the Phased Containment Option. Normally, when containment would be used for a test shot, the blast products would remain in the containment vessel or building element designed to contain the test. Hence, a containment vessel would contain the blast debris; the debris would be taken to appropriate LANL facilities according to the nature of the debris. For the containment options, potential releases from containment vessels or the containment building are described by two conservative performance assumptions: no more than 1 percent of the blast byproducts could escape a normal test, and no more than 5 percent of the tests could cause a rupture of the containment vessel or building. While containment vessels and buildings would be designed not to fail and are not expected to fail, these assumptions address the possibility of failure. A rupture of a containment vessel means the development of a crack, not a catastrophic explosion of the entire containment vessel. Thus, a 6 percent release of inventory as blast byproducts for all contained test shots represents a highly unlikely result. To be conservative, it is also assumed that all blast byproducts that escape contained tests (i.e., in Vessel Containment, Building Containment, and Phased Containment options) would be in the soils surrounding the firing point and not removed from the site by any routine cleanup activity.

Under the Vessel Containment and Phased Containment options, some uncontained experiments would be conducted. In the case of the vessel containment option, up to 25 percent of the inventory would be shot in uncontained tests. In the case of the phased containment option, three phases would occur in the uncontained-to-contained percentages: 95 percent uncontained and 5 percent contained for 5 years, 60 percent uncontained and 40 percent contained for 5 years, and finally 25 percent uncontained and 75 percent contained for 20 years. All uncontained testing would be conducted under site cleanup protocols similar to those used today, and consequently only 30 percent of the depleted uranium inventory expended in uncontained tests would remain in the soil at the firing site. However, all beryllium and lead released in uncontained tests is assumed to remain in the soils at the firing site.

D.6 SOIL CONTAMINATION CIRCLE RADIUS AND SOIL CONTAMINATION LEVELS

The estimate of the soil contamination circle radius from the aerial radiological survey (i.e., 460 ft or 140 m) is comparable to the 420-ft (128-m) radius calculated by Fresquez and Mullen (1995) as defining the 95 percent upper-confidence level of enclosing all above-background total-uranium soil contamination. The soil survey conducted by Fresquez (1994) only characterized an ~200-ft (~61-m) radius circle centered on the firing point and may reflect only a portion of the fragment and aerosol size fractions. However, the aerial radiological survey takes into account uranium (uranium-238) concentration levels associated with the complete range of fragment sizes as well as the aerosol fraction. Based on the similarity of tests to be run in the future as compared to past PHERMEX operations (e.g., explosive charges, the range and pattern of large and small tests), we conclude that the soil contamination area around PHERMEX [defined approximately by a circle with radius 460 ft (140 m) centered on the firing point] is appropriate for application to alternatives involving either PHERMEX or DARHT sites.

The inventory of depleted uranium used at PHERMEX over the last 32 years is ~35,000 lb (~16,000 kg). Of this, 30 percent, or 11,000 lb (4,800 kg) of depleted uranium, is estimated to remain within the soil contamination circle. Clearly, this is greater than the estimated 1,300 lb (568 kg) of uranium accounted for in the surface soils (i.e., to 3 in or 7.5 cm depth) within 200 ft (61 m) of the firing point at PHERMEX. However, a circle of radius 200 ft (61 m) represents only ~20 percent of the area of the soil contamination circle that has a radius of 460 ft (140 m). If 11,000 lb (4,800 kg) of depleted uranium

were uniformly distributed in the upper ~1 ft (~30 cm) of soil within an ~460-ft (~140-m) radius soil contamination circle, the resulting uranium concentration would be ~190 ppm.

Under the No Action Alternative, the total inventory of depleted uranium used at PHERMEX after an additional 30 years would be 82,000 lb (37,000 kg) of depleted uranium. Of this, 30 percent, or ~24,000 lb (~11,000 kg), of depleted uranium would remain onsite within the soil contamination circle and contribute to soil contaminant concentrations. If initially distributed uniformly in the upper ~1 ft (30 cm) of the soil contamination circle, the resulting uranium concentration would be 430 ppm.

While total uranium concentration in soils in the immediate vicinity of firing points is known to be significantly higher (e.g., average values of 3,789 and 4,650 ppm values calculated for PHERMEX and E-F firing sites), these areas represent a relatively small fraction of the overall soil contamination circle in an area-weighted average. Area-weighted average concentrations calculated at E-F (542 ppm for a 660-ft or 200-m radius) and PHERMEX (456 ppm for a 200-ft or 61-m radius) are comparable to those calculated for the uranium inventory forecast to be within the soil contamination circle of PHERMEX operations (i.e., 190 ppm current and 430 ppm future).

The soil contamination circle radius of current PHERMEX operations, 460 ft (140 m), is assumed to apply to alternatives involving either the PHERMEX or DARHT sites. Based on soils contamination data from PHERMEX and E-F firing sites and the ratio of inventory planned for usage versus that used at PHERMEX, the maximum average soil contamination level for depleted uranium at the firing point of the DARHT site is not anticipated to be greater than 5,300 ppm (i.e., 4,000 ppm x 46,000 lb (21,000 kg) depleted uranium/35,000 lb (16,000 kg) depleted uranium). Similarly, the maximum average soil contamination level observed at PHERMEX in the vicinity of the firing point under either the No Action or Upgrade PHERMEX alternatives is not anticipated to be greater than double that observed currently at PHERMEX or 9,300 ppm [i.e., 4,000 ppm x 82,000 lb (37,000 kg) depleted uranium/35,000 lb (16,000 kg) depleted uranium].

It is apparent from the recent surface soil survey of PHERMEX (Fresquez 1994) that beryllium and lead contamination drops to background levels inside of the soil contamination circle for depleted uranium. However, no information is available on site cleanup and removal of beryllium and lead. Therefore, the entire original inventory of both beryllium and lead is assumed to be dispersed within the soil contamination circle and available for migration in hydrologic pathways.

There is no information on the distribution of copper and aluminum in the soils surrounding the PHERMEX firing point. Nor is there information about periodic cleanup activities at the firing point removing either copper or aluminum. Consequently, total inventories of copper and aluminum are assumed to be in the soils and available for migration via surface water and ground water pathways.

D.7 REFERENCES CITED IN APPENDIX D

Anderson, A.B., 1995, *Materials Expended Report for Phermex,* LANL Memorandum No. DX-11-95-109, March 16, Los Alamos National Laboratory, Los Alamos, New Mexico.

Fresquez, P., 1994, *Results of the Soil Sampling Survey Conducted Over Active RCRA Firing Site TA-15-184 (PHERMEX),* LANL Memorandum No. ESH-8/EFM-94-111, May 26, Los Alamos National Laboratory, Los Alamos, New Mexico.

Fresquez, P., 1995, *Documentation of a Soil Uranium and Beryllium Study Conducted at PHERMEX in 1987,* LANL Memorandum No. ESH-20/EARE-95-0449, February 23, Los Alamos, New Mexico.

Fresquez, P., and M. Mullen, 1995, *Regression Analysis on Soil Uranium Data Collected from PHERMEX,* LANL Memorandum No. ESH-20/EARE-95-0367, February 2, Los Alamos National Laboratory, Los Alamos, New Mexico.

Fritzsche, A.E., 1989, *An Aerial Radiological Survey of Technical Area 15 and Surroundings, Los Alamos National Laboratory,* EGG-10282-1095, September, EG&G Energy Measurements, Albuquerque, New Mexico.

Hanson, W.C., and F.R. Miera, Jr., 1976, *Long-Term Ecological Effects of Exposure to Uranium,* LA-6269, July, Los Alamos National Laboratory, Los Alamos, New Mexico.

Hanson, W.C., and F.R. Miera, Jr., 1977, *Continued Studies of Long-Term Ecological Effects of Exposure to Uranium,* LA-6742/AFATL-TR-77-35, June, Los Alamos National Laboratory, Los Alamos, New Mexico.

Hanson, W.C., and F.R. Miera, Jr., 1978, *Further Studies of Long-Term Ecological Effects of Exposure to Uranium,* LA-7162/AFATL-TR-78-8, July, Los Alamos National Laboratory, Los Alamos, New Mexico.

LATA (Los Alamos Technical Associates, Inc.), 1992, *Appendix E to the Operable Unit 1086 RFI Work Plan, Calculation of Acceptable Levels of Surface Contamination at Technical Area-15 (PHERMEX),* November, Los Alamos, New Mexico.

McClure, D.A., 1995, *DARHT EIS Section 3.1.3.2 Effluents (Mass Balance),* internal memorandum to S.T. Alexander March 21, Los Alamos National Laboratory, Los Alamos, New Mexico.

Appendix E
Water Resources

DARHT EIS

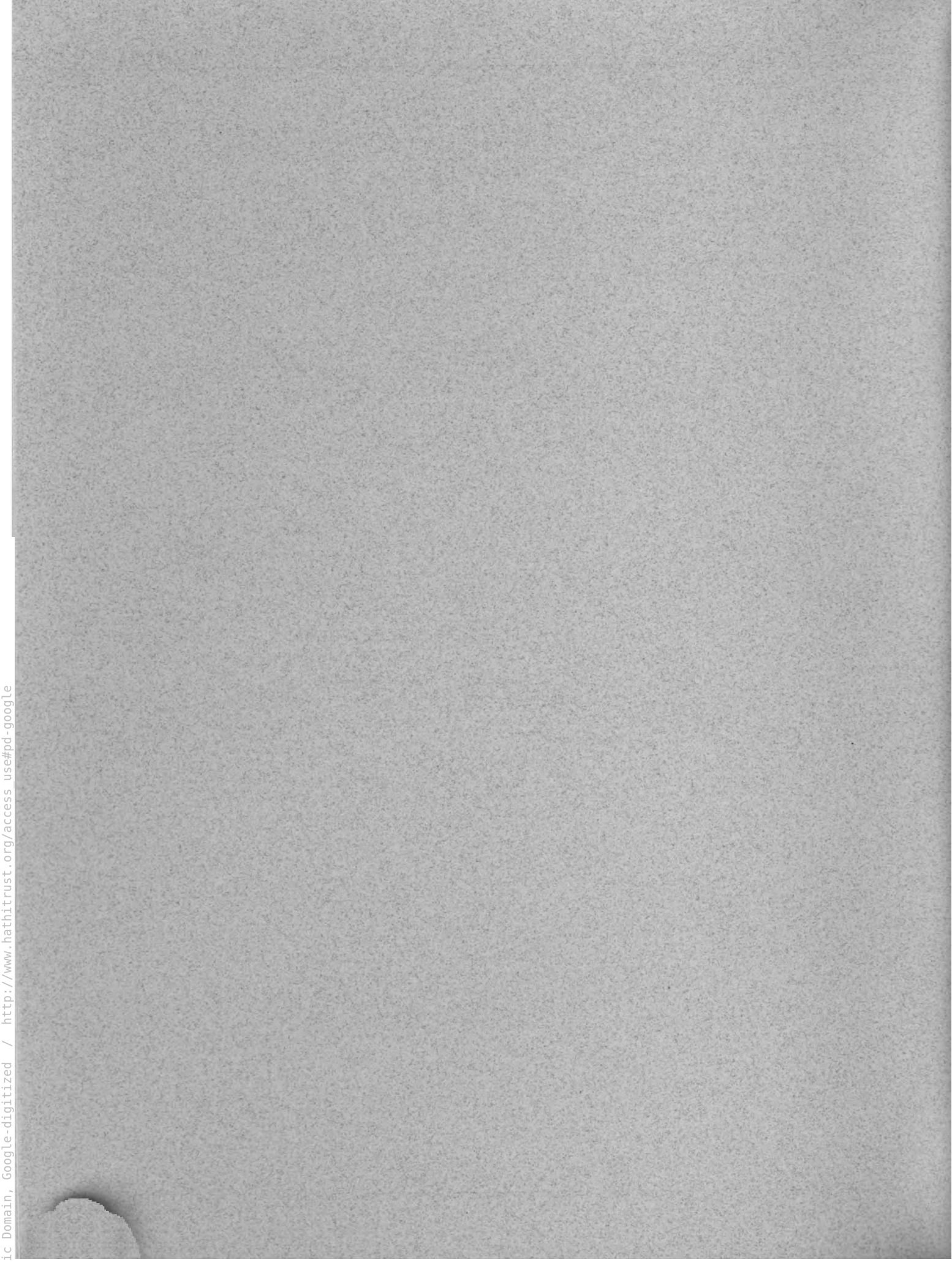

APPENDIX E
WATER RESOURCES

This appendix provides background information on 1) estimates of recharge at the mesa top (i.e., firing sites), 2) the solubilities and distribution coefficients associated with the metals of interest when associated with LANL site sediments, 3) the approach taken to model surface water pathway, and 4) the approach taken to model the vadose zone and ground water pathways.

APPENDIX E1: DEEP DRAINAGE BENEATH THE DARHT AND PHERMEX SITES

E1.1 ABSTRACT

Meteoric water that drains well below the lowest level of plant roots is called deep drainage and can transport solubilized contaminants through vadose zone deposits to ground water. This pathway for contaminant migration to the accessible environment must be evaluated to understand the potential for surface soil contamination to migrate through the mesa and underlying vadose zone to ground water. The objective of this study was to estimate the deep drainage rates at two locations, the DARHT and PHERMEX sites. Estimates of deep drainage were performed using the UNSAT-H computer code, daily weather data from 1980 to 1994, and, in lieu of site-specific data, surrogate information for the hydrologic properties of vegetation and soils. Drainage rates were determined for a variety of soil and vegetation scenarios; the actual rates depend explicitly on the site-specific surface conditions. For the scenarios studied, the drainage rates ranged from 4.7 to 520 mm/yr. For the center of the DARHT site, the rates for an unvegetated surface were 265 and 360 mm/yr depending on the soil type. Modifying the surface with a gravel cover increased the drainage rate to 520 mm/yr. For the center of the PHERMEX site, the rate was 124 mm/yr for the unvegetated surface. Allowing shrubs and grasses to grow on the sites reduced, but did not eliminate, deep drainage. The potential exists for deep drainage at both sites. Whether deep drainage actually exists can only be determined with site-specific measurements.

E1.2 INTRODUCTION

One component of the DARHT EIS is an analysis of the potential for deep drainage beneath the DARHT and PHERMEX sites to carry contaminants to the main aquifer. At other DOE sites, deep drainage has transported solubilized contaminants to underlying ground water systems. While such transport is not apparent beneath Threemile Mesa on which DARHT and PHERMEX are located, it does represent a pathway of interest and must be evaluated. The objective of this portion of the EIS was to estimate the deep drainage rate beneath the DARHT and PHERMEX sites.

E1.3 PRIOR ESTIMATES

Information on the rates of deep drainage beneath the DARHT and PHERMEX sites was unavailable. However, occasional monitoring at other locations at LANL indicates that deep drainage rates are highly variable, ranging from near zero to more than the annual precipitation rate, depending on the surface conditions at each of the specific locations.

Abeele et al. (1981) and Nyhan (1989a) reported water content profiles measured with neutron probes in several deep access wells. Some wells had low water contents in the tuff, indicating little, if any, deep drainage. Other wells had high water contents, particularly in the upper zones of tuff, possibly indicative of recent deep drainage. In one well, the high water contents implied that water was added in excess of precipitation rates. Nyhan (1989) speculated that an unlined drainage ditch routed surface water to the vicinity of the well, where the water subsequently infiltrated. Abeele et al. (1981) also alluded to the influence of surface topography as a factor in affecting infiltration rates and thus deep drainage rates.

Abeele et al. (1981) reported that the flux in the overburden above a waste disposal pit was always directed downward below a depth of about 13 ft (4 m) during a two-year period. In 1978, it was 3.5 in/yr (90 mm/yr); in 1979, it was 6 in/yr (150 mm/yr). The difference was attributed to extremely high precipitation at the end of 1978 and the beginning of 1979. At another location at LANL, Abeele et al. (1981) estimated a downward rate of 0.01 in/yr (0.3 mm/yr). It has been summarized as follows:

> "Where the soil cover has not been disturbed, little if any water from precipitation infiltrates the underlying tuff (Purtymun and Kennedy 1971). Where the soil cover was disturbed, as in the waste disposal areas, the moisture content of the tuff indicates a much higher degree of infiltration than the one that might have been implied by the moisture content fluctuations found in the undisturbed tuff (Abeele et al. 1981)."

Rogers and Gallaher (Rogers 1995) reviewed the hydraulic properties of the Bandelier Tuff as well as other units. Their review included core data from several areas at the LANL facility; the data came from both mesa tops and canyon bottoms. They concluded that "[t]he canyon bottom and mesa top hydraulic head profiles suggest that downward flow of water occurs beneath the surface of the Pajarito Plateau" (Rogers 1995). They noted two exceptions where there was the suggestion of upward flow, one of which they speculated was caused by "increased external air circulation through the mesa sides."

Core data were unavailable for the DARHT and PHERMEX sites. In lieu of site-specific data, data reported by Rogers and Gallaher (Rogers 1995) for other mesa tops were used to estimate deep drainage. Assuming a hydraulic gradient close to unity, one can equate the in situ hydraulic conductivity to the drainage rate. Rogers and Gallaher lumped core data together to calculate mean in situ conductivity values. In their table 5, Rogers and Gallaher report both harmonic and arithmetic mean values of hydraulic conductivity. For Area TA-54, Rogers and Gallaher reported values ranging from 1.7×10^{-6} to 0.06 in/yr (4.3×10^{-5} to 1.5 mm/yr) for the harmonic and arithmetic means, respectively. For Area TA-16, the rates ranged from 3 to 55 in/yr (79 to 1,390 mm/yr). For Area TA-53, the rates ranged from 7 to 3,660 in/yr (180 to 93,000 mm/yr). While not from the DARHT or PHERMEX sites, these ranges indicate clearly that deep drainage can vary greatly from site to site.

The impact of early and recent LANL operations may not always be reflected in core data – and this makes interpretation difficult. For example, Allison et al. (1994) related the case of land clearing in Australia in which the recharge rate increased from 0.003 to 1.8 in/yr (0.08 to 45 mm/yr). The pressure front generated by the increase in recharge took nine years to reach the 25-ft (7.5-m) depth. Foxx and Tierney (1984) related the historical occurrence of grazing and logging as well as the impact of recent disturbances from LANL operations. Generally, such changes alter plant communities and reduce their ability to transpire water, thus increasing the potential for deep drainage. Depending on the pre-disturbance drainage rate, an increase in drainage may take decades or centuries to propagate downward through the tuff. Thus, core data collected today must be interpreted and used cautiously, especially if one does not know or account for the history of surface conditions at specific sites.

E1.4 METHOD

Deep drainage was estimated at the DARHT and PHERMEX sites using simulation modeling. Simulations were conducted using the UNSAT-H Version 2.02 computer code (Fayer and Jones 1990). The UNSAT-H computer code, developed for the Hanford site, was selected because it was developed for and has been applied to estimate deep drainage at DOE sites in the arid and semi-arid western United States. The code models one-dimensional, deep drainage, accounting for the hydrological characteristics of soil media, climate, and vegetation. The exhibit E1-1 contains a listing of an example input file for UNSAT-H. The model requires information on the domain, soil properties, initial conditions, boundary conditions, and plants.

E1.4.1 Domain

The model domain extended to 16 ft (5 m). This depth is well below the zone of evapotranspiration for most species. Some roots have been observed at greater depths within fractures (Tierney and Foxx 1987), but these were not considered in this one-dimensional modeling exercise. Also, because of the one-dimensional nature of this analysis, processes such as interflow (subsurface lateral drainage) were not addressed. The node spacing ranged from 0.1 in (0.2 cm) at the soil surface to 20 in (50 cm) at the 16-ft (5-m) depth. At the transition between different materials, the node spacing was reduced to 0.8 in (2.0 cm).

E1.4.2 Soil Properties

The soil at the center of the DARHT site is mapped as Pogna sandy loam (Nyhan et al. 1978). Some of the soil samples collected at the DARHT site for a geotechnical investigation report (Korecki 1988) indicated that there is more clay than expected for a Pogna sandy loam. Nyhan et al. (1978) indicated that the Pogna sandy loam has small inclusions of other soil types. Based on the descriptions reported by Korecki (1988), a likely candidate for some of the soil at the DARHT site is the "Typic Eutroboralf, fine," which includes layers of sandy loam, sandy clay, and clay. In the blueprints for the DARHT Facility (LANL 1993a), several drawings indicate surface modifications that include stripping the soil off and building directly on the tuff as well as covering the surface near the firing point with gravel. At some distance from the center of the DARHT site is another soil type, the Seaby loam,

EXHIBIT E1-1.—*Example Input File for UNSAT-H Computer Code*

```
DP1:  Typic Eutroboralf, fine, with grass-shrub cover 40%,
day 74 and 288
    1    1    1    1    0    0    0
iplant,lower,ngrav,iswdif,etc.
    0  365  365    1    1    0       0.0
nprint,dayend,ndays,nyears,etc.
    1    2    0    1    0
nsurpe,nfhour,itopbc,et_opt,icloud
    4    1    1    0    3    1
kopt,kest,ivapor,sh_opt,inmax,inhmax
       0.0  1.00e+05       0.0       0.0
hirri,hdry,htop,dhmax
   5.0e-05  1.00e+00   1.0e-08      24.0
dmaxba,delmax,delmin,stophr
      0.66    288.46      0.24       1.0
tort,tsoil,vapdif,qhtop
       0.0       0.0       0.0       0.0
tgrad,tsmean,tsamp,qhleak
       0.5       1.6   1.0e-06   0.0e-00
wtf,rfact,rainif,dhfact
    5   68                                        matn,npt
   1       0.0   1       0.2   1       0.4   1       0.6
   1       0.8   1       1.0   1       1.4   1       1.8
   1       2.4   1       3.0   1       4.0   1       5.5
   1       7.0   1       9.0   1      11.0   1      13.0
   1      15.0   1      17.0   5      19.0   5      21.0
   5      23.0   5      25.0   5      27.0   5      29.0
   5      31.0   5      33.0   5      35.0   5      38.0
   5      41.0   5      44.0   5      46.0   5      48.0
   5      50.0   4      52.0   4      54.0   4      56.0
   4      59.0   4      63.0   4      68.0   4      74.0
   4      80.0   4      84.0   4      86.0   4      89.0
   4      91.0   4      93.0   3      95.0   3      97.0
   3      99.0   3     102.0   3     106.0   3     110.0
   3     115.0   3     123.0   3     135.0   3     150.0
   3     175.0   3     200.0   3     225.0   3     250.0
   3     275.0   3     300.0   3     325.0   3     350.0
   3     375.0   3     400.0   3     450.0   3     500.0
 Sandy loam retention
    0.4100    0.0650    0.0750    1.8900
 Sandy loam conductivity
         2      4.43    0.0750    1.8900       0.5
 Gravel retention
     0.419    0.0050    4.9300      2.19
 Gravel conductivity
         2    1260.0    4.9300      2.19       0.5
 Tuff retention
    0.4690    0.0450    0.0029     1.884
 Tuff conductivity
         2    0.1188    0.0029     1.884       0.5
 Sandy clay retention
    0.3800    0.1000    0.0270     1.230
 Sandy clay conductivity
         2    0.1200    0.0270     1.230       0.5
 Clay retention
    0.3800    0.0680    0.0080     1.090
 Clay conductivity
         2    0.2000    0.0080     1.090       0.5

*** Initial matric suction values go here
```

EXHIBIT E1-1.—*Example Input File for UNSAT-H Computer Code – Continued*

```
Plant information for shrubs and grasses
    1     1     1     1    74   288                          leaf,nfroot,nuptak,nfpet,etc
   12   0.6                                                  npoint,bare
    0  0.70    91  0.70   105  1.00   121  1.33   135  1.70 ngrow,flai
  213  1.70   227  1.60   244  1.50   258  1.28   274  1.08 ngrow,flai
  305  0.70   366  0.70                                     ngrow,flai
     0.000     0.0000     1.0000                            aa,b1,b2
    0     0     0     0     0     0     0     0     0     0 ntroot
    0     0     0     0     0     0     0     0     0     0
    0     0     0     0     0     0     0     0     0     0
    0     0     0     0     0     0     0     0     0     0
  366   366   366   366   366   366   366   366   366   366
  366   366   366   366   366   366   366   366   366   366
  366   366   366   366   366   366   366   366
   4.0e+04    1.0e+03       30.0                            hw,hd,hn
   4.0e+04    1.0e+03       30.0                            hw,hd,hn
   4.0e+04    1.0e+03       30.0                            hw,hd,hn
   4.0e+04    1.0e+03       30.0                            hw,hd,hn
   4.0e+04    1.0e+03       30.0                            hw,hd,hn

*** Meteorological data go here
```

which should be considered. Thus, five soil scenarios were envisioned for this analysis: 1) tuff, 2) gravel above tuff, 3) Pogna sandy loam, 4) Typic Eutroboralf, fine, and 5) Seaby loam. Table E1-1 shows the soil profile description for each scenario.

The soil type at the center of the PHERMEX site is mapped as Nyjack loam (Nyhan et al. 1978). Nearby soil types include the Seaby loam (included in the DARHT scenario list) and the Hackroy sandy loam. The Nyjack loam and Hackroy sandy loam were added to the list in table E1-1 to bring the total number of soil profile scenarios to seven.

Hydraulic properties were assigned to each porous material in table E1-1. Specifically, water retention and hydraulic conductivity were described using the van Genuchten (1980) retention function and the Mualem (1976) conductivity model; table E1-2 shows the parameters. Hydraulic properties specific to the site soils were unavailable. Instead, the particle size description (e.g., sandy loam, clay) was used to assign parameters based on the correlations reported by Carsel and Parrish (1988). For those materials with gravel, the hydraulic parameters reported by Carsel and Parrish (1988) were modified using the method proposed by Bouwer and Rice (1983). The actual properties of the tuff unit beneath the surface of the DARHT site were unknown. For this study, the properties of the Tshirege Unit 3 were used (Rogers 1995). This unit appears to be the highest in elevation for which hydraulic properties are available. All hydraulic properties were assumed to be isothermal and non-hysteretic. Soil freezing was not addressed.

E1.4.3 Initial Conditions

There was no information on the 1980 matric suction distribution at the DARHT or PHERMEX sites. Therefore, the first year (1980) of every simulation was repeated until the water balance variables (i.e.,

TABLE E1-1.—*Soil Profile Descriptions for the Computer Simulations*

Soil Profile	Depth Interval (cm)	Porous Material
Tuff	0 to 500	tuff
Gravel Above Tuff	0 to 30	gravel
	30 to 500	tuff
Pogna Sandy Loam	0 to 30	sandy loam
	30 to 500	tuff
Typic Eutroboralf, fine	0 to 18	sandy loam
	18 to 51	clay
	51 to 94	sandy clay
	94 to 500	tuff
Seaby Loam	0 to 13	loam
	13 to 25	clay loam, 40 percent gravel
	25 to 30	clay loam, 55 percent gravel
	30 to 66	gravel
	66 to 500	tuff
Nyjack Loam	0 to 8	loam
	8 to 61	clay loam
	61 to 99	sandy loam, 25 percent gravel
	99 to 500	tuff
Hackroy Sandy Loam	0 to 8	sandy loam
	8 to 25	clay
	25 to 30	clay, 25 percent gravel
	30 to 500	tuff

evaporation, transpiration, drainage, and runoff) changed by less than 0.004 in (0.1 mm) from one year to the next. The reason for the iteration was to lessen the impact of the unknown initial conditions.

E1.4.4 Boundary Conditions

The surface boundary was described with weather data, which were summarized by Bowen (1990). The daily precipitation data were obtained for the TA-59 site for 1980 to 1990 and the TA-6 site for 1991 to 1994. During each day, the precipitation was added at the rate of 0.4 in/h (1 cm/h) until the day's total was applied to the surface. Snow was treated as an equivalent rainfall. No adjustment was made for delays in snowmelt.

Daily potential evapotranspiration (PET) values were calculated using the Penman Equation in Doorenbos and Pruitt (1977) and daily weather parameters from the TA-59 and TA-6 sites. These parameters included wind speed at 75 ft (23 m), maximum and minimum air temperature and dew-point temperature at 4 ft (1.2 m), solar radiation, and cloud cover. The dew-point temperature data set was sparse. When data existed, a comparison to measured minimum air temperature showed the dew-point temperature to

TABLE E1-2.—*Parameters Used to Describe Hydraulic Properties in the Simulations*

Porous Material	Gravel (vol %)	θ_s	θ_r	α (1/cm)	n	K_s (cm/h)
Tuff	0	0.469	0.045	0.0029	1.88	0.119
Gravel	100	0.419	0.005	4.93	2.19	1260.0
Sandy loam	0	0.410	0.065	0.075	1.89	4.42
Sandy loam	25	0.308	0.049	0.075	1.89	2.83
Sandy clay	0	0.380	0.100	0.027	1.23	0.12
Loam	0	0.430	0.078	0.036	1.56	1.04
Clay loam	0	0.410	0.095	0.019	1.31	0.26
Clay loam	40	0.246	0.057	0.019	1.31	0.122
Clay loam	55	0.185	0.043	0.019	1.31	0.0846
Clay	0	0.380	0.068	0.008	1.09	0.200
Clay	25	0.285	0.051	0.008	1.09	0.130

θ_s Saturated moisture content.
θ_r Residual moisture content.
α Fitted van Genuchten parameter, 1/cm.
n Fitted van Genuchten parameter.
K_s Saturated hydraulic conductivity, cm/h.

Note: The van Genuchten parameter m was set equal to 1-1/n. The standard value of 0.5 was used for the pore interaction term.

be less than or equal to the minimum air temperature. Because a relatively complete record of daily minimum air temperature existed, the daily dew-point temperature was approximated as the minimum air temperature. Cloud cover data were not available. Instead, cloud cover was approximated using the measured solar radiation and calculations of the potential solar insolation for Los Alamos (Campbell 1985).

During the evaporation process, the matric suction of the surface node was not allowed to exceed a predetermined value. For most of the simulations, the value was 1,450 lb/in^2 (10 MPa). For the gravel surface scenario, however, this limit increased the difficulty of the solution. Instead, a value of 14.5 lb/in^2 (0.1 MPa) was used.

The bottom boundary was described with a unit gradient condition. Observations at other sites indicate that unit gradient conditions exist in the tuff in certain zones at certain sites, but it is not universal. For these simulations, plant roots were assumed to be no more than 3.3 ft (1 m) deep. As long as the simulations indicated that deep drainage was greater than 0.04 in/yr (1 mm/yr), the unit gradient condition at 16 ft (5 m) was assumed to be valid.

E1.4.5 Plants

Plant information consisted of the method to partition potential evapotranspiration, active season, bare fraction, root length density, and maximum root depth during the year, as well as the effectiveness of plant water withdrawal as a function of soil matric suction. According to the Environmental Restoration Program (ERP), the plant community on the PHERMEX mesa is the piñon-ponderosa-juniper association (LANL 1993b). In the vicinity of the facilities, however, this community has been eliminated and replaced by structures (e.g., roads, parking lots, buildings), bare ground, and shrubs and grasses. Data for those plants pertinent to the DARHT and PHERMEX sites were not available. Instead, literature parameters or reasonable estimates of parameters were chosen. Plant responses to precipitation and temperature variations, fire, disease, nutrient cycling, grazing, and land use changes were not addressed in the simulations.

The leaf area method was used to partition potential evapotranspiration into potential evaporation and potential transpiration. Leaf area as a function of season was described using values reported by Nyhan (1989b) for a 40 percent cover of shrubs and grasses.

The active season of the plants determined when to calculate transpiration and when roots started or stopped growing. The active season was specified with starting and ending days during the year. The shrubs and grasses were started on March 15 (day 74) and stopped on October 15 (day 288). These dates were estimates only but are reasonable given the monthly temperatures experienced at Los Alamos (Bowen 1990).

The bare fraction of soil was used to scale potential transpiration based on the amount of soil surface covered by the vegetation. If the bare fraction was zero, the cover percentage would be 100 percent and there would be no reduction in potential transpiration. For the grasses and shrubs cover, the bare fraction was assigned as 0.6. This means that the vegetation covered 40 percent of the ground surface (Nyhan 1989b); therefore, potential transpiration was appropriately reduced by 60 percent. Any reduction to potential transpiration caused by a less than 100 percent cover is added to potential evaporation. After all the manipulations, the sum of potential evaporation and potential transpiration must equal potential evapotranspiration.

Root length density data were unavailable. The roots of the grasses and shrubs were considered to be at their maximum depth throughout the growing season. The maximum depth was defined as the surface of the uppermost tuff unit. This depth ranged from 12 in (30 cm) in the Pogna sandy loam to 39 in (99 cm) in the Nyjack loam. Roots have been observed in cracks and fissures in the tuff (Tierney and Foxx 1987). For this one-dimensional analysis, however, cracks and fissures were not considered in the conceptual model.

Data on plant water uptake as a function of matric suction were also unavailable. A matric suction of 0.4 lb/in^2 (0.003 MPa) was assumed to be the limit below which plants ceased transpiration because of anaerobic conditions. From 0.4 to 14.5 lb/in^2 (0.003 to 0.1 MPa), plants were assumed to withdraw water at the potential rate. Above 14.5 lb/in^2 (0.1 MPa), but below the permanent wilting point, plants were assumed to withdraw progressively less water as the matric suction increased. Typically, the matric suction above which plants cease to transpire is 220 lb/in^2 (1.5 MPa) (i.e., the permanent wilting point).

Sagebrush was reported to operate in soils with matric suctions as high as 1,000 lb/in^2 (7.0 MPa) (Fernandez and Caldwell 1975; Branson et al. 1976). For this study, as an approximation, an intermediate value of 580 lb/in^2 (4.0 MPa) was chosen.

E1.5 RESULTS

Table E1-3 shows that the deep drainage rate is highly dependent on the soil profile and the presence of vegetation. Table E1-3 also shows that, for a given combination of soil profile and vegetation, the year-to-year rates [as estimated at the 16-ft (5.0-m depth)] can vary by more than a factor of two. Figures E1-1 to E1-6 illustrate the yearly variation more clearly.

The deep drainage rate at the center of the DARHT site was estimated to be 10 or 14 in/yr (265 or 360 mm/yr) depending on the soil type and assuming vegetation was not allowed to grow. Table E1-3 shows that the estimated rates were reduced by more than half when plants were included. If the immediate center of the site was covered with a layer of gravel (LANL 1993b), the drainage rate would nearly double to 20 in/yr (520 mm/yr), or 95 percent of the precipitation. If the tuff were left exposed at any point, the results in table E1-3 suggest that the drainage rate would be only 1.3 in/yr (34 mm/yr), which is much lower than the rates estimated for the soils. The reason is that the tuff holds infiltrating water relatively near the surface, and its soil hydraulic properties are conducive to upward unsaturated flow. Thus, higher evaporation rates occur from exposed tuff surfaces.

At some distance from the center of the DARHT site is the Seaby loam soil. The simulation results indicate the drainage rate in this soil type is much less than for either the Pogna sandy loam or Typic Eutroboralf soils.

The deep drainage rate at the center of the PHERMEX site was estimated to be 5 in/yr (124 mm/yr) (assuming vegetation was not allowed to grow). At some distance from the center of the PHERMEX site are the Seaby loam, with rates slightly higher than the Nyjack loam, and the Hackroy sandy loam, with rates three times greater than the Nyjack loam without plants, and thirty times greater than the Nyjack loam with plants.

These results are in accord with previous simulation results (Nyhan 1989a) for seepage through covers over waste disposal areas. Nyhan estimated seepage rates of 2.4 and 4.8 in/yr (60 and 120 mm/yr) for a cover with range grass and a bare cover, respectively, assuming a saturated conductivity of 0.08 in/h (0.2 cm/h) for the cover. For the years 1977 to 1987, Nyhan showed that the seepage rate varied between 0 and 6.3 in/yr (0 and 160 mm/yr) for the bare cover and for a cover with a poor range grass.

When the precipitation rate exceeds the ability of the soil to accept infiltration, water begins to accumulate on the soil surface. Once the storage capacity of the soil surface is exceeded, overland flow, or runoff, begins. The UNSAT-H model assumes zero surface storage; thus, water that does not infiltrate is considered to be runoff. Table E1-3 shows the average annual runoff for each of the simulations. Only those soil profiles that had one or more clay layers had runoff. The Nyjack loam, Seaby loam, and Hackroy sandy loams had the highest rates; the Seaby loam was highest with 1.2 in/yr (30 mm/yr). Some of these high rates were comparable to the drainage rate. For the Nyjack loam, the runoff rate was actually twice the drainage rate [which, in this case, was quite low at 0.02 in/yr (4.7 mm/yr)]. The impact of frozen soil, snow, and rapid snowmelt on runoff and deep drainage was not evaluated.

TABLE E1-3.—*Summary of Simulation Results for 1981 to 1994*

Soil[a] Profile	Max. Root Depth (cm)	Average Annual Rates (mm/yr)				Annual Drainage Rates (mm/yr)		Average Annual Mass Error	
		Evaporation	Transpiration	Runoff	Drainage	Max	Min	mm	% of drain
Tuff	na	505.5	0.0	0.4	33.8	44.3	16.5	0.1	0.3
Gravel	na	21.5	0.0	0.0	519.5	653.6	394.1	3.0	0.6
Pogna	na	183.5	0.0	0.0	359.9	449.2	261.4	0.5	0.1
Pogna	30	209.3	166.5	0.0	164.9	211.6	88.7	1.1	0.7
Typic Eutroboralf	na	272.6	0.0	3.7	265.3	328.1	192.4	1.5	0.6
Typic Eutroboralf	94	279.1	196.7	1.9	57.1	80.8	18.0	2.3	4.1
Seaby	na	464.8	0.0	30.0	32.4	54.1	5.1	0.5	1.5
Seaby	30	337.9	164.7	13.2	9.5	23.8	1.5	0.5	4.9
Nyjack	na	395.9	0.0	22.4	124.0	168.2	67.5	0.1	0.1
Nyjack	99	310.8	200.8	11.8	4.7	11.5	0.8	0.4	7.8
Hackroy	na	200.0	0.0	25.0	318.4	397.8	248.2	1.3	0.4
Hackroy	30	189.0	190.6	15.4	142.6	197.6	91.5	7.6	5.3

[a] Tuff, Gravel, Pogna sandy loam, Typic Eutroboralf (fine), Seaby loam, Nyjack loam, Hackroy sandy loam.

At LANL, Wilcox (1994) reported that runoff accounted for 10 to 18 percent of the precipitation received during a two-year study of the intercanopy zone of a piñon-juniper woodland. The soil was from the Hackroy series and the slope was about 4.4 to 5.3 percent. While not directly applicable to the DARHT and PHERMEX sites, the results from Wilcox (1994) demonstrate that runoff can be a significant component of the water balance at LANL and thus impacts the estimation of deep drainage rates at these two sites. The Wilcox study did consider snow and snowmelt processes. If actual runoff is higher than predicted (table E1-3) at the two sites, the predicted drainage rates are higher than they should be.

E1.6 SENSITIVITIES

Several issues that arose during this study included hourly versus daily precipitation, the use of the 14-yr record versus the longer term precipitation record, the calculation of the daily average dew-point temperature, the calculation of internodal conductances, the effect of initial conditions, and mass balance. Most of these issues were evaluated by conducting additional simulations and comparing to the originals summarized in table E1-3.

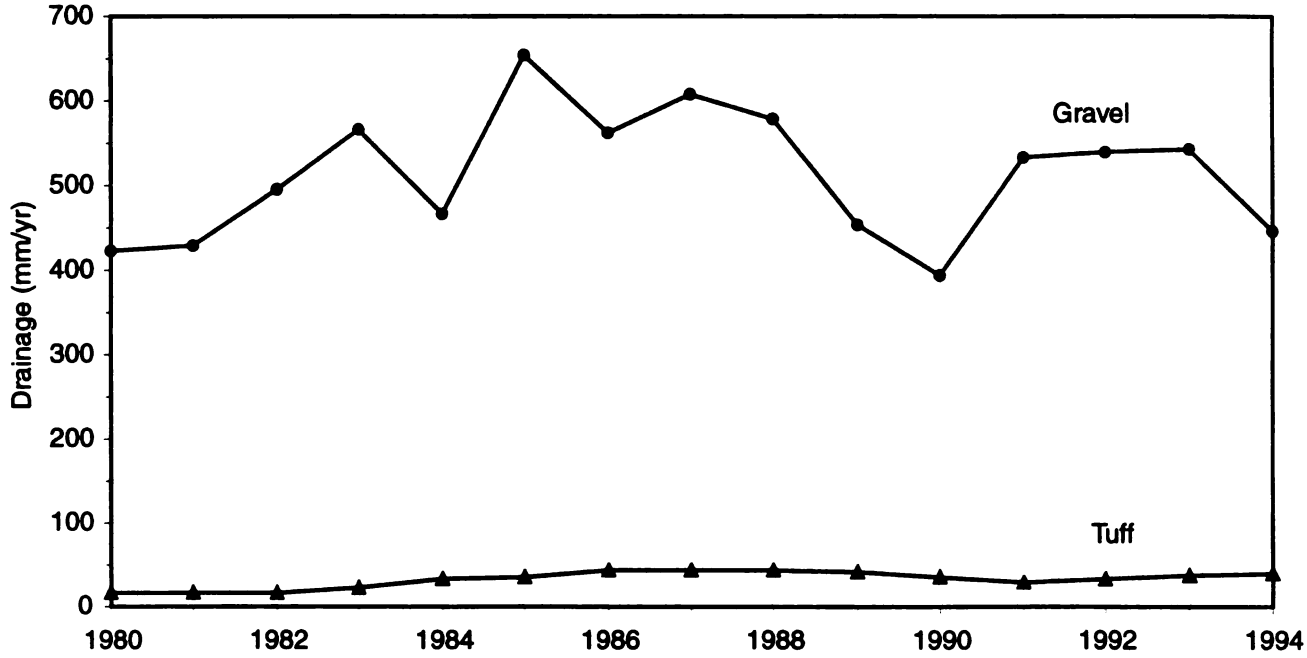

FIGURE E1-1.—*Simulation Results Showing Annual Drainage from the Tuff and Gravel Soil Profiles.*

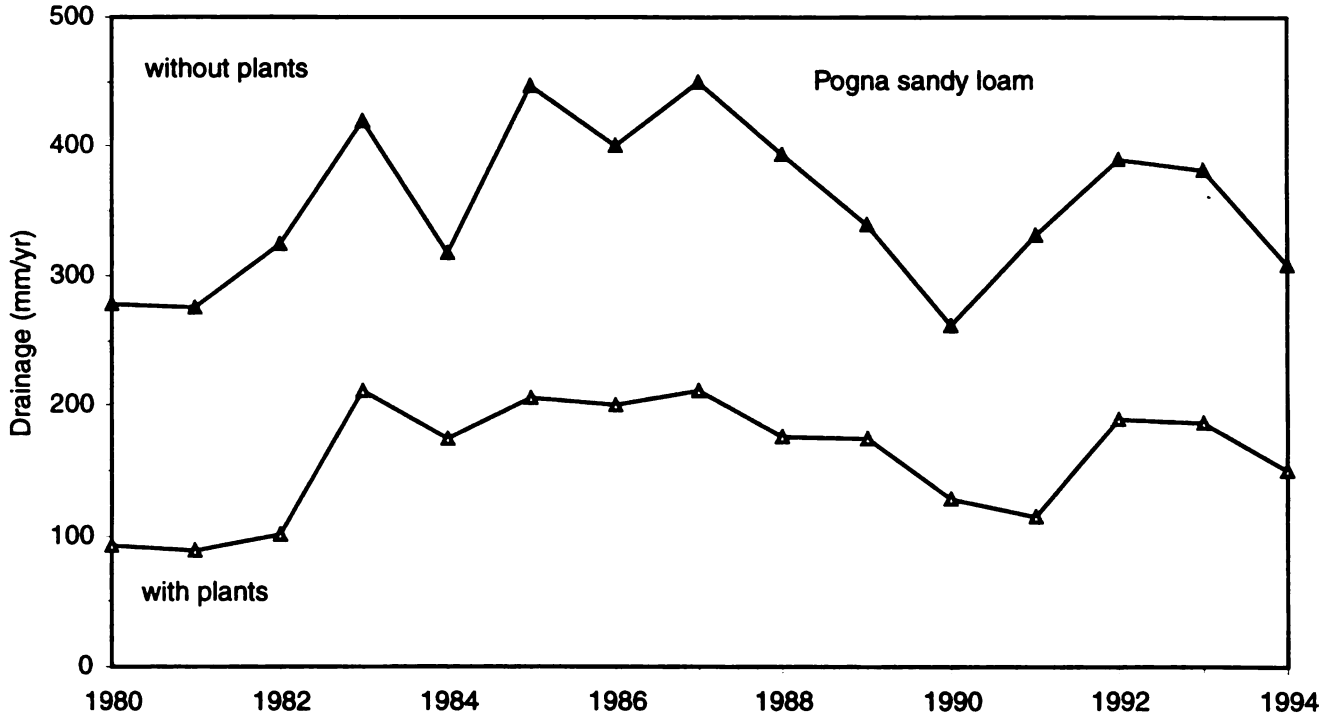

FIGURE E1-2.—*Simulation Results Showing Annual Drainage from the Pogna Sandy Loam Soil Profile.*

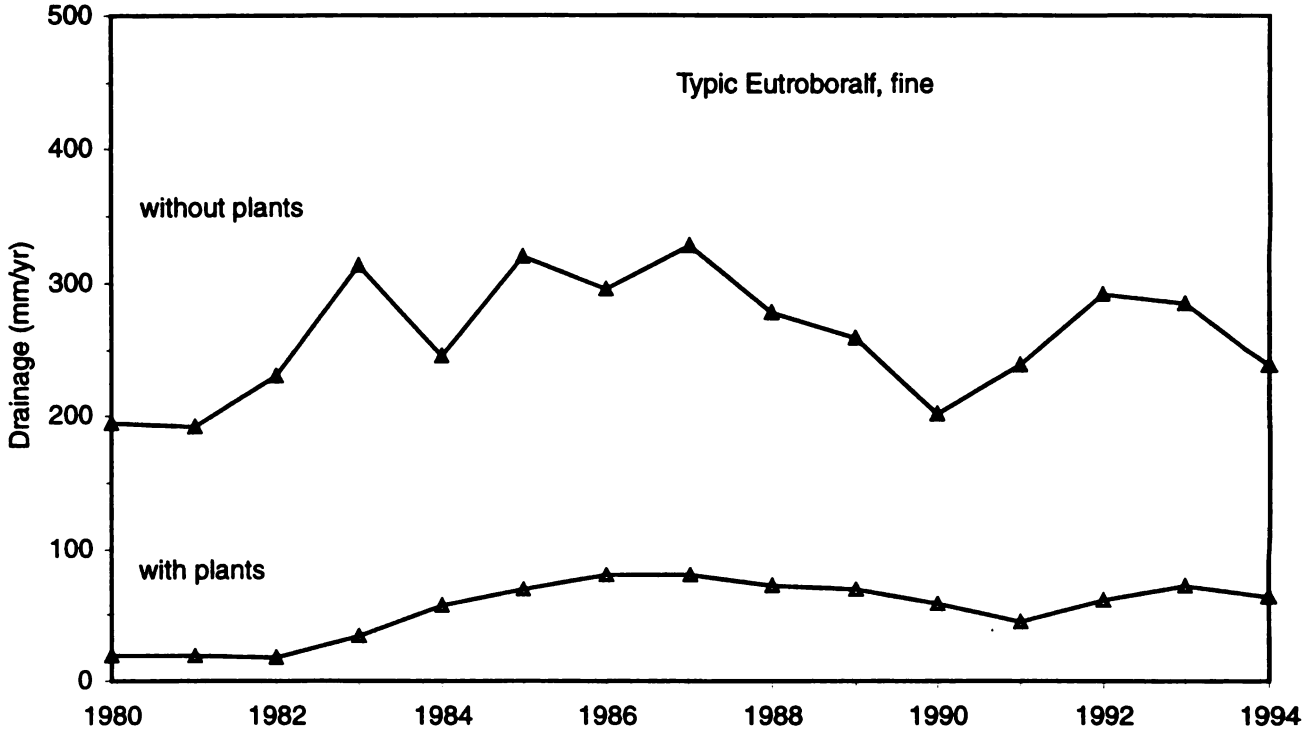

FIGURE E1-3.—*Simulation Results Showing Annual Drainage from the Typic Eutroboralf Soil Profile.*

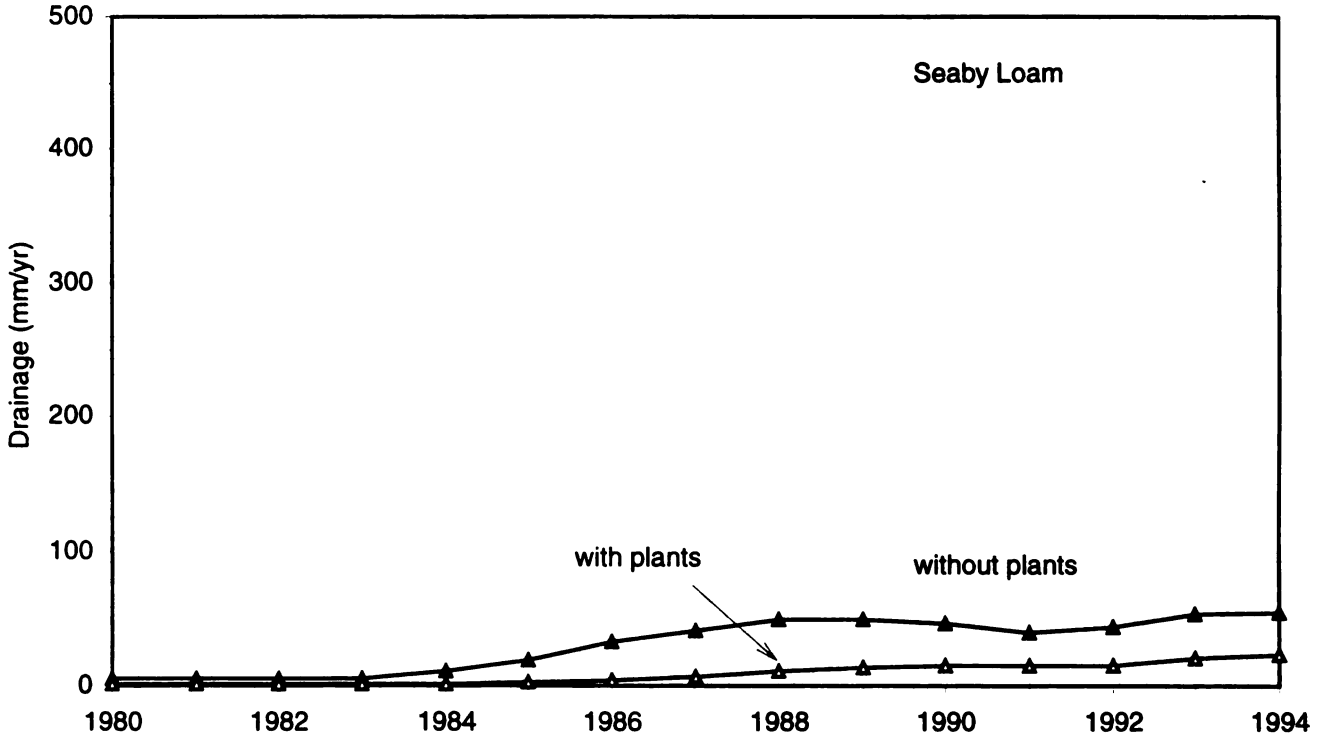

FIGURE E1-4.—*Simulation Results Showing Annual Drainage from the Seaby Loam Soil Profile.*

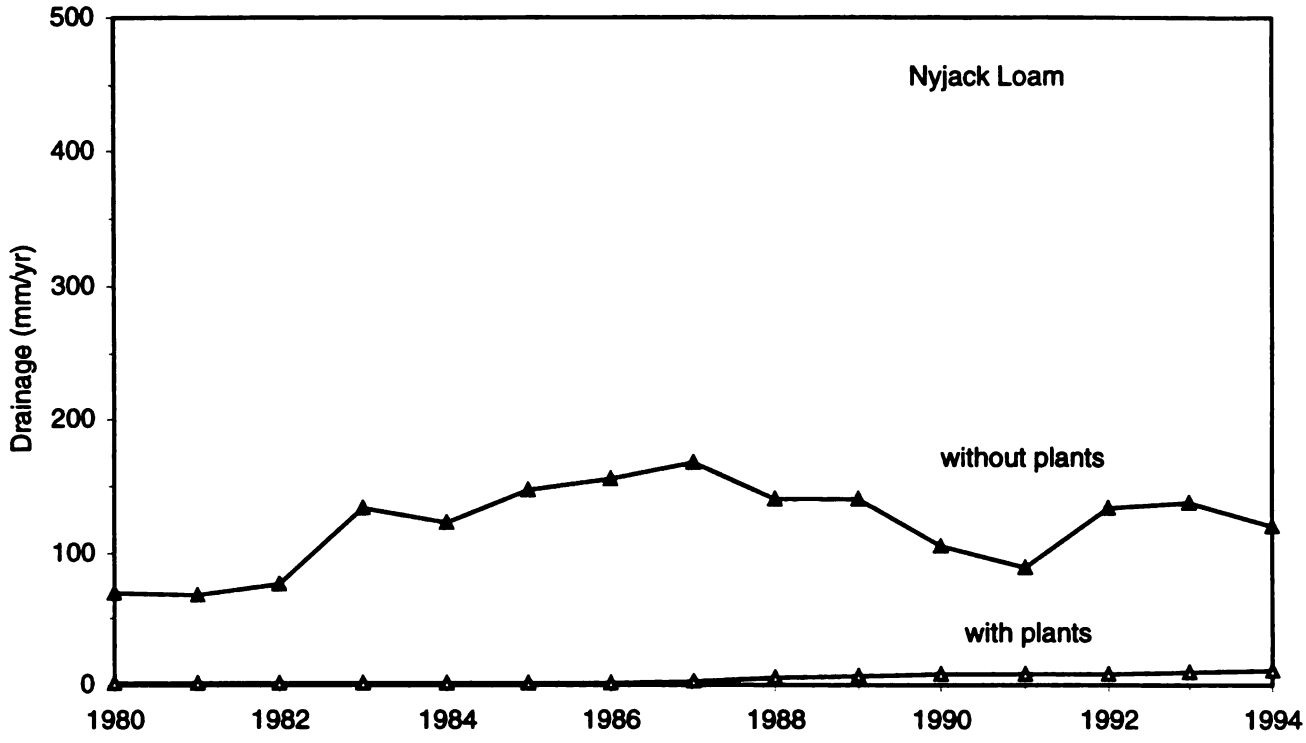

FIGURE E1-5.—*Simulation Results Showing Annual Drainage from the Nyjack Loam Soil Profile.*

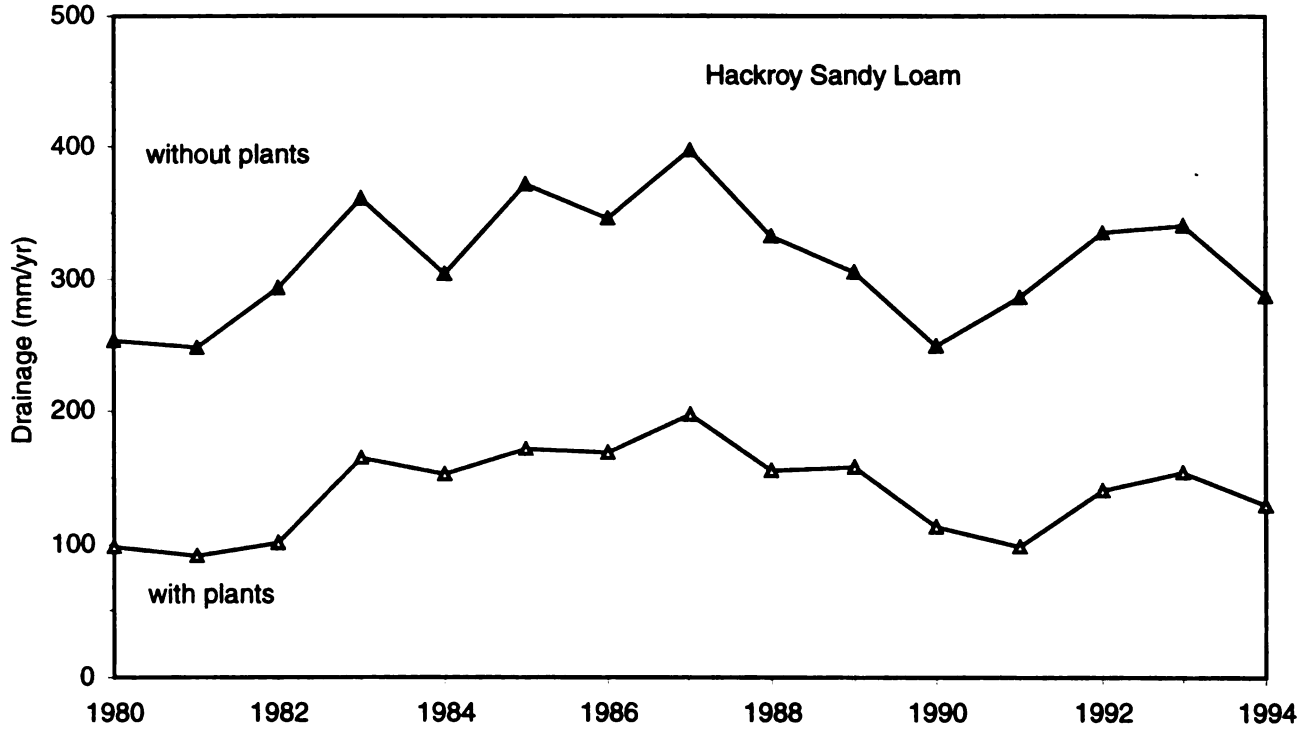

FIGURE E1-6.—*Simulation Results Showing Annual Drainage from the Hackroy Sandy Loam Soil Profile.*

E1.6.1 Hourly Precipitation

As configured, the UNSAT-H computer code applies daily precipitation at the rate of 0.4 in/h (10 mm/h) starting at 0000 h until the day's amount has been applied to the soil surface. The concern is that the daily rates will underestimate runoff because they fail to represent the high intensities that sometimes occur. Four years (1991 to 1994) of 15-min precipitation data were used to provide hourly precipitation input for the UNSAT-H code. The Pogna sandy loam and Seaby loam profiles without plants were simulated. The Pogna sandy loam had no runoff using either daily or hourly precipitation data. In fact, the hourly precipitation resulted in a slight reduction in evaporation, mainly because hourly precipitation that occurred during the day reduced evaporation. Overall, estimated drainage increased by about 0.04 in/yr (1 mm/yr). For the Seaby loam, the hourly precipitation data resulted in a 13 percent reduction in runoff. The seemingly contradictory result is understandable. For the daily precipitation, all the rates were 0.4 in/h (10 mm/h). For the hourly precipitation, most of the rates were far less than 0.4 in/h (10 mm/h) while some rates were more. The net result of using hourly precipitation was a 0.05 in/yr (1.3 mm/yr) reduction in annual runoff.

E1.6.2 Precipitation Record

The drainage rate varies from year to year as a function of the precipitation distribution and amounts and the weather. The question that remains unanswered is whether the 14-yr record used for this study adequately represents the longer term weather that has been observed or can be reasonably expected to occur. Bowen (1990) reported precipitation extremes for LANL for the period from 1911 to 1988. The record shows that the largest annual precipitation amount was 30.3 in (770.6 mm), which occurred in 1941. That amount is about 17 percent greater than the highest value used in this study. Bowen (1990) also reported that the highest seasonal snowfall occurred in 1986-1987. That period is within the period used for this study. Both the highest annual precipitation and seasonal snowfall records are very near the estimated 100-yr values reported by Bowen (1990). If this analysis of deep drainage were to extend much beyond 100 years, consideration would have to be given to analyzing for greater precipitation amounts and intensities than used for this study.

E1.6.3 Dew-point Temperature

A clean and continuous record of daily average dew-point temperature was not available for the period 1980 to 1994. In lieu of actual data, daily dew-point temperatures were approximated as equivalent to the minimum daily air temperatures. Daily dew-point temperature from 1982 showed that the minimum air temperature may be roughly 9°F (5°C) higher than the dew-point temperature. The Pogna sandy loam scenario with and without plants was simulated using dew-point temperatures that were 9°F (5°C) lower than the minimum daily air temperature. In both cases, estimated evapotranspiration increased and drainage decreased (2 percent reduction without plants; 16 percent with plants). Similar results are expected for the other soil profiles.

E1.6.4 Internodal Conductance

For all of the simulations without plants, the geometric mean was used to approximate internodal conductances. The Pogna sandy loam simulation without plants was repeated with arithmetic averaging. The result was a much higher evaporation rate and a 24 percent reduction in the drainage rate. All of the simulations with plants were conducted using the arithmetic mean. The Pogna sandy loam simulation with plants was repeated with geometric averaging. The result was significantly reduced evaporation and a 25 percent increase in the drainage rate. One way to view the results overall, in the context of the averaging scheme, is that the simulations with plants and arithmetic averaging represent the lower estimate of deep drainage, and the simulations without plants but with geometric averaging represent the upper estimate.

E1.6.5 Initial Conditions

To overcome the lack of initial conditions, the simulation of 1980 was repeated until there was less than a 0.004-in (0.1-mm) annual change in the water balance components and in the drainage flux through the tuff. This requirement was relaxed for some of the simulations with plants because the rates under the 1980 weather conditions were either very low or the flux was actually upward. Using these initial conditions, the simulation results for some soil profiles showed drainage rates that increased slowly during part or all of the 14-yr period, indicating some sensitivity to the initial conditions. To ascertain the degree of sensitivity to initial conditions, the Pogna sandy loam and Seaby loam profiles without plants were simulated with a uniform initial matric suction profile of 39 in (100 cm), which is very wet. Figure E1-7 shows that, after two years, the annual drainage rates from the initially wet (open triangles) Pogna sandy loam were nearly identical to what was predicted using the drier initial conditions (filled triangles). The 14-yr average rate was also nearly identical to the average rate predicted using drier initial conditions. In contrast, figure E1-7 shows that the annual drainage rates from the initially wet Seaby loam took the entire 14 years to come within 3 percent of the original simulation reported in table E1-3. Also, the 14-yr average rate was double the average rate predicted using drier initial conditions. When drainage rates are high, the initial conditions appear to become unimportant after only 1 to 2 years. When the rates are low, the initial conditions appear to influence the simulation results for at least as long as 14 years. The technique of conducting two simulations, one initially dry and one initially wet, can be used to illustrate the impact and provide bounding drainage predictions. Based on testing, the limited results suggest that the initial conditions used in the study caused an underestimate of deep drainage of no more than 12 to 16 in/yr (30 to 40 mm/yr).

E1.6.6 Mass Balance

The allowable mass balance error of a given simulation is controlled by the user. As more control is exerted, the simulation time requirement increases. Generally, the mass balance error was kept to less than 1 percent of the drainage rate. For the very low rates, this requirement was relaxed to 10 percent. In two cases, the Seaby loam and Nyjack loam, even this requirement was initially not met. These soil profiles with vegetation were simulated again with tighter convergence criteria. The estimated water balance components changed by less than 0.04 in/yr (1 mm/yr), but the mass balance errors were reduced to less than 10 percent relative to the drainage estimates. Further reductions in the mass balance errors could be obtained but the results and conclusions would not likely be affected.

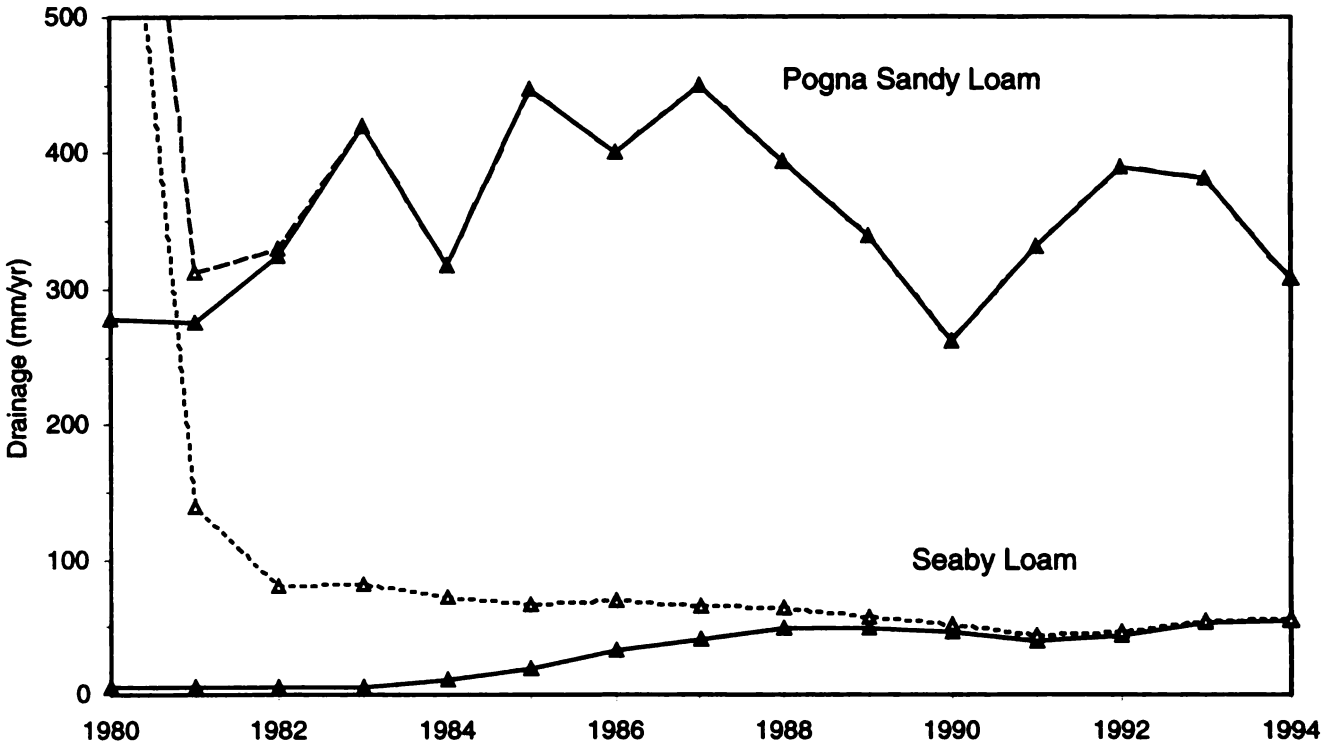

FIGURE E1-7.—*Simulation Results Showing the Impact of Initial Conditions on Annual Drainage from the Pogna Sandy Loam and Seaby Loam Soil Profiles.*

E1.7 SUMMARY

The results of this study showed clearly that deep drainage at the DARHT and PHERMEX sites is possible. Estimated rates ranged from 0.2 to 14 in/yr (4.7 to 360 mm/yr) and could be as high as 20 in/yr (520 mm/yr) if the surface was graveled and unvegetated. These estimates are reasonably similar to other estimates (e.g, Abeele et al. 1981; Rogers 1995).

APPENDIX E2: SOLUBILITY AND SORPTION OF METALS

Mobilization of contaminants from the firing sites to and within Potrillo and Water canyons, and the associated subsurface environment is significantly affected by the contaminants' solubility in water and sorption onto soil and sediments. Thus, estimated solubility limits and distribution coefficients were determined for depleted uranium, beryllium, lead, nickel, copper, aluminum, iron, and silver at the LANL sites. The metals studied represent two classes: 1) those metals assigned annual expenditure rates (e.g. depleted uranium, beryllium, lead, and copper) (see chapter 3, table 3-4) and 2) those metals identified as included in the "other metals" category of the materials expended (see appendix B, table B-4) that were

also listed in the primary and secondary drinking water standards (i.e., 40 CFR 141 and 143) (e.g. aluminum, iron, nickel, and silver). Note, aluminum and stainless steel (hence iron) make up the majority of the "other metals" category of materials expended during tests.

Because the numerical values for solubilities, distribution coefficients (K_d), and constants in the equations defining K_d are interrelated, these numerical values are given only in the metric units used by geochemists.

E2.1 METHODOLOGIES FOR ESTIMATION OF SOLUBILITY AND DISTRIBUTION COEFFICIENTS

Since no solubility experiments specific to the DARHT and PHERMEX sites were conducted previously, these values, except for depleted uranium, were obtained by running the geochemical model, MINTEQ (Felmy et al. 1984) with water quality data measured at Beta Hole in the Water Canyon and in Well PM-4 of the Pajarito Field (LANL 1988; LANL 1989; LANL 1990; LANL 1993c; Purtymun et al. 1994). The MINTEQ computer code was selected because it is a state-of-the-art geochemical code capable of calculating complex geochemical equilibria for reactions involving gases, aqueous solutions, adsorbed species, and minerals within a wide range of geochemical conditions and constraints. The code has associated with it a thermochemical database containing aqueous speciation and solubility data. The code was developed in the mid-1980s for the EPA as part of a system to model the migration and fate of pollutant metals; the code was subsequently modified for the Nuclear Regulatory Commission and DOE. For depleted uranium, field data measured at the E-F site (Hanson and Miera 1977), Aberdeen Proving Ground in Maryland (Erickson et al. 1993), and Yuma Proving Ground in Arizona (Erickson et al. 1993) were used to estimate solubility. Water quality data for the surface and subsurface water used for the MINTEQ modeling are shown in table E2-1. Distribution coefficients for depleted uranium, beryllium, lead, nickel, copper, aluminum, iron, and silver were estimated by using laboratory experimental results from other sites (e.g., Yucca Mountain in Nevada and the Hanford Site in Washington).

TABLE E2-1.—*Water Quality at the Beta Hole in Water Canyon and Well PM-4 in the Pajarito Field*

Location	Calcium (mg/L)	Magnesium (mg/L)	Potassium (mg/L)	Sodium (mg/L)	Carbonate plus Bicarbonate (mg/L)	Chloride (mg/L)	Sulfate (mg/L)	pH
Beta Hole	12	4	3.3	17	51	11	7.5	7.8
PM-4	14	4	3	15	60	2	2.5	7.85

E2.2 DEPLETED URANIUM

Depleted uranium is the isotopic form present in the studies cited here. The physical chemistry of various isotopic forms of uranium is essentially identical, so the general term "uranium" is used in this section.

E2.2.1 Solubility of Uranium

Many studies have obtained data on uranium distributions at LANL and physical/chemical characteristics (Hanson 1974; Hanson and Miera 1976; Hanson and Miera 1978; Elder et al. 1977; and Becker 1993). Common oxidation states of uranium are designated as uranium(III), uranium(IV), uranium(V), uranium(VI), but in the LANL geologic environment uranium(IV) and uranium(VI) are the most important (Onishi et al. 1981). Uranium(VI) species control the total uranium concentration in oxidizing environments. The uranyl ion (UO_2^{+2}) is a dominant species under oxidizing conditions. This cation can form many soluble and stable complexes with common ground water anions such as carbonate and sulfate (Onishi et al. 1981). In reducing conditions, uranium (IV) dominates and generally precipitates as uranium dioxide. Uranium content in solution, and thus also a distribution coefficient K_d, are a function of oxidation-reduction potential (Eh), pH, solution carbonate content, sediment characteristics (particle size, carbonate, phosphorous, and hydrous oxide contents), and organic matter content (organic carbon and humic substances) (Onishi et al. 1981). Data reviewed by Onishi et al. (1981) indicate that the uranium K_d for sediments from the Great Miami River (Ohio) ranged between 1,000 and 1,600 mL/g, while K_d values for sediments in 40 Japanese rivers varied between 1,000 and 6,000 mL/g.

Erickson et al. (1993) performed a series of experiments and geochemical modeling to determine corrosion rate, solubility, and adsorption potential for uranium at Aberdeen Proving Ground in Maryland and the Yuma Proving Ground in Arizona. Uranium pieces corrode with a corrosion rate of 0.02 to 0.04 in/yr (0.05 to 0.10 cm/y) to form uranium (VI) hydrated oxides, mostly the yellowish mineral schoepite ($UO_3 \cdot H_2O$). The corrosion rate is fast enough that uranium is available for transport through dissolution of schoepite and subsequent surface and subsurface migration. The LANL E-F site exhibits a yellow corrosion product of uranium on the soil surface, a sign of schoepite. Soils (two types) at Aberdeen Proving Ground are predominantly silt with moderate cation exchange capacity (CEC), low calcium carbonate content, and low paste pH values (pH of 4 to 6). Soils (one set) at Yuma Proving Ground are predominantly gravel and sand with higher CEC, high carbonate minerals, and slightly basic (pH of 8 to 8.5) saturation paste. Erickson et al. (1993) reported that the solubility of uranium at Aberdeen Proving Ground and Yuma Proving Ground is 10 to 280 mg/L, and 20 to 130 mg/L, respectively. They attributed the higher corrosion rate and uranium mobility measured at Yuma Proving Ground as primarily controlled by the higher dissolved carbonate, derived from the dissolution of carbonate minerals in this soil. Soil characteristics (especially carbonate content) at the LANL site fall between one of the Aberdeen Proving Ground soils and the Yuma Proving Ground soil types (LANL 1995).

Furthermore, uranium concentrations in standing water at the detonation center of the E-F site were 86 and 235 mg/L in 1975 and 1976, respectively, with nearly all of the uranium being in solution as opposed to suspended as fine solids (Hanson and Miera 1977). The uranium concentration in standing water at 66 ft (20 m) to the southwest away from the detonation center was only 63 μg/L in 1975, i.e., three orders-of-magnitude less than the concentration measured in standing water at the detonation center. A uranium concentration in runoff water measured in 1975 at 330 ft (100 m) to the southwest (still on mesa top) away from the detonation center was 52 μg/L. These concentration differences between the detonation center and the short distances away imply that not enough uranium was transported from the firing point to maintain the uranium concentration in solution at the solubility limit of uranium even 65 ft (20 m) away.

Based on these studies, we selected uranium solubility limit to be 300 mg/L for the current study. We also assumed that corrosion of uranium is fast enough for uranium to be available for subsequent surface/ subsurface migration.

E2.2.2 Sorption of Uranium

Erickson et al. (1993) also conducted adsorption experiments and geochemical modeling with the chemical code, MINTEQ (Felmy et al. 1984). Experimental values for uranium distribution coefficients on the two soil types at Aberdeen Proving Ground were reported to be 4,360 and 328 mL/g. The Yuma Proving Ground site has the lowest K_d value (54 mL/g) due to the high carbonate solution concentrations despite the Yuma Proving Ground environment having the highest pH and CEC, two attributes that normally portend high adsorption. Since soil characteristics (especially carbonate concentrations) at the LANL site (Longmire 1995) fall between one of the Aberdeen Proving Ground soil types and the Yuma Proving Ground soil type, an expected K_d value with soil at the LANL site is estimated to be between 54 and 328 mL/g. We selected distribution coefficient values for the LANL soil to be 50 mL/g, and 100 mL/g as conservative and more realistic estimates. Since suspended sediment in LANL canyon streams have finer particle size, and since it is generally believed that finer sediments exhibit greater K_d values (Onishi et al. 1981; Becker 1993), we selected K_d values of 100 and 200 mL/g to be conservative and more realistic estimates for the in-stream suspended sediment.

E2.3 LEAD

E2.3.1 Solubility of Lead

The release rate of lead from the metal compounds into water depends largely on the oxidation rate of metallic lead, the dissolution of secondary minerals (e.g., lead carbonates), and the amount of water available to react with lead (Rhoads et al. 1992). However, we are not aware of any solubility and adsorption data for lead in contact with LANL waters or tuff. Thus, we performed geochemical modeling with MINTEQ to obtain lead solubility estimates for the LANL sites. The water quality data shown in table E2-1 was used to represent the LANL surface water and ground water conditions. The mineral cerrusite ($PbCO_3$) was imposed as the solubility limiting solid in this case.

MINTEQ predicted lead solubility in canyon streams and ground water to be 48.2 and 45.7 μg/L, respectively. Hence, we selected the lead solubility to be 50 μg/L for both surface and subsurface waters at the LANL sites.

Rhoads et al. (1992) conducted experiments and chemical modeling to determine the lead solubility in Hanford ground water. Assuming lead was in equilibrium with cerrusite, they used the geochemical code MINTEQ (Felmy et al. 1984) to predict the lead solubility to be 287 μg/L, which is close to solubility limits of 236 to 482 μg/L which they obtained in laboratory experiments. This result confirms the general validity of the MINTEQ simulation with cerrusite limiting lead solubility.

E2.3.2 Sorption of Lead

Adsorption of dissolved lead depends on water and soil chemistry, and properties of the lead species in solution (Rhoads et al. 1992). However, a main factor affecting lead adsorption is the amount of iron oxides in the soil.

According to Rhoads et al. (1992), batch experiments with Hanford ground water and relatively fine sediment (sand, silt, and clay mixture) yielded distribution coefficients varying from 1,190 mL/g at dissolved lead concentration of 200 μg/L to 56,000 mL/g at dissolved lead concentration of 0.005 μg/L, showing the following functional relationship:

$$K_d = 9550\ C^{-0.335}$$

where C is a dissolved lead concentration in μg/L. This relationship yields K_d values of 2,580 mL/g at the dissolved lead concentration of 50 μg/L, 1,410 mL/g at the dissolved lead concentration of 300 μg/L, and 1,150 mL/g at the dissolved lead concentration of 550 μg/L.

Based on this Hanford study, conservative and realistic distribution coefficient values of 1,000 and 10,000 mL/g, respectively, for lead transport in the subsurface of the LANL site were selected. Because of the finer suspended sediment in canyon streams, their conservative and realistic distribution coefficient values were selected to be twice the values of ground water, e.g., 2,000 and 20,000 mL/g, respectively.

E2.4 BERYLLIUM

E2.4.1 Solubility of Beryllium

Beryllium solubility was calculated using the geochemical code MINTEQ (Felmy et al. 1984) by imposing beryllium hydroxide ($Be(OH)_2$) as the solubility limiting solid. Thermodynamic data used for this study on beryllium hydride were not a part of the original MINTEQ code but are incorporated in MINTEQA2 (Version 3.0) and are reported in Serne et al. (1993). Beryllium solubility was calculated for water from Water Canyon at the Beta Hole, and ground water from water supply Well PM-4 in the Pajarito Field (see table E2-1).

Beryllium solubility for Water Canyon at the Beta Hole and Well PM-4 predicted by the MINTEQ geochemical code are 3.95 and 3.62 μg/L, respectively. The MINTEQ simulation shows the strong dependency of beryllium solubility to pH. By using MINTEQA2 (i.e., with the same thermodynamic data base as those used under the current study), Serne et al. (1993) calculated beryllium solubility for Hanford ground water (pH of 8.1) to be 2.3 μg/L, which is comparable to the 3.62 to 3.95 μg/L range we estimated for the LANL waters.

Based on these model results, the beryllium solubility selected was 4 μg/L for both the canyon streams and subsurface flow.

E2.4.2 Sorption of Beryllium

Very few data are available for beryllium adsorption on soil (Serne et al. 1993), and we are not aware of any beryllium adsorption data for LANL soils and sediments. Beryllium adsorption data for 11 soils reviewed by Rai et al. (1984) show that beryllium adsorption is greater than adsorption of other divalent metals such as zinc, cadmium, nickel, and the monovalent metal mercury.

Adsorption of divalent beryllium is expected to be somewhat similar to that of divalent strontium. Thus, we used a strontium distribution coefficient obtained from experiments on tuff deposits for beryllium adsorption values. Strontium adsorption is significantly influenced by calcium and magnesium ions. There are many strontium adsorption studies performed with Yucca Mountain tuff. These include strontium distribution coefficients of:

- 50 to 84 mL/g obtained in batch tests and 30 to 52 mL/g obtained by column tests (Erdal et al. 1980)
- 50 to 300 mL/g with batch tests and 30 to 106 mL/g with column tests (Vine et al. 1981a)
- 51 to 283 mL/g with batch tests and 19 to 395 mL/g with column tests (Vine et al. 1981b)

Based on data from five samples of devitrified tuff, the range in strontium K_d values for the LANL soil was reported to be 53 to 190 mL/g with an average value of 116 mL/g (Wolfsburg 1980).

Based on these values, we selected conservative and realistic strontium distribution coefficient values to be 50 and 100 mL/g, respectively, for subsurface water. Because beryllium adsorption by soil is expected to be similar to that of strontium, these values were also used for the beryllium distribution coefficient for subsurface flow modeling.

Because the suspended sediments in canyon streams are expected to be finer than soils in the subsurface (Becker 1993), and the finer the sediment the greater the K_d values (Onishi et al. 1981), we selected conservative and realistic beryllium K_d values for canyon stream modeling to be 100 and 200 mL/g, respectively.

E2.5 NICKEL

E2.5.1 Solubility of Nickel

The solubility of nickel was estimated by using the MINTEQ code with its existing data base, and the LANL water quality data shown in table E2-1. Geochemical simulation indicates that the most stable solid phase of nickel in both surface and ground water is nickel hydroxide ($Ni(OH)_2$) as was found for a Hanford ground water case (Serne et al. 1993). The calculated nickel solubilities for canyon streams and ground water were 1.16 and 0.904 mg/L, respectively, assuming equilibrium with nickel hydroxide. Thus, we selected the nickel solubility to be 1.0 mg/L for both surface and subsurface waters at the LANL sites.

E2.5.2 Sorption of Nickel

No nickel adsorption experiments have been conducted with LANL soils and water. Thus, we used Hanford Site nickel adsorption data to obtain an appropriate nickel distribution coefficient for this study. By using Hanford ground water with Trench-8 soil, Serne et al. (1993) obtained K_d values of 440 mL/g and 2,350 mL/g after 5 and 44 days. With Trench-94 soil, they obtained K_d values of 48 and 337 mL/g at a dissolved nickel concentration of 2 and 1,000 μg/L, respectively. Serne et al. (1993) then derived the following empirical K_d expression:

$$K_d = 240\ C^{-0.155}$$

where C is the dissolved nickel concentration in μg/L, and the K_d is the distribution coefficient in mL/g. The above equation yields K_d values of 118, 167, and 240 mL/g at the dissolved nickel concentrations of 100, 10, and 1 μg/L, respectively. Note that a dissolved nickel concentration at the LANL sites is expected to be less than 100 μg/L.

In addition, Brookins (1984) and Serne (1994) reported the conservative nickel distribution coefficients to be 50 mL/g for devitrified tuff and 20 mL/g for sandy soil, respectively.

From these data, we selected conservative and realistic nickel distribution coefficients to be 20 and 200 mL/g, respectively, for the LANL ground water. For the LANL canyon streams suspended sediments, we selected conservative and realistic values of 40 and 400 mL/g, respectively.

E2.6 COPPER

E2.6.1 Solubility of Copper

The mineral malachite ($Cu_2CO_3(OH)_2$) was specified as the copper solubility controlling solid for MINTEQ calculations of copper solubility in the canyon stream and ground water described in table E2-1. MINTEQ predicted the copper solubility to be 10.5 μg/L for both the LANL site surface and ground water. Thus, the copper solubility for this study was selected to be 10 μg/L for both canyon stream and subsurface modeling.

E2.6.2 Sorption of Copper

There are no copper adsorption data available for the LANL waters and soils or sediments. Since copper and nickel are both divalent and are expected to have similar sorption behavior, we elected to use the same K_d values for copper as for nickel. Serne (1994) reported the conservative copper K_d value for Hanford sandy soil to be 20 mg/L, the same as our conservative K_d value for nickel.

Thus we assigned the conservative and realistic K_d values for the LANL ground water to be 20 and 200 mL/g, respectively. The conservative and realistic K_d values for the canyon stream water were assigned 40 and 400 mL/g, respectively.

E2.7 ALUMINUM

E2.7.1 Solubility of Aluminum

Aluminum solubility was also calculated using the geochemical code MINTEQ (Felmy et al. 1984) by assigning the solubility limiting solid to be the mineral gibbsite ($Al(OH)_3$). With the water quality data shown in table E2-1 for Water Canyon and Well PM-4, MINTEQ predicted the aluminum solubility at equilibrium with gibbsite to be 1.22 and 1.36 μg/L for the canyon streams and ground water in the study area. Thus, we selected aluminum solubility to be 1 μg/L for both surface and subsurface flow modeling.

E2.7.2 Sorption of Aluminum

Since aluminum is a major constituent of soil, and the bulk of aluminum in the soil is not undergoing adsorption/desorption reactions with water, no meaningful adsorption experimental data for aluminum exist. Nonetheless, we selected the conservative aluminum K_d value to be 300 mL/g for the LANL ground water, as indicated by Serne (1994) for the Hanford sandy soil's conservative value. We selected a more realistic K_d value for aluminum to be 5,000 mL/g for the ground water. Because suspended sediment is finer than the bulk surface soil, we selected K_d values for the canyon streams to be twice the corresponding K_d values of the subsurface. Thus, the conservative and more realistic K_d values for canyon streams were assigned to be 600 and 10,000 mL/g, respectively.

E2.8 IRON

E2.8.1 Solubility of Iron

The solubility of iron was estimated using the MINTEQ code with its existing data base and water quality data shown in table E2-1. Because there were no redox data available for Water Canyon stream water and Well PM-4 ground water, we assumed that the water is oxidized. With this assumption, the geochemical simulation indicates that the most probable controlling solid phase of iron in both surface and ground water is amorphous iron hydroxide ($Fe(OH)_3$). The predicted iron solubility for both the canyon stream and ground water was 0.0022 μg/L. This value is very similar to the 0.002 μg/L value Morel (1983) reported for the ferric iron solubility at equilibrium with iron hydroxide at a pH of 7.8. Thus, we selected the iron solubility to be 0.002 μg/L for both surface and subsurface waters in the study area. Note that if the ground water of Well PM-4 is in a reduced condition, the iron solubility would be much higher than 0.002 μg/L due to the higher solubility of ferrous iron.

E2.8.2 Sorption of Iron

Similar to the aluminum case discussed above, iron is also a major constituent of soil and the bulk of the iron in the soil is not undergoing adsorption/desorption reactions with water. Thus, there is no meaningful adsorption experimental data for iron. However, Serne (1994) found a conservative K_d value for iron in sandy soil to be 15 mL/g, and we selected this value for subsurface flow modeling at the LANL sites. We assigned a realistic iron K_d value of 1,000 mL/g for the subsurface model. Conservative and realistic K_d values for iron in canyon streams were assigned to be 30 and 2,000 mL/g, respectively.

E2.9 SILVER

E2.9.1 Solubility of Silver

Silver chloride (AgCl) was specified as the silver solubility controlling solid for MINTEQ calculations of silver solubility in the canyon streams and ground water whose chemical quality is shown in table E2-1. MINTEQ predicted silver solubility to be 76.4 and 286 μg/L for the LANL sites' surface and ground water, respectively. Thus, the silver solubility for this study was selected to be 80 and 300 μg/L for canyon stream and subsurface models, respectively.

E2.9.2 Sorption of Silver

Serne (1994) stated that 1 mL/g may be taken as a conservative K_d value for silver in a sandy soil. Consequently, we selected the conservative K_d for the LANL subsurface water to be 1 mL/g. For canyon streams water, we assigned a conservative silver K_d value of 2 mL/g. Since silver is monovalent, we assumed a realistic K_d value for silver to be half of the divalent nickel K_d value. Thus, we selected realistic K_d values for silver in the subsurface environment and canyon streams at the LANL study area to be 100 and 200 mL/g, respectively.

E2.10 SUMMARY OF SOLUBILITY AND SORPTION OF METALS IN LANL SURFACE AND GROUND WATERS

Mobilization of contaminants released to surrounding surface and subsurface water environments from the firing sites is significantly affected by their solubility and affinity to sorb onto soils and sediments. Thus, the solubility and distribution coefficients of depleted uranium, beryllium, lead, nickel, copper, aluminum, iron, and silver were estimated here for LANL site surface and ground waters.

Except for depleted uranium, the solubility of the metals of interest were obtained by running the geochemical model, MINTEQ (Felmy et al. 1984). Water quality data from samples taken at the Beta Hole on Water Canyon and at Well PM-4 of the Pajarito Field (LANL 1988; LANL 1989; LANL 1990; LANL 1993c; Purtymun et al. 1994) were assumed to be representative of surface and ground water quality for the study area (see table E2-1). For depleted uranium, solubility was estimated using field data measured at the E-F site at LANL (Hanson and Miera 1977), Aberdeen Proving Ground in Maryland (Erickson et al. 1993), and Yuma Proving Ground in Arizona (Erickson et al. 1993).

Table E2-2 shows a summary of both the solubility and sorption values estimated for the metals of interest in LANL surface and ground waters. Note that except for silver, solubility for each metal is the same for surface and ground waters of the LANL study area. Both conservative and realistic estimates of distribution coefficients, K_d, are shown in the table for depleted uranium, lead, beryllium, nickel, copper, aluminum, iron, and silver.

TABLE E2-2.—*Estimated Solubilities and Distribution Coefficients for Metals in LANL Surface and Ground Water*

Metals	Solubility, μg/L unless otherwise noted	Distribution Coefficients, K_d, (mL/g)			
		Subsurface Sediments and Ground Water		Suspended Sediment and Surface Water	
		Conservative	Realistic	Conservative	Realistic
Depleted Uranium	300 mg/L	50	100	100	200
Lead	50	1,000	10,000	2,000	20,000
Beryllium	4	50	100	100	200
Nickel	1000	20	200	40	400
Copper	10	20	200	40	400
Aluminum	1	300	5,000	600	10,000
Iron	0.002	15	1,000	30	2,000
Silver	300 and 80 for surface and ground water	1	100	2	200

APPENDIX E3: SURFACE WATER MODELING

Contaminant movement in runoff, stream flow, and sediment transport from both PHERMEX and DARHT has been identified as a key set of processes leading to exposure and health effects. Pathways of interest include stream flow and sediment discharge through the Water and Potrillo Canyon watersheds leading to the Rio Grande and stream flow transmission losses to the underlying ground water. This section of the appendix describes the modeling procedures used to estimate the transport and fate of depleted uranium, beryllium, and lead in the Water and Potrillo Canyon watersheds.

E3.1 MODEL DESCRIPTION

The transport and fate of depleted uranium, beryllium, and lead in the Water and Potrillo Canyon watersheds were estimated using one-dimensional event-based procedures (Lane et al. 1985) originally developed to simulate the movement of plutonium in the Los Alamos Canyon watershed. The procedures developed by Lane et al. (1995), hereafter referred to as the Lane model, were selected because they were specifically formulated to represent the hydrologic, hydraulic, sediment, and contaminant transport processes occurring in the Los Alamos region. The Lane model accounts only for the transport of contaminants sorbed to sediments and does not consider contaminant transport in the dissolved phase.

Since this EIS is concerned with the transport of depleted uranium, beryllium, and lead which are soluble in LANL waters, the Lane model procedures were extended to include dissolved phase transport and sorption/desorption with sediments using partition coefficients as described by Mills (Mills et al. 1985). The model was also extended to include the transport of dissolved contaminants from the firing sites into the neighboring canyon channels. The extended model transports contaminants sorbed to sediments or dissolved in the water column. The model also estimates dissolved contaminants that infiltrate to the subsurface from mesa top firing sites and through channel transmission losses. It is important to note that the long-term observations of precipitation, stream flow, and sediment yield necessary to calibrate and validate the model were not available for the Water and Potrillo Canyon watersheds. A very conservative approach has been taken in this model to account for the substantial uncertainty that exists in the performance of the water resource system. The simulated concentrations leaving the LANL site are well below drinking water standards.

E3.2 MODEL APPLICATION

The extended Lane model was developed and applied to the Water Canyon and Potrillo Canyon watersheds. These watersheds were divided into a series of representative channel reaches. Figure E3-1 shows a schematic of the channel network and the individual reach identification numbers.

Total daily precipitation values used to drive the model for the 32-year historical period of PHERMEX operations were obtained from gage data collected at LANL (Bowen 1990). Snowmelt runoff was not explicitly included because there was not adequate information to characterize these events. Precipitation occurring as snow was simply applied as rainfall on the day of occurrence. Following Lane et al. (1985), the daily average precipitation was converted to a 1-hour rainfall and used as the input to the hydrology model.

Because stream flow in Water and Potrillo Canyons is ephemeral, a very long time may be required for contaminants to be transported downstream from the release point and attain a maximum concentration. Since the model is driven entirely by rainfall events, a hypothetical future precipitation record was required. A 5,000-year daily average precipitation record was created using the methods described by Sharpley and Williams (Sharpley and Williams 1990) and statistics computed from the measured daily rainfall record from 1947 through 1994.

Watershed subbasin areas, composite runoff curve numbers, channel widths, lengths, and slopes were obtained from McLin (1992) and are listed in table E3-1. Note that overbank areas (floodplains) were not included and the active channels were assumed to have a rectangular cross section. These assumptions are conservative in that they lead to increased rates of sediment and contaminant transport and thus an accelerated movement of contaminants toward the Rio Grande. Channel widths of 3 ft (0.91 m) have been used except for the section of Potrillo Canyon (reach 3) termed the "discharge sink" by Becker (Becker 1993). The discharge sink has been noted to be a wide area without a distinct channel with a high vertical infiltration rate (Becker 1993).

Additional channel characteristics used in the model (hydraulic conductivity, Manning's n, median grain size, and silt-clay fraction) were estimated using the values chosen by Lane (Lane et al. 1985) for Los Alamos Canyon as guidance. Only two sediment size classes were considered in the model; bedload was represented as material with a median grain size diameter (d_{50}), and suspended load was represented by

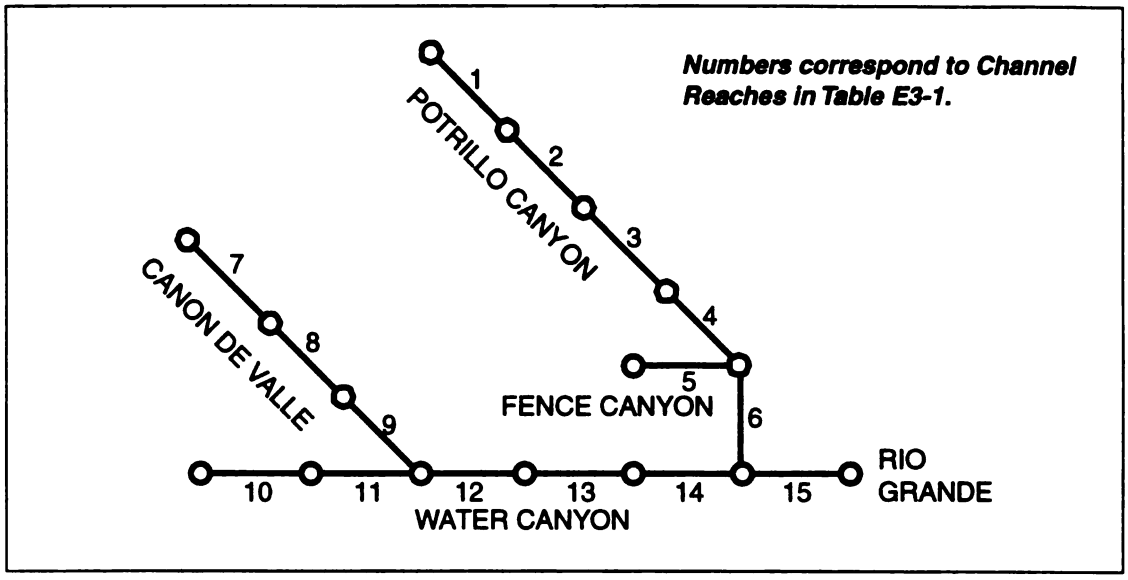

FIGURE E3-1.—***Schematic of Runoff-sediment-contaminant Transport Model Channel Network.***

the silt-clay size fraction. As recommended by Lane (Lane et al. 1985), a constant value of 5 was used for the suspended sediment transport coefficient in the model. To improve confidence in model results, future studies should be undertaken to characterize the channel sediments in Water and Potrillo Canyons. The values selected for each channel reach are listed in table E3-1. The depth of channel bed sediments available for contaminant storage was assumed to be 11.81 in (30 cm) for all reaches, which is consistent with the value selected by Lane (Lane et al. 1985).

For each reported simulation, the entire yearly contaminant mass release is assumed to be distributed uniformly over a 100-ft (30-m) radius circle centered at the firing site (PHERMEX or DARHT) at the start of each year. For days during which rainfall occurs, the contaminants are mobilized by assuming that they go into solution at the solubility limit. The volume of rainfall and associated contaminant mass is split between infiltration to the vadose zone and runoff to the canyons using the curve number method (Lane et al. 1985). Use of the runoff curve method neglects evapotranspiration; all precipitation is used for transporting contaminant as infiltration and runoff. Note, the runoff curve number used for the firing site area is the same as that used for the watershed subbasin containing the firing site listed in table E3-1. This assumes that the firing site area will be restored to natural soil and vegetation conditions after the facility is closed. Contaminants travel from the firing site to the canyon channel only through runoff; soil erosion and contaminant movement associated with the eroded soil was not considered. This assumption was made in order to avoid the additional complexities and uncertainties associated with the simulation of soil erosion and overland contaminant transport from the firing sites to the channel system. The dissolved contaminants associated with rainfall runoff are input to Potrillo Canyon in reach number 1 and to Water Canyon in reach number 12 (see figure E3-1).

Application of the curve number for the natural soils and vegetation to partition between runoff and infiltration at the DARHT Facility implies one of two situations: 1) the grounds of the DARHT Facility are seeded after construction and maintained during operation such that only a small portion of the facility grounds contaminated with depleted uranium, beryllium, and lead (e.g., the firing point) exhibit altered storm water runoff characteristics, and/or 2) the release is so long term (e.g., hundreds to tens of thousands

TABLE E3-1.—*Channel Characteristics*

Canyon	Reach No	Drainage Area (mi^2)	Curve Number	Length (mi)	Average Width (ft)
Water	10	4.07	54	3.41	3.0
	11	2.63	62	3.36	3.0
	12	0.52	72	1.33	3.0
	13	0.90	72	2.27	3.0
	14	1.97	72	2.60	3.0
	15	0.32	77	0.95	3.0
Cañon de Valle	7	2.33	53	4.26	3.0
	8	0.78	63	1.42	3.0
	9	1.17	64	2.37	3.0
Potrillo	1	0.68	70	1.33	3.0
	2	0.68	70	1.33	3.0
	3	0.49	70	0.95	40.0
	4	0.93	70	1.80	3.0
	6	0.96	75	1.85	3.0
Fence	5	1.03	71	3.41	3.0

Canyon	Hydraulic Conductivity (in/hr)	Slope	Manning n	Median Grain Size (mm)	Silt-Clay Percentage
Water	1.5	0.13	0.040	1.3	2.5
	1.5	0.04	0.040	1.3	2.5
	1.5	0.02	0.040	0.8	0.5
	1.5	0.02	0.040	0.8	0.5
	1.5	0.04	0.040	0.8	2.5
	1.5	0.08	0.040	0.8	1.5
Cañon de Valle	1.5	0.12	0.040	1.6	3.5
	1.5	0.05	0.040	1.6	3.5
	1.5	0.04	0.040	1.6	3.5
Potrillo	1.5	0.03	0.040	1.2	2.0
	1.5	0.02	0.040	1.2	2.0
	1.5	0.02	0.040	1.2	2.0
	1.5	0.02	0.040	0.9	2.5
	1.5	0.02	0.040	0.9	2.5
Fence	1.5	0.02	0.040	1.1	0.5

of years) that the different storm water runoff characteristics of the 30-year operational period are not significant to the overall release. The facility and its surrounding grounds, including access roads and parking, will certainly increase impervious surface area, and, therefore, increase peak rates of runoff from the facility. However, runoff from these surfaces will be routed into rip-rap lined ditches and culverts. The increased runoff caused by the structure and asphalt surfaces will, by design, be routed away from the firing point and surrounding contaminated soils. The storm water pollution prevention plan being implemented under the construction program calls for the placement of rip-rap at site drainage areas to

protect against erosion, and the revegetation of all areas disturbed and not covered by pavement, structures, or rip-rap. Thus, storm water runoff that would impact the contaminated soils of the firing point and adjacent grounds may not be significantly greater than that experienced in a natural setting. Concerning the second situation, the release is believed to be very long term. Becker (1993) estimated that the majority of the uranium inventory used in experiments during the last 50 years remains on the firing sites. Furthermore, the results of the present analysis demonstrated that beryllium and lead releases will require tens of thousands of years to leave the firing site. Thus, it is believed that conditions are met for the application of the curve number representative of long-term site conditions.

A source of additional runoff associated with operation of the facility is the cooling water blowdown discharge. When the facility is in operation, an estimated average of 2,000 gal/d (267 ft^3/d; 7.6 m^3/d) of cooling water will be discharged underground to a rip-rap lined trench that is drained by a culvert to a discharge point to the southeast of the east accelerator hall of the DARHT Facility. (Note, discharge of this cooling tower blowdown water has been approved and it is included in the National Pollutant Discharge Elimination System (NPDES) Permit issued to LANL by the EPA.) The discharge point is approximately 370 ft (113 m) from the firing point and is shielded from the firing point by the east accelerator hall. At this distance and being shielded, it is not anticipated that the discharge point will exhibit depleted uranium concentrations in soils that are significantly above background. Furthermore, because the culvert discharges to a rip-rap drainage area, it is anticipated that this cooling water will infiltrate into the subsurface and not discharge to Water Canyon except when cooling water discharge coincides with storm water discharge. Because this discharge is not expected to contact firing site soils and is expected to seep into the mesa rather than discharge to Water Canyon, the cooling water discharge has been neglected in this analysis.

Inclusion of runoff from storm water and cooling water discharges during the 30-year operation of the DARHT Facility could lead to minor increases in discharge to Water Canyon from the facility grounds (e.g., the 7 ac (3 ha) of the facility including structures and paved surfaces) but would not result in significantly greater flows within the canyon. Water Canyon and Cañon de Valle provide drainage to approximately 7,000 ac (11 mi^2) of upstream watershed. The relatively small increase in discharge from operation of this 7-acre facility will not significantly impact the total discharge of the canyon.

In all cases, the partition coefficients (K_d) and solubility limits for the depleted uranium, beryllium, and lead used were the conservative estimates for suspended sediments as given in appendix E2.

E3.3 NO ACTION ALTERNATIVE SIMULATIONS

In this alternative, the transport by surface runoff during the past 32 years for releases of depleted uranium, beryllium, and lead and for releases during the next 30 years from the PHERMEX site were assumed to be evenly split between Water and Potrillo Canyons with 50 percent of the release going to each canyon. The amount of depleted uranium released is assumed to be 30 percent of total mass indicated in section 2 of appendix E. For the next 30 years in the No Action Alternative, the annual releases of depleted uranium, beryllium, and lead would be 460, 22 and 33 lb/yr (210, 10, and 15 kg/yr), respectively. Table 5-3 shows the simulated peak concentration of contaminants in the infiltrated water at the discharge sink in Potrillo Canyon (reach 3) and at Water Canyon channels below the source (Reaches 12, 13, 14, and 15).

Because of their low solubility, the concentrations of beryllium and lead reach a plateau at the end of the 5,000-year simulation, but still remain well below drinking water standards. Using the average simulated transport rates, the inventories of beryllium and lead at the firing site will be exhausted in approximately 300,000 and 40,000 years, respectively. Although beryllium and lead have relatively low solubilities, depleted uranium has a relatively higher solubility in LANL surface and ground waters. Consequently, the source of depleted uranium on the soil surface would be completely removed from the firing site in less than 1,000 years.

Table 5-3 also lists the peak concentration of dissolved and sediment-sorbed contaminant concentrations entering the Rio Grande. The Rio Grande is the nearest off-LANL access point for surface water carrying contamination from the firing point. The quality of surface water entering the Rio Grande is forecast to be more than an order-of-magnitude below the proposed water quality standard for uranium and several orders-of-magnitude below the drinking water standard MCLs for beryllium and lead.

The long-term average annual water volume (over the 5,000-year simulation) infiltrating at the Potrillo Canyon discharge sink was computed to be 37,400 ft^3/yr (1,000 m^3/yr). This is lower, but in the range of the 183,600 ft^3 (5,200 m^3) volume that was reported for 1990 from the short-term measurements by Becker (Becker 1993). The average annual simulated water discharge and sediment discharges entering the Rio Grande from the Water-Potrillo Canyon watersheds were 237,000 ft^3/yr (6,700 m^3/yr) and 165 tons/yr (150,000 kg/yr), respectively. No direct measurements of stream flow volume and sediment discharge to the Rio Grande were available for Water Canyon.

E3.4 DARHT BASELINE ALTERNATIVE SIMULATIONS

The annual expenditures from the DARHT site of depleted uranium, beryllium, and lead were 460, 22, and 33 lb/yr (210, 10, and 15 kg/yr), respectively. The amount of depleted uranium released is assumed to be 30 percent of total mass indicated in section 2 of appendix E. These annual expenditures from DARHT were released onto the firing site for the first 30 years of the simulation. All surface runoff from the firing site was directed to Water Canyon. Table 5-8 shows the peak concentration of contaminants and years to peak in the infiltrated water along Water Canyon (Reaches 12, 13, 14, and 15).

Because of their low solubility, the concentrations of beryllium and lead reach a plateau at the end of the 5,000-year simulation, but still remain well below drinking water standards. Using the average simulated transport rates, the inventories of beryllium and lead at the firing site will be exhausted in approximately 74,000 and 9,000 years, respectively. Although beryllium and lead have relatively low solubilities, depleted uranium has a relatively high solubility in LANL surface and ground waters. Consequently, the source of depleted uranium on the soil surface would be completely removed from the firing site in less than 1,000 years.

Table 5-8 also lists the peak and time to peak for the dissolved and sediment-sorbed contaminant concentrations entering the Rio Grande. The Rio Grande is the nearest off-LANL access point for surface water carrying contamination from the firing point. The quality of surface water entering the Rio Grande is forecast to be more than an order-of-magnitude below the proposed water quality standard for uranium and several orders-of-magnitude below the drinking water standard MCLs for beryllium and lead.

E3.5 ENHANCED CONTAINMENT ALTERNATIVE SIMULATIONS

Under this alternative three options were analyzed: the Vessel Containment Option, the Building Containment Option, and the Phased Containment Option (preferred alternative). The annual expenditures of depleted uranium, beryllium, and lead for each of these options are listed in table E3-2.

These annual expenditures from DARHT were released onto the firing site for the first 30 years of the simulation. All surface runoff from the firing site was directed to Water Canyon. Table 5-11 shows the peak concentration of contaminants and years to peak in the infiltrated water along Water Canyon (Reaches 12, 13, 14, and 15) for the three options.

Because of their low solubility, the releases of beryllium and lead are long term. Beryllium concentrations plateau before the end of the 5,000-year simulation and remain well below drinking water standards. Based on release projections, we estimate beryllium release will require 4,420, 22,000, and 34,000 years for the Vessel Containment, Building Containment, and Phased Containment options, respectively. Similarly, lead concentrations plateau within the 5,000-year simulation and remain well below drinking water standards. Because its solubility is greater than that of beryllium, lead release times are shorter. We estimate lead release to the environment will require 530, 2,590, and 4,062 years for the three options, respectively. Depleted uranium has a relatively high solubility in LANL surface and ground waters. Based on this high solubility concentration, the source of depleted uranium at the soil surface would be completely removed from the firing site in 30 years for the various containment options. Such a release is conservative or aggressive because it routes the depleted uranium into the environment more quickly than field observations (Becker 1993) indicate is occurring. The model indicates that the reach of Water Canyon (reach 12) receiving runoff from the facility could discharge water to the streambed or to the downstream reach (depending on canyon flow conditions) containing concentrations of depleted uranium at or slightly above the drinking water standard for uranium (i.e., 20 μg/L).

Table 5-11 also lists the peak and time to peak for the dissolved and sediment-sorbed contaminant concentrations entering the Rio Grande. The Rio Grande is the nearest off-LANL access point for surface water carrying contamination from the firing point. The quality of surface water entering the Rio Grande is forecast to be more than an order-of-magnitude below the proposed drinking water standard for uranium and several orders-of-magnitude below the drinking water standards for beryllium and lead.

APPENDIX E4: VADOSE ZONE AND GROUND WATER MODEL

E4.1 INTRODUCTION

Ground water constitutes one potential environmental pathway by which contaminants originating at the DARHT and PHERMEX firing sites may, after centuries to millennia, become accessible to members of the public. Some canyons in the Los Alamos area (notably Los Alamos and Mortandad Canyons to the north of TA-15) have shallow alluvial and intermediate-depth perched aquifer systems that provide a relatively fast path for contaminants leached through canyon bottoms to appear in ground water. However, the canyons of concern in this study, Water Canyon and Potrillo Canyon, do not appear to have

TABLE E3-2.—*Annual Expenditures of Depleted Uranium, Beryllium, and Lead for the Enhanced Containment Alternative*

Containment Option	Depleted Uranium lb (kg)	Beryllium lb (kg)	Lead lb (kg)
Vessel			
(30 yr)	185 (84)	6.5 (3)	10 (4.4)
Building			
(30 yr)	92 (42)	1.3 (0.6)	2 (0.9)
Phased			
(0 to 5 yr)	444 (200)	21 (9.5)	31 (14)
(6 to 10 yr)	315 (143)	14 (6.2)	21 (9.4)
(11 to 30 yr)	185 (84)	6.5 (3)	10 (4.4)

such shallow aquifer systems. Potrillo Canyon is cut directly on the Bandelier Tuff, and there is little to no alluvial fill in the upper reaches of the watershed. Therefore, it is unlikely that a permanent alluvial aquifer exists in this canyon (LANL 1993b). Water Canyon is a large canyon that heads on the flanks of the Sierra de Los Valles. A short distance downstream from the confluence of Water Canyon and Cañon de Valle, near the DARHT and PHERMEX sites, is Beta Hole, a dry well extending 187 ft (57 m) into the Bandelier Tuff (LANL 1993b; Purtymun 1995). The lack of water in Beta Hole and two other shallow wells completed in the alluvium confirm that Water Canyon in the vicinity of TA-15 contains no permanent perched or alluvial aquifers, though there is a possibility of perched zones at intermediate depth (LANL 1993b).

In the absence of a perched aquifer, water infiltrating through the vadose (unsaturated) zone may transport contaminants in liquid phase from the surface to the regional or main aquifer. However, this would occur over a long period of time, and has not been observed at LANL. Once in the main aquifer, contaminants may be transported down gradient through the saturated zone down gradient to the Rio Grande, where these contaminants may be discharged in springs or directly to the Rio Grande and become accessible in that surface water body to members of the public. Alternatively, once in the main aquifer, contaminated water might be pumped from wells for municipal and industrial use, again becoming accessible. Although no water supply wells currently exist in TA-15, which includes the DARHT and PHERMEX sites, Purtymun (Purtymun 1984) identified an area that included TA-15 as most suitable for additional water supply wells for Los Alamos County based on the desired attributes of high yield and low drawdown wells. It is surmised that these desirable attributes for well placement will make the area subject to future water well development. However, regulations would require testing before public use, and during subsequent use. The average yield from the five wells in the Pajarito Field [the PM wells are located in the zone identified by Purtymun (Purtymun 1995)] was 1,215 gpm (2.7 ft^3/s, 0.08 m^3/s) (Purtymun 1984). Therefore, well extraction of dissolved contaminant mass from the regional aquifer, if transported to the aquifer, is a possible consideration.

In spite of the above considerations with regard to the main aquifer, it may be unnecessary to model the flow and transport of contaminants in the main aquifer depending on the results of vadose zone modeling. To reach the main aquifer, contaminant mass must 1) be available at the surface for leaching into the soil profile and 2) be transported vertically downward from the surface to the water table. The travel time for recharge water through unsaturated volcanic tuffs in a semi-arid climate can be centuries to millennia. Sorption further extends the time required for contaminants to migrate to the main aquifer, and dispersion acts to reduce peak concentrations.

Ground water modeling and analysis for this study necessarily follows the assumptions made for the runoff-sediment-contaminant transport model (see appendix E3, Surface Water Modeling). Water infiltration into the bottom sediments of Water Canyon and the contaminant mass loading associated with that water as predicted by the runoff-sediment-contaminant transport model constitute the inputs to the vadose zone model for Water Canyon.

The discharge sink in Potrillo Canyon identified by Becker (1993) is taken to be the controlling feature in that canyon. Evidence in Becker (1993) demonstrated that all surface water from the Potrillo Canyon watershed above this feature drains to the subsurface very rapidly via the discharge sink (except for flood events with a recurrence frequency greater than a 1-in-10-year event). The mechanism that enables such large water intake rates to the subsurface is not well characterized. Becker (1993) concluded that the discharge sink is an area of increased sedimentation, that it contains significant amounts of uranium adsorbed onto the surface soils with depth, and that leaching and deep infiltration transport uranium (dissolved phase) to ground water. Becker (1993) could only hypothesize as to the feature that creates the discharge sink, an underlying fault with a 29-ft (9-m) offset. Because no defensible mechanism can be proposed to account for the discharge sink's hydrologic behavior at this time, no attempt was made to model the discharge sink. Instead, the approach to stream flow losses in Potrillo Canyon was to compute the concentrations of contaminants in water arriving at the sink (as all water in the upper reach of Potrillo Canyon usually collects at the discharge sink), and if those concentrations are low enough to meet regulatory criteria, no further analysis is required. If not, we would make the conservative assumption that contaminated water from the discharge sink is transferred instantly to the main aquifer (i.e., taking no credit for time delay and dispersion in the vadose zone), and examine the consequences of water supply well uptake or surface water discharge of contaminated water at the Rio Grande.

Water Canyon does not appear to exhibit any feature analogous to the discharge sink Becker discovered in Potrillo Canyon (Becker 1993). Nor does Water Canyon appear to have a perched aquifer system, based on the dry Beta Hole located in Water Canyon adjacent TA-15 (LANL 1993b; Purtymun 1995). Therefore, it was decided that modeling the vadose zone below Water Canyon might enable evaluation of the downward flow of water and transport of contaminants from stream losses to the stream bed as predicted by the surface water and sediment transport analysis model.

Finally, the vadose zone from the firing sites atop Threemile Mesa to the main aquifer was modeled. The mesa top in the vicinity of DARHT and PHERMEX is over 300 ft (91 m) above the bottom of Water Canyon. Thus, a model of vadose zone flow and transport from the bottom of Water Canyon to the main aquifer simulates a significantly shorter pathway. However, the contaminant loading at the firing sites into the soil is large enough (e.g., infiltration carrying contaminants at their solubility limit) to require vadose zone flow and transport modeling also.

E4.2 VADOSE ZONE STRATIGRAPHY

There are no deep wells in TA-15 that would provide certain knowledge of the geologic stratigraphy at the DARHT, PHERMEX, or nearby Water Canyon and Potrillo Canyon locations (LANL 1993b; Purtymun 1995). The closest wells that penetrate to the regional aquifer are the test wells DT-5A, DT-9, and DT-10 to the south of TA-15, and the municipal and industrial supply wells PM-2 and PM-4 located to the northeast of TA-15. Figure E4-1 depicts the locations of these wells and the DARHT and PHERMEX firing sites. A cross-section from test well DT-5A to supply well PM-4, based on well log data reported in Purtymun (Purtymun 1995), is shown in figure E4-2. The Tshirege, Otowi, and Guaje members are all sequences within the Bandelier Tuff. Figure E4-2 illustrates the transition in geologic units expected over the area in the vicinity of DARHT and PHERMEX. Based on this cross-section, the location of the DARHT site, and the anticipated stratigraphy (LANL 1993b), the expected geologic stratigraphy for this EIS was developed, and is shown in figure E4-3. The elevation axis at the left of figure E4-3 shows how the expected stratigraphy corresponds to elevation above mean sea level, and includes arrows to show the elevations at the DARHT and PHERMEX sites, Water Canyon (near Beta Hole), and the Potrillo Canyon discharge sink location. The water table elevation at 6,000 ft (1,830 m) (Purtymun 1984; Volzella 1994; LANL 1993b; Purtymun 1995) is shown on the stratigraphic column at 800 ft (244 m) below the well head surface. The depth of the alluvium is designated as 8 ft (2 m) based on the geologic log of the Beta Hole (Purtymun 1995). The fingered layers of Basalt Unit 2 shown in figure E4-2 are assumed not to be present based on the stratigraphy presented in the *RFI Work Plan* (LANL 1993b) and the trend of basalt layers fingered into the Fanglomerate Member of the Puye Formation to decrease from east to west as a result of the geologic processes in which they were laid down.

E4.3 VADOSE ZONE HYDROLOGIC PROPERTIES

The expected stratigraphy for Water Canyon depicted in figure E4-3 shows five hydrogeologic units in the vadose zone for which hydrologic properties are required for modeling purposes: alluvium, three members of the Bandelier Tuff (Tshirege, Otowi, and Guaje), and the Puye Formation. The properties required for water flow modeling are saturated hydraulic conductivity, porosity or saturated moisture content, residual moisture content, and the empirical curve-fitting van Genuchten (van Genuchten 1980) water retention parameters α and n for use in the water retention and liquid relative permeability models chosen for this analysis.

Values for the vadose zone flow model parameters for each unit are reported in table E4-1. All values for the alluvium and Bandelier Tuff members are based on mean values reported in Rogers and Gallaher (Rogers and Gallaher 1995). No values were reported in that document directly for the Guaje Member, so the average of all Bandelier Tuff measurements was used to provide the hydrologic properties given in table E4-1 for the Guaje Member. Figure E4-4 provides the graphical interpretation of the water retention and relative permeability parameters by showing the retention and conductivity curves resulting from the use of the parameter values given in table E4-1.

No published hydrologic data, other than field coefficients of conductivity (Purtymun 1984), were found in the literature pertaining to the Puye Formation. The Puye Formation is derived from the Tschicoma volcanic centers located in the northeastern range of the Jemez Mountains. It consists of stream flow

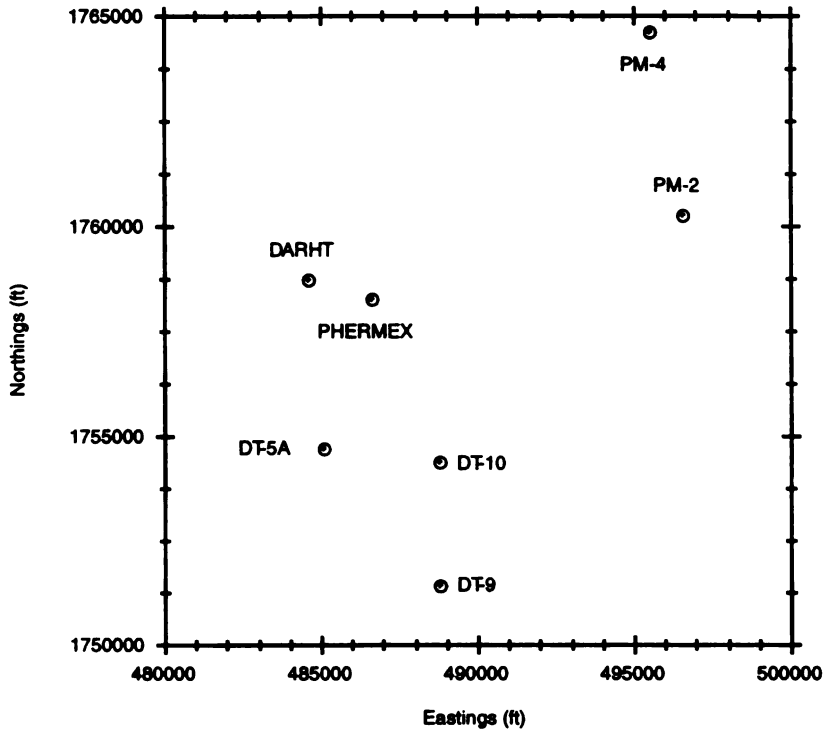

FIGURE E4-1.—***Locations of Deep Wells Relative to DARHT and PHERMEX Sites.***

TABLE E4-1.—***Hydrologic Properties for Vadose Zone Flow Modeling***

Stratigraphic Layer	Water Content Parameters		van Genuchten Model Parameters		Saturated Hydraulic Conductivity
	θ_r Residual	θ_s Saturated	α (1/m)	n	K_s (m/s)
Alluvium	0.038	0.433	3.85	1.558	4.40×10^{-6}
Tshirege	0.021	0.498	1.20	1.759	6.00×10^{-7}
Otowi	0.026	0.469	0.66	1.711	1.30×10^{-6}
Guaje	0.022	0.492	1.13	1.716	7.00×10^{-7}
Puye§	0.0283	0.4982	1.76	1.338	2.42×10^{-8}

θ_r Residual water content.
θ_s Saturated water content.
α Fitted van Genuchten parameter, 1/m.
n Fitted van Genuchten parameter.
K_s Saturated hydraulic conductivity, m/s.
§ Ringold Unit (Rockhold et al. 1993) properties used as analogue for Puye Formation.

deposits, debris flow and block flow deposits, and ash fall and pumice fall deposits (LANL 1993b). The hydrologic properties of a similar undifferentiated unit, the Ringold Unit found at the Hanford Site in Washington State, were chosen. The Ringold Unit is taken to be an analogue to the Puye Formation, and

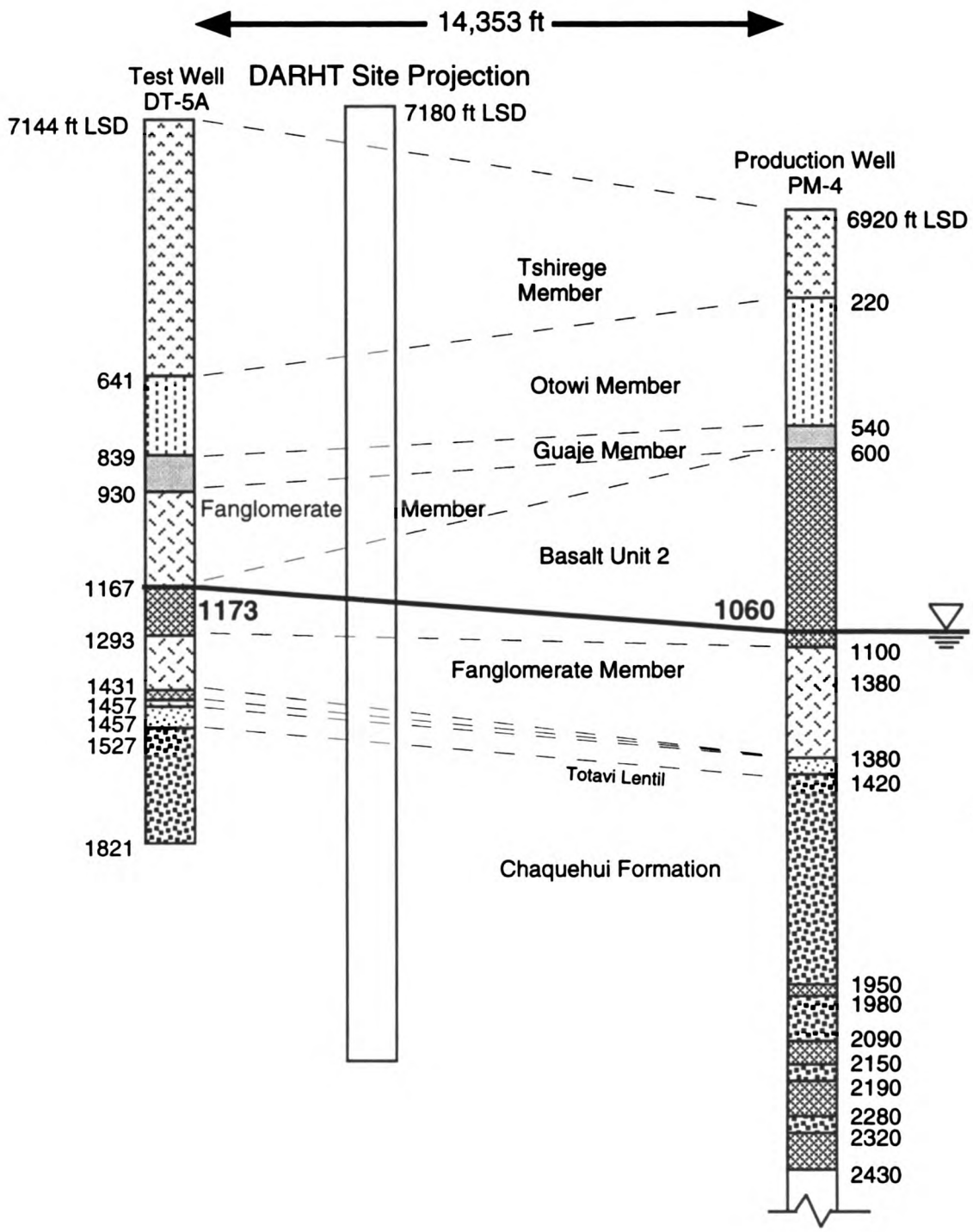

FIGURE E4-2.—*Stratigraphic Cross-section from Test Well DT5A to Production Well PM-4, Indicating Projected Location of DARHT Site on the Cross Section.*

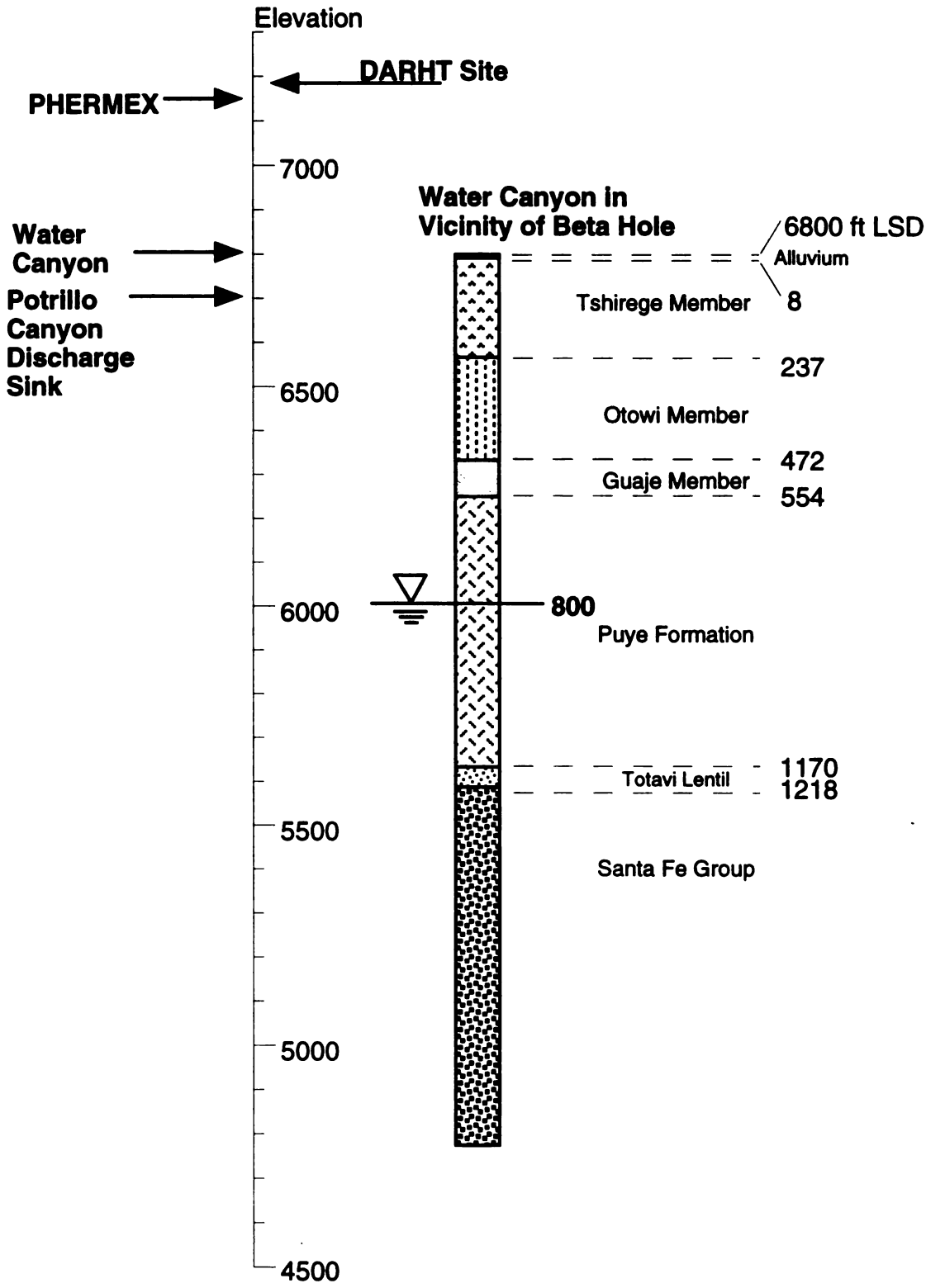

FIGURE E4-3.—*Expected Stratigraphy at Vicinity of Beta Hole in Water Canyon.*

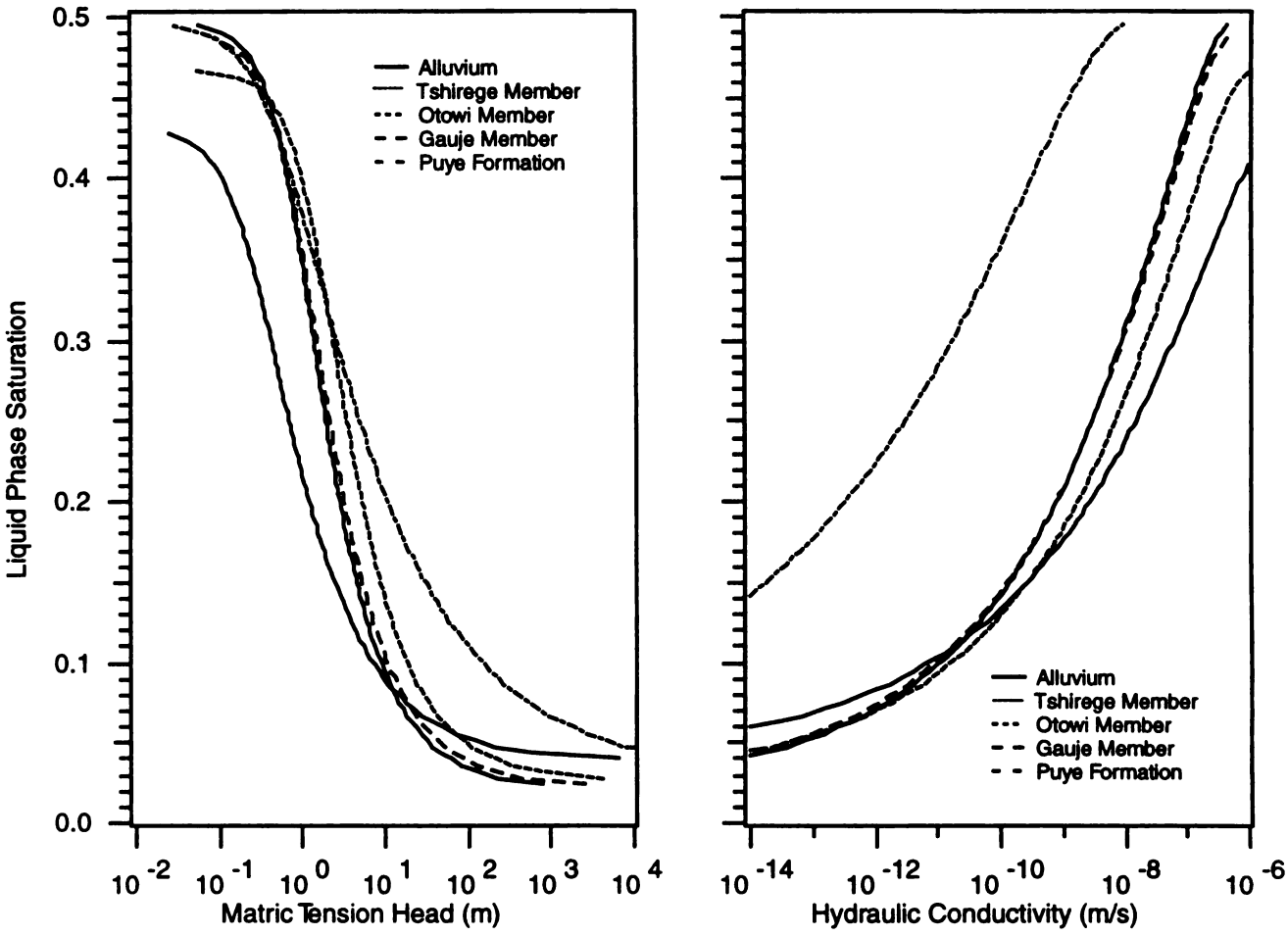

FIGURE E4-4.—*Unsaturated Water Retention and Relative Permeability Relationships for Vadose Zone Units.*

therefore properties used are largely approximate. Further precision will require a characterization and data collection program aimed at the Puye Formation and would only be necessary if the results of this analysis indicated that the unit imposed a significant control over the flow and transport results, which it did not. Properties for the Ringold Unit, reported in table E4-1, were taken from those reported in Rockhold et al. (1993).

E4.4 VADOSE ZONE MODELING APPROACH

We modeled the vadose zone below Water Canyon and Threemile Mesa as one-dimensional vertical stratigraphic columns extending from the regional aquifer piezometric surface (water table) at the lower boundary to the surface of Water Canyon or Threemile Mesa at the upper boundary. The upper boundary was treated as a Neumann boundary with a constant water flux rate based on the average water infiltration predicted by the runoff-sediment-contaminant transport model. Temporal variation in water infiltration was neglected because such variation is greatly damped within a few meters of the surface. The lower boundary was treated as a Dirichlet boundary and assigned a constant atmospheric pressure to represent

the presence of the water table. Fracture flow was neglected because published information on this flow mechanism is incomplete (Loeven and Springer 1992); fractures are sparse features where documented (Purtymun et al. 1978), and in the low-saturation regimes such as that modeled here, fractures constitute barriers to moisture flow rather than preferential pathways (Klavetter and Peters 1986).

A computer code was used to perform the flow and transport simulations. The code we chose was the Multiphase Subsurface Transport Simulator, or MSTS (White and Nichols 1993; Nichols and White 1993). The MSTS computer code was chosen based on the following considerations:

- MSTS solves the nonlinear water mass conservation equation for variably saturated media necessary to model the vadose zone
- MSTS was developed for the Yucca Mountain Site Characterization Project, a program concerned with deep vadose zone flow and transport in arid site volcanic tuff environments, characteristics similar to the site under consideration in this study
- MSTS simulates dilute species mass transport using a convection-dispersion model with linear sorption coupled with the water mass conservation simulation, providing an integrated capability for flow and transport modeling that is much simpler than using separate flow and transport models
- Radioactive decay in the transport equation (dilute species mass conservation equation) is accounted for by the MSTS code
- The code is well documented, has been favorably reviewed (Reeves et al. 1994), and has a proven track record for flow and transport simulation in the numerically difficult volcanic tuff environment (Eslinger et al. 1991).

Numerical stability criteria were examined to construct a grid of computational cells and enable stable simulation of water flow and contaminant transport for this vadose zone model. Calculations indicated that a grid discretization of 0.5 ft (0.15 m) or less would be required, yielding 1,600 grid elements over the 800 ft (244 m) high stratigraphic column. Other calculations indicated that time steps for the transport simulations should not exceed 20 years to avoid numerical dispersion effects. Because the transport model was restricted to 1-yr time steps to match the temporal rate of contaminant mass loading resulting from the runoff-sediment-contaminant transport model, and 20-yr time steps after mass loading ended, this criterion presented no additional limitation.

E4.5 VADOSE ZONE FLOW MODEL RESULTS

Hydrologic conditions (e.g., water flow) in the unsaturated zone will depend on similar occurrences under any of the alternatives. For example, the presence of the DARHT and PHERMEX facilities does not affect the hydrology of Water Canyon appreciably, and infiltration would move water through Threemile Mesa at either location of the firing point. Therefore, the results of the vadose zone flow simulations were performed and the results reported here for all alternatives and options. Contaminant mass transport simulations that are based on the water pressure fields calculated here are reported with respect to individual alternatives and options in section 5.

A steady-state pressure field was simulated for Reach 12 of Water Canyon. Reach 12 in the surface water model is immediately downstream of the confluence of Cañon de Valle and Water Canyon (see

appendix E3). Another was simulated for a location representative of the DARHT and PHERMEX facilities on Threemile Mesa. The surface elevation difference between the two sites was neglected; the firing sites differ in elevation by approximately 36 ft (11 m) (Fresquez 1994; Korecki 1988). The conditions vary in the different reaches of the Water Canyon model depending upon the water infiltration predicted in each reach by the runoff-sediment-contaminant transport model. The liquid-phase pressure and saturations predicted from the steady-state simulation with the MSTS code for Reach 12 are plotted in figure E4-5. The abrupt changes in pressure and saturation shown in figure E4-5 reflect the variations in hydrologic properties corresponding to the stratigraphic units identified. Liquid-phase mean travel time, that is, the mean time for water to travel from the base of Water Canyon to the regional aquifer, was predicted with the MSTS code. Travel times for Reaches 12 and 13, and for the mesa-top-to-aquifer vadose zone model, are reported in table E4-2. Water travel times provide an upper bound on the arrival time of the mean concentration of a nonretarded, nondecayed contaminant. Retarded (sorbed) species, such as those under consideration in this study, will have even longer arrival times.

E4.6 CONTAMINANT TRANSPORT SIMULATIONS

Review of the similarities between alternatives for the concentration of infiltration waters predicted by the runoff-sediment-contaminant transport model reduced the number of vadose zone contaminant transport cases that were necessary to simulate for this EIS. The ground water impacts of the Plutonium Exclusion and Single Axis alternatives were the same as the DARHT Baseline Alternative; and the Upgrade PHERMEX Alternative was the same as the No Action Alternative. This review implied that simulations were necessary only under the No Action, DARHT Baseline, and Enhanced Containment alternatives. For these three alternatives, the peak concentrations of depleted uranium, beryllium, and lead in water infiltrating into the vadose zone in the four reaches of Water Canyon downstream from the firing sites, and on Threemile Mesa at the firing sites, were compared to the drinking water standards for these metals. Because transport and dispersion in the vadose zone will only further decrease the concentrations of these metals in solution, it was necessary to simulate only those cases in which the concentration of contaminants in infiltrating water at the surface exceeded the drinking water standard. Finally, comparison of concentrations of contaminants in infiltrating water in the four reaches of Water Canyon showed that the uppermost reach (Reach 12) was always subject to the highest infiltration contaminant concentration levels of the four reaches. Because no simulation of Reach 12 resulted in contaminant concentrations at the regional water table exceeding the drinking water standard for any contaminant, no simulation was necessary for the less-impacted reaches downstream. Thus, a total of 10 simulation cases were required for depleted uranium: transport through Threemile Mesa for the No Action, DARHT Baseline, and Enhanced Containment alternatives (including the three options) and transport through the sediments beneath the uppermost reach of Water Canyon (Reach 12) for the same five alternatives and options. We also simulated beryllium and lead transport from the mesa and the uppermost reach of Water Canyon to the main aquifer to examine the transport of these dissolved contaminants in the vadose zone.

Initial conditions for all simulations specified the liquid pressure field obtained for the respective reach or mesa top simulation (section E4.5, above) and zero contaminant concentration throughout the profile. Mass transport was simulated using the one-year constant time steps of the surface water model (matching the temporal rate for which the contaminant mass input values were provided by the runoff-sediment-contaminant transport model) and then using 20-year constant time steps for periods after mass input rates specified by the surface water model ceased (20-year steps being the maximum permissible under the Courant Number stability criteria). Parameters related to dilute contaminant species mass transport include

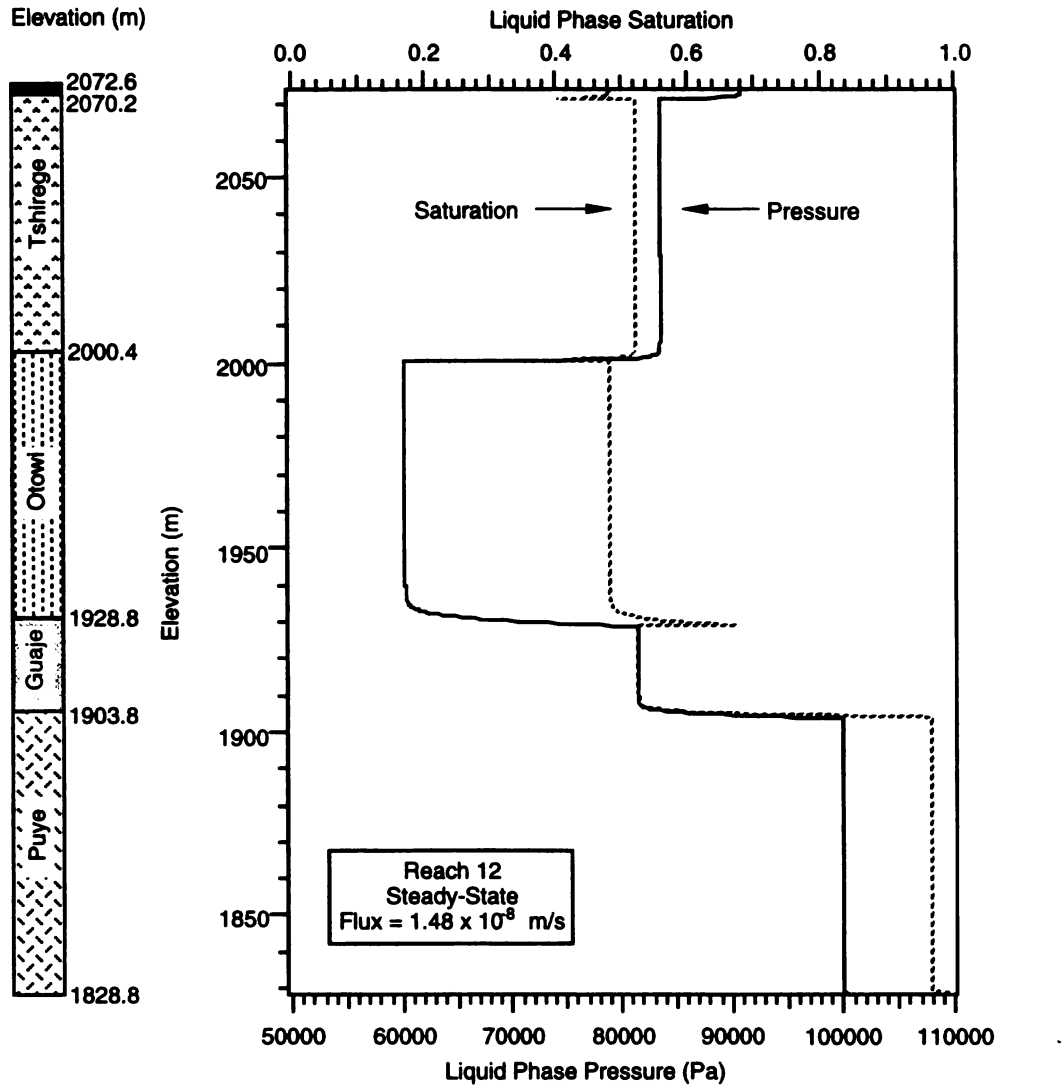

FIGURE E4-5.—*Liquid Phase Pressure and Saturation Profiles Predicted for Water Canyon Reach 12.*

TABLE E4-2.—*Liquid Phase Vadose Zone Water Travel Times for Threemile Mesa and Water Canyon Reaches 12 and 13 Predicted by MSTS*

Vadose Zone	Water Travel Time (yr)
Threemile Mesa	298
Water Canyon Reach 12	179
Water Canyon Reach 13	174

values of the sorption coefficient (K_d), longitudinal hydraulic dispersivity coefficient (α_L), and molecular dispersion coefficient (D_{dl}). Sorption coefficient values were estimated in appendix E2 ("Solubility and Distribution Coefficients") where both conservative and best-estimate values were provided. We chose to use conservative (i.e., less sorption) values in all vadose zone modeling of contaminant transport. For moderate travel distances (on the order of kilometers), longitudinal dispersivity roughly varies between 0.01 and 0.1 of the mean travel distance of the solute. Choosing the more often used and higher value, with the travel distance through the vadose zone of 800 ft (240 m), we obtained the 80 ft (24 m) value. The molecular diffusion coefficient was that of water, 1.076×10^{-8} ft^2/s (1.0×10^{-5} cm^2/s).

Contaminant mass input rates were obtained from the results of the runoff-sediment-contaminant transport model. The infiltrated volume for each year reported by the runoff-sediment-contaminant transport model was multiplied by the corresponding water concentration of the infiltrated water, and divided by the channel reach area or the area for mass distribution around the firing point to obtain a value for annual mass flux per unit area. This value was converted to appropriate units for the vadose zone flow and transport code and treated as a mass source rate in the uppermost node of the model. For each simulated case, contaminant transport was modeled for 100,000 years. For depleted uranium, 1,000 years of mass input was provided, after which the surface supply of depleted uranium on the mesa surface and in the channel reaches was exhausted (the remainder of the simulation was carried out with no contaminant source term). For beryllium and lead, 5,000 years of mass input was provided. For the simulation beyond 5,000 years, estimates (based on surface modeling) of the time to "plateau" for releases for beryllium and lead and average input concentrations thereafter were used to specify an average contaminant mass source rate and duration for the balance of the 100,000-year simulations. Table E4-3 presents the peak concentration of water arriving at the regional main aquifer for each simulated case and time of the peak occurrence, and the related drinking water standard. The significance of the arrival concentrations listed in table E4-3 is provided in the discussions of individual alternatives in sections 5.1.4.2, 5.2.4.2, and 5.4.4.2.

E4.7 GROUND WATER ISSUES AT LANL

Two issues exist with respect to ground water resources in the vicinity of LANL. The first involves the recent discovery of tritium in the main aquifer at four points in the northern portion of the LANL site. The second involves the general observation that private ground water wells located north of Pojoaque can exhibit levels of alpha contamination in excess of drinking water standards.

E4.7.1 Tritium in the Main Aquifer

Since 1991, advanced techniques, not commonly applied to ground water samples, have been used to detect tritium at ultra-low levels and to determine that recent water (no more than a few decades old) has recharged the main aquifer from the land surface in several locations at LANL (Gallaher 1995). Many samples of well and spring water taken at LANL have shown only the natural background levels of tritium and no apparent recent recharge. However, four locations have indicated tritium migration to the main aquifer from overlying contaminated perched aquifers. The levels of tritium measured range from approximately 1 percent to less than a hundredth of a percent of current drinking water standards. Thus, measured levels of tritium are significantly below drinking water standards and below levels measurable using standard measurement techniques. All four confirmed main aquifer tritium measurements indicating

TABLE E4-3.—*Vadose Zone Numerical Transport Simulation Predictions of Peak Concentrations and Associated Times for Water Arriving at the Regional Main Aquifer from the Vadose Zone for All Simulated Cases*

Alternative, Location	Contaminant		
	DU (μg/L)	Be (μg/L)	Pb (μg/L)
Drinking Water Standard	20 [56 FR 33050]	4 [40 CFR 141.62]	15 [40 CFR 141.80]
No Action, Threemile Mesa (PHERMEX)	145 (42,850 yr)	3.4 (>100,000 yr)	26 (55,740 yr)
No Action, Water Canyon Reach 12	0.017 (18,450 yr)	0.00069 (>100,000 yr)	2.6×10^{-6} (>100,000 yr)
DARHT Baseline, Threemile Mesa (DARHT)	81 (42,950 yr)	3.1 (84,680 yr)	6.3 (33,800 yr)
DARHT Baseline, Water Canyon Reach 12	0.018 (18,430 yr)	0.0014 (>100,000 yr)	5.2×10^{-6} (>100,000 yr)
Vessel Containment Option Threemile Mesa (DARHT)	32 (42,880 yr)	1.2 (41,880 yr)	0.0012 (>100,000 yr)
Vessel Containment Option Water Canyon Reach 12	0.054 (18,390 yr)	0.0027 (>100,000 yr)	1.0×10^{-5} (>100,000 yr)
Phased Containment Option Threemile Mesa (DARHT)	43 (42,060 yr)	1.8 (50,640 yr)	0.0018 (>100,000 yr)
Phased Containment Option Water Canyon Reach 12	0.055 (18,430 yr)	0.0027 (>100,000 yr)	1.0×10^{-5} (>100,000 yr)
Building Containment Option Threemile Mesa (DARHT)	16.1 (41,980 yr)	0.233 (45,099 yr)	1.5×1.0^{-7} (>100,000 yr)
Building Containment Option Water Canyon Reach 12	0.0365 (18,468 yr)	3.4×10^{-4} (>20,870 yr)	4.5×10^{-7} (>100,000 yr)

young water are in Los Alamos, Pueblo, and Mortandad Canyons, all in the northern part of the Los Alamos site. No main aquifer samples from the southern portion of the site have shown tritium concentrations above natural background. LANL scientists are studying whether the communication between intermediate perched and deep aquifer formations is a result of poor well construction (leaks in well bore seals with casing) or recharge of the main aquifer through either fractures or faults. If the ongoing studies determine the old construction methods are resulting in communication, efforts may be undertaken to abandon and plug the older test wells (Gustafson 1995).

E4.7.2 Alpha Concentrations in Regional Ground Water

High alpha concentrations have been observed in ground water drawn from private wells in the vicinity of Nambe and Pojoaque, New Mexico (Nickeson 1994). These wells are located on the opposite side of

the Rio Grande from LANL and to the north of Pojoaque. The relationship between LANL activities and the observed alpha concentrations was questioned at the DARHT public hearings. Nickeson noted there was no one to blame for the high alpha concentrations found in her well water. The levels found are related to the abundance of naturally occurring uranium deposits in the highly volcanic region of northern New Mexico. The Santa Fe Reporter (Bird 1995) presented a broader portrait of the high alpha contamination problem in the region, and its relation to natural uranium levels in the region. Bird indicated that the Ground Water Division of the Environment Department (State of New Mexico) was being asked to consider a study of the area's private wells. Such a study may relate the levels of natural uranium in the aquifer formation to levels observed in ground water, determine the origin of ground water in the Pojoaque area (i.e., origin to the east or west of the Rio Grande), or determine isotopic ratios of uranium species (i.e., identifying natural versus depleted uranium sources, man-made isotopes, or other alpha emitters). Because it is a regional water quality issue and is acknowledged by State of New Mexico officials as being related to natural uranium levels, resolution of this issue is clearly beyond the scope of the DARHT EIS.

E.5 REFERENCES CITED IN APPENDIX E

Abeele, W.V., et al., 1981, *Geohydrology of Bandelier Tuff.* LA-8962-MS, Los Alamos National Laboratory, Los Alamos, New Mexico.

Allison, G.B., et al., 1994, Vadose-zone Techniques for Estimating Groundwater Recharge in Arid and Semiarid Regions, *Soil Sc. Sac. Am. J.* 58:6-14.

Becker, N.M., 1993, *Influence of Hydraulic and Geomorphologic Components of a Semi-Arid Watershed on Depleted Uranium Transport,* LA-UR-93-2165, Los Alamos National Laboratory, Los Alamos, New Mexico.

Bird, K., 1995, "Northern Wells Exceed Uranium Limits," *Santa Fe Reporter*, January 18-24, p. 18, Santa Fe, New Mexico.

Bouwer, H., and R.C. Rice, 1983, "Effect of stones on hydraulic properties of vadose zones," *In Proceedings of the Characterization and Monitoring of the Vadose (Unsaturated) Zone*, National Water Well Association, Worthington, Ohio.

Bowen, B.M, 1990, *Los Alamos Climatology,* LA-11735-MS, Los Alamos National Laboratory, Los Alamos, New Mexico.

Branson, F.A., et al., 1976, "Moisture Relationships in Twelve Northern Desert Shrub Communities Near Grand Junction, Colorado," *Ecology* 57:1104-1124.

Brookins, D.G., 1984 *Geochemical Aspects of Radioactive Waste Disposal*, Springer Verlag, New York, New York.

Campbell, G.S, 1985, *Soil Physics with BASIC*, Elesevier, Inc., New York, New York.

Carsel, R.F., and R.S. Parrish, 1988, "Developing Joint Probability Distributions for Soil Water Retention Characteristics," *Water Resour. Res.* 24:755-769.

Doorenbos, J., and W.O. Pruitt, 1977, *Guidelines for Predicting Crop Water Requirements*, FAO Irrigation Paper No. 24, pp. 1-107, Food and Drainage Agriculture Organization of the United Nations, Rome, Italy.

Elder, J.C., et al., 1977, *Hazard Classification Test of Mixed-Loas 30-mm GAU-8 Ammunition by Bonfire Cookoff and Sympathetic Detonation Testing*, LA-6711-MS, February, Los Alamos National Laboratory, Los Alamos, New Mexico.

Erdal, B.R., et al., 1980, "Laboratory Studies of Radionuclide Distribution Between Selected Groundwaters and Geologic Media," *In Task 4, Third Contractor Information Meeting*, pp. 453-522, Vol. I, J.F. Relyea, Chairman, CONF-7910160, PNL-S-8571, Pacific Northwest Laboratory, Richland, Washington.

Erickson, R.L., et al., 1993, *Geochemical Factors Affecting Degradation and Environmental Fate of Depleted Uranium Penetrators in Soil and Water*, PNL-827, February, Pacific Northwest Laboratory, Richland, Washington.

Eslinger, P.W., et al., 1993, *Preliminary Total-System Analysis of a Potential High-Level Nuclear Waste Repository at Yucca Mountain*, PNL-8444/UC-814, January, Pacific Northwest Laboratory, Richland, Washington.

Fayer, M.J., and T.L. Jones, 1990, *UNSAT-H Version 2.0: Unsaturated Soil Water and Heat Flow Model*, PNL-6779, Pacific Northwest Laboratory, Richland, Washington.

Felmy, A.R., et al., 1984, MINTEQ: *A Computer Program for Calculating Aqueous Geochemical Equilibria,* EPA-600-3-84-032, PB84-157148, National Technical Information Service, Springfield, Virginia.

Fernandez, O.A., and M.M. Caldwell, 1975, "Phenology and Dynamics of Root Growth of Three Cool Semi-desert Shrubs Under Field Conditions," *J. Ecol.* 63:703-714.

Foxx, T.S., and G.D. Tierney, 1984, *Status of the Flora of the Los Alamos National Environmental Research Park: A Historical Perspective*, LA-8050-NERP, Vol. II, September, Los Alamos National Laboratory, Los Alamos, New Mexico.

Fresquez, P.R., 1994, *Results of the Soil Sampling Survey Conducted Over Active RCRA Firing Site TA-15-184 (Phermex),* Memo to T. Grieggs, ESH-8, May, Los Alamos National Laboratory, Los Alamos, New Mexico.

Gallaher, B., 1995, *Update on Tritium in Los Alamos Groundwater*, LANL Memorandum No. ESH-18/WQ & H-95-0044, February 1, Los Alamos National Laboratory, Los Alamos, New Mexico.

Gustafson, J.R., 1995, "New Data Released on Los Alamos Water Supply," *Newsbulletin, The Newsweekly for Laboratory Employees and Retirees*, March 10, Los Alamos National Laboratory, Los Alamos, New Mexico.

Hanson, W.C., 1974, *Ecological Considerations of Depleted Uranium Munitions*, LA-5559, June, Los Alamos National Laboratory, Los Alamos, New Mexico.

Hanson, W.C., and F.R. Miera, Jr., 1976, *Long-Term Ecological Effects of Exposure to Uranium*, LA-6269, July, Los Alamos National Laboratory, Los Alamos, New Mexico.

Hanson, W.C., and F.R. Miera, Jr., 1977, *Continued Studies of Long-Term Ecological Effects of Exposure to Uranium*, LA-6742, AFATL-TR-77-35, June, Los Alamos National Laboratory, Los Alamos, New Mexico.

Hanson, W.C., and F.R. Miera, Jr., 1978, *Further Studies of Long-Term Ecological Effects of Exposure to Uranium*, LA-7163/AFATL-TR-78-8, July, Los Alamos National Laboratory, Los Alamos, New Mexico.

Klavetter, E.A., and R.R. Peters, 1986, *Fluid Flow in a Fractured Rock Mass*, SAND85-0855, March, Sandia National Laboratories, Albuquerque, New Mexico.

Korecki, N.T., 1988, *Geotechnical Investigation Report: Dual-Axis Radiographic Hydrotest Facility Los Alamos National Laboratories, Los Alamos, New Mexico*, SHB Job No. E88-1154, Sergent, Hauskins and Beckwith, Albuquerque, New Mexico.

Lane, L.J., et al., 1985, *New Estimating Procedures for Surface Runoff, Sediment Yield, and Containment Transport in Los Alamos County, New Mexico*, LA-10335-MS, April, Los Alamos National Laboratory, Los Alamos, New Mexico.

LANL (Los Alamos National Laboratory), 1993a, *Dual-Axis Radiographic Hydrotest Facility, 11/19/93, Civil Drawings*, Drw. No. C46477, Lab Job No. 6976-15, Los Alamos National Laboratory, Los Alamos, New Mexico.

LANL (Los Alamos National Laboratory), 1993b, *RFI Work Plan for Operable Unit 1086, Environmental Restoration Program*, LA-UR-92-3968, July, Los Alamos National Laboratory, Los Alamos, New Mexico.

LANL (Los Alamos National Laboratory), 1993c, *Environmental Surveillance at Los Alamos During 1991*, LA-12572-ENV, August, Los Alamos National Laboratory, Los Alamos, New Mexico.

LANL (Los Alamos National Laboratory), 1990, *Environmental Surveillance at Los Alamos During 1989*, LA-12000-ENV, December, Los Alamos National Laboratory, Los Alamos, New Mexico.

LANL (Los Alamos National Laboratory), 1989, *Environmental Surveillance at Los Alamos During 1988*, LA-11628-ENV, June, Los Alamos National Laboratory, Los Alamos, New Mexico.

LANL (Los Alamos National Laboratory), 1988, *Environmental Surveillance at Los Alamos During 1987*, LA-11306-ENV, May, Los Alamos National Laboratory, Los Alamos, New Mexico.

Loeven, C.A., and E.P. Springer, 1992, *Validation of Continuum Concepts for Flow and Transport in Unsaturated Fractured Bandelier Tuff*, LQ-UR-93-2873, Los Alamos National Laboratory, Los Alamos, New Mexico.

Longmire, P., et al., 1995, *Natural Background Geochemistry, Geomorphology, and Pedogenesis of Selected Soil Profiles and Bandelier Tuff, Los Alamos, N.M.*, LA-13913-MS, January, Los Alamos National Laboratory, Los Alamos, New Mexico.

McLin, S.G., 1992, *Determination of 100-Year Floodplain Elevations at Los Alamos National Laboratory*, LA-12195-MS, August, Los Alamos National Laboratory, Los Alamos, New Mexico.

Mills, W.B., et al., 1985, *Water Quality Assessment: A Screening Procedure for Toxic and Conventional Pollutants in Surface and Ground Water, Part 1*, EPA/600/6-85/002a, September, U.S. Environmental Protection Agency, Athens, Georgia.

Morel, F.M.M., 1983, *Principles of Aquatic Chemistry*, John Wiley & Sons, New York, New York.

Mualem, Y., "A New Model for Predicting the Hydraulic Conductivity of Unsaturated Porous Media," *Water Resour. Res.*, 12, 513-522, 1976.

Nichols, W.E., and M.D. White, 1993, *MSTS Multiphase Subsurface Transport Simulator User's Guide and Reference*, PNL-8637, May, Pacific Northwest Laboratory, Richland, Washington.

Nickeson, D., 1994, "Secret of Poor Health? It May be in the Water," *The New Mexican*, November 27, pp. D-1 and D-4, Santa Fe, New Mexico.

Nyhan, J.W., 1989a, *A Hydrologic Modeling Study of Water Balance Relationships at the Area P Landfill in Los Alamos, New Mexico*, LA-11521-MS, March, Los Alamos National Laboratory, Los Alamos, New Mexico.

Nyhan, J.W., 1989b, *Hydrologic Modeling to Predict Performance of Shallow Land Burial Cover Designs at the Los Alamos National Laboratory*, LA-11533-MS, March, Los Alamos National Laboratory, Los Alamos, New Mexico.

Nyhan, J.W., et al., 1978, *Soil Survey of Los Alamos County, New Mexico*, LA-6779-MS, June, Los Alamos National Laboratory, Los Alamos, New Mexico.

Onishi, Y., et al. 1981, *Critical Review: Radionuclide Transport, Sediment Transport, and Water Quality Mathematical Modeling; and Radionuclide Adsorption/Desorption Mechanisms*, NUREG/CR-1322/PNL-2901, January, Pacific Northwest Laboratory, Richland, Washington.

Purtymun, W.D., 1995, *Geologic and Hydrologic Records of Observation Wells, Test Holes, Test Wells, Supply Wells, Springs, and Surface Water Stations in the Los Alamos Area*, LA-12883-MS, January, Los Alamos National Laboratory, Los Alamos, New Mexico.

Purtymun, W.D., et al., 1994, *Water Supply at Los Alamos during 1991*, LA-12770-PR, June, Los Alamos National Laboratory, Los Alamos, New Mexico.

Purtymun, W.D., 1984, *Hydrologic Characteristics of the Main Aquifer in the Los Alamos Area: Development of Ground Water Supplies*, LA-9957-MS, January, Los Alamos National Laboratory, Los Alamos, New Mexico.

Purtymun, W.D., and W.R. Kennedy, 1971, *Geology and Hydrology of Mesita del Buey*, LA-4660, Los Alamos National Laboratory, Los Alamos, New Mexico.

Purtymun, W.D., et al., 1978, *Geologic Description of Cores from Holes P-3 MH-1 Through P-3 MH-5, Area G, Technical Area 54,* LA-7308-MS, May, Los Alamos National Laboratory, Los Alamos, New Mexico.

Rai, D., and J.M. Zachara, 1984, *Chemical Attenuation Rates, Coefficients, and Constants in Leachate Migration, Volume I: A Critical Review*, EPRI EA-3356, February, Electric Power Research Institute, Palo Alto, California.

Reeves, M., et al., 1994, *Review and Selection of Unsaturated Flow Models,* WBS: 1.2.5.4.6/QA: NA, April, INTERA Inc., Las Vegas, Nevada.

Rhoads, K., et al., 1992, *Estimation of the Release and Migration of Lead Through Soils and Groundwater at the Hanford Site 218-E-12B Burial Ground*, PNL-8356, Vols. 1 and 2, October, Pacific Northwest Laboratory, Richland, Washington.

Rockhold, M.L., et al., 1993, *Physical and Hydraulic Properties of Sediments and Engineered Materials Associated with Grouped Double-Shell Tank Waste Disposal at Hanford,* PNL-8813, September, Pacific Northwest Laboratory, Richland, Washington.

Rogers, D.B., and Gallaher, B., 1995, *Review of Unsaturated Hydraulic Characteristics of the Bandelier Tuff,* Memo to J. Turin, M. Ankeny, D. Broxton, and A. Stoker, January 31, Los Alamos National Laboratory, Los Alamos, New Mexico.

Serne, R.J., 1994, *Hanford Sediment Kd's – Regional Perspective*, memorandum to Gene Whelan (Pacific Northwest Laboratory) April 18, 1994.

Serne, R.J., et al., 1993, *Solid-Waste Leach Characteristics and Contaminant-Sediment Interactions, Volume I: Barch Leach and Adsorption Tests and Sediment Characterization*, PNL-8889, October, Pacific Northwest Laboratory, Richland, Washington.

Sharpley, A.N., and J.R. Williams, 1990, *EPIC—Erosion/Productivity Impact Calculator, 1. Model Documentation,* Technical Bulletin Number 1768, September, United States Department of Agriculture.

Tierney, G.D., and T.S. Foxx, 1987, *Root Lengths of Plants on Los Alamos National Laboratory Lands*, LA-10865-MS, Los Alamos National Laboratory, Los Alamos, New Mexico.

van Genuchten, M. Th., 1980, "A Closed-Form Equation for Predicting the Hydraulic Conductivity of Unsaturated Soils," *Soil Science Society of America Journal*, 44:892-898.

Vine, E.N., et al., 1981a, "Current Status of Crushed Rock and White Rock Column Studies," in *Waste/Rock Interactions Technology Program FY-80 Information Meeting*, pp. 183-193, J.F. Relyea, Chairman, PNL-3387, February, Pacific Northwest Laboratory, Richland, Washington.

Vine, E.N., et al., 1981b, "Current Status of Laboratory Sorption Studies" in *Waste/Rock Interactions Technology Program FY-80 Information Meeting*, pp. 194-203, J.F. Relyea, Chairman, PNL-3387, February, Pacific Northwest Laboratory, Richland, Washington.

Vozella, J.C., 1994, *Water Level Maps for Los Alamos National Laboratory (LANL)*, Letter to W.K. Honker, December 27, Los Alamos National Laboratory, Los Alamos, New Mexico.

White, M.D., and W.E. Nichols, 1993, *Multiphase Subsurface Transport Simulator Theory Manual*, PNL-8636/UC-814, May, Pacific Northwest Laboratory, Richland, Washington.

Wilcox, B.P., 1994, "Runoff and Erosion in Intercanopy Zones of Pinyon-Juniper Woodlands," *J. Range Mgmt*, 47:285-295.

Wolfsburg, K., 1980, "Sorptive Properties of Tuff and Nuclide Transport and Retardation," in *Evaluation of Tuff as a Medium for Nuclear Waste Repository: Interim Status Report on the Properties of Tuff*, J.K. Johnstone and K. Wolfsberg, Eds., SAND80-1464, pp. 39-48, Sandia National Laboratory, Albuquerque, New Mexico.